Experimental Assessment of Constraint Release Physics in Entangled Polymers and Its Implication for Rheological Modeling

by

Ryan Justin Hall

A dissertation submitted in partial fulfillment
of the requirements for the degree of
Doctor of Philosophy
(Macromolecular Science and Engineering)
in the University of Michigan
2019

Doctoral Committee:

Professor Ronald G. Larson, Chair
Professor Brian J. Love
Professor Emeritus Richard E. Robertson
Professor Michael J. Solomon
Professor Alan S. Wineman

Ryan J. Hall

rjhall@umich.edu

ORCID iD: 0000-0002-5567-4016

Dedication

To my friends, mentors and family – you all have imparted to me unique life lessons and supported me in my pursuit of advanced education

Acknowledgements

It is with great joy and anticipation that I bring this chapter of my life to close. My graduate school journey has been a challenging but rewarding experience that has expanded my polymer research knowledge and provided both professional and personal growth opportunities. Most importantly, my journey has introduced to me a great number of friends and research collaborators.

First, I want to express deep gratitude to Prof. Ronald Larson. During my first couple of years in graduate school, I wanted to focus on theoretical research; however, progress was slow. After deep contemplation, I eventually realized that my research strength was in experiments. Prof. Larson patiently stood by me throughout this self-reflection process and exercised flexibility in allowing me to carve out my unique research path after my strength was realized.

I also want to thank Prof. Michael Solomon. After recognizing my strength in experimental research, and with the blessings of Prof. Larson, I sought out Prof. Solomon with the hope of gaining more experience in rheology and other characterization techniques that would complement my ongoing research under Prof. Larson. Prof. Solomon warmly welcomed me into his lab and opened the door to additional research projects for me to explore.

Third, I want to thank my dissertation committee members: Prof. Alan Wineman, Prof. Richard Robertson and Prof. Brian Love. I appreciate Prof. Wineman for his refreshing sense of humor and willingness to serve as my advisor for graduate program's literature review requirement. I appreciate Prof. Robertson for his enthusiasm in the classroom and unwavering

commitment to bettering the lives of students in my graduate program. I appreciate Prof. Love for his openness and the years of knowledge that he shared in the classroom.

Fourth, I want to thank my colleagues in the Larson, Solomon, and Glotzer laboratory groups for their support in friendship and research advice. I especially thank Luis Rivera, Dr. Priyanka Desai, Dr. Soroush Moghadam, Dr. Kyle Huston, Dr. Aly Salehi, Dr. Ali Ramazani, Keara Saud, and Nina Gasbarro for the fun experiences shared over the years.

I offer special thanks to my colleagues in the Macromolecular Science and Engineering Program; you all have been like a family to me. Particularly, I want to thank my friends and cohort Harry van der Laan, Dr. Leanna Foster and Rosy Adorf for their close friendship, personal adventures shared, and for their contributions to the ACS POLY/PMSE (American Chemical Society Division of Polymer Chemistry and the Division of Polymeric Materials Science and Engineering) student organization. I also want to thank the efforts of the past Macro Program coordinator and director, respectively Adam Mael and Prof. Mark Banaszak Holl. Adam has been steadfast in providing support as I navigated the rigors of graduate school and was fun to collaborate with when I was serving in various roles within the ACS POLY/PMSE student organization. I appreciate Mark for his energy and the new opportunities that he brought to the Macro Program. I will forever look fondly back on my first international research conference trip with Mark and other Macro students, to NAIST (Nara Institute of Science and Technology) in Japan.

I also want to thank my personal family and friends, especially my partner Drew, for their support throughout my graduate school journey. My grandparents were particularly supportive and accommodating during the earlier years of my PhD. I've stayed in their home on numerous

occasions while running special rheology experiments at the Illinois Institute of Technology in Chicago.

Last, but not least, I would like to thank the funding sources for my graduate school experience: National Science Foundation (NSF) and the Rackham Merit Fellowship (RMF) Program. In addition, I thank my research collaborators Dr. Maria Katzarova, Dr. Beom-Goo Kang, Dr. Maksim Shivokhin, Qifan Huang, Dr. Sanghoon Lee, Prof. Taihyun Chang, Prof. David C. Venerus, Prof. Jimmy Mays, Dr. Konstantinos Ntetsikas, Dr. George Polymeropoulos, Prof. Nikos Hadjichristidis, and Prof. Jay Schieber for their contributions. I especially appreciate Maria, Jay and David for their research insight and support during my trips to Illinois Institute of Technology for conducting special rheology experiments.

Table of Contents

List of Tables

List of Figures

Abstract

Innovations in the predictive theory, particularly tube models such as the Hierarchical 3.0 model (Wang et al. *J. Rheol.*, 54(2): 223-260, 2010), Branch-on-Branch (BoB) model (Das et al. *J. Rheol.*, 50(2), 207-234, 2006), and the Time-Marching Algorithm (van Ruymbeke et al. *J. Non-Newtonian Fluid Mech.*, 128, 7-22, 2005), have contributed greatly towards the improvement of industrial-scale polymer processing. However, recent studies conducted by Desai et. al. (*Macromolecules*, 49(13): 4964-4977, 2016) and Park et al. (*Macromolecules*, 37, 597-604, 2004) concerning the accuracy of Hierarchical and BoB model predictions have uncovered shortcomings in the tube theory. These shortcomings include 1) confusion in the choice of model parameters, particularly the dilution exponent; 2) the failure of Dynamic Tube Dilation (DTD) physics, especially in predicting the rheology of branched polymers; and 3) uncertainty of Constraint Release-Rouse (CR-Rouse) physics, which is important in predicting the rheology of polydisperse linear polymers, binary linear blends, and star-linear blends. In the two studies presented here, we attempt to address all three of the above shortcomings and provide a foundation for rebuilding tube theory.

First, we determine experimentally the dilution exponent for entangled polymers from the scaling of terminal crossover frequency with entanglement density from the linear rheology of three 1,4-polybutadiene star polymers that are blended with low-molecular-weight, unentangled linear 1,4-polybutadiene at various star volume fractions. Assuming that the rheology of monodisperse stars depends solely on the plateau modulus, the number of entanglements per chain, and the tube-segment frictional Rouse time, we show that only a dilution exponent of

unity, and not the alternative of 4/3 superposes the dependence of the terminal crossover frequency of the blends on entanglement density with those of pure stars obtained from literature. This is the first determination of the dilution exponent for star polymers that does not rely on any particular tube model implementation. We also show that the Hierarchical model, using the "Das" parameter set, which assumes a dilution exponent value of unity, reasonably predicts the rheological data of the melts and blends.

Second, we generate the most comprehensive dataset of star-linear blends (over 50 blends in total) to investigate further the failings of DTD and uncertainty of CR-Rouse physics. This work is coherent with the study of Desai et al. (*Macromolecules*, 49(13): 4964-4977, 2016) that showed the failure of the Hierarchical and BoB models to predict the linear rheological star-linear blend data when the pure linear polymer has a shorter relaxation time, but within 3-4 orders of magnitude, of the star polymer.. However, when the linear polymer has a longer relaxation time than the star, this new work, surprisingly, finds that both experimental data and model predictions are non-monotonic in the dependence of terminal relaxation time on star volume fraction.. We suspect that multiple regimes of constraint-release dynamics exist in star-linear polymer blends, only some of which are captured by current tube models. In addition to illuminating polymer relaxation physics, this vast dataset of star-linear blends serves as a rigorous benchmark for all existing predictive models, as well as for models that may be developed in the future.

Chapter 1: Introduction

I. Overview of Tube Theory

Material selection, processing optimization, and cost reduction has been an everlasting quest internalized by engineers and related professionals that work within industrial polymer manufacturing. Polymer processing innovations such as thermoforming, compression molding, injection molding, blow molding, and extrusion have greatly expanded the capabilities of processing plants over the years. However, in tandem with these growing polymer processing options, the need for rheological characterization has also grown in order to meet the demands of customers and manufacturing requirements in a timely manner.

Fortunately, in 1979, two scientists by the names Mosao Doi and Sam F. Edwards published a series of four papers describing a mathematical model that predicts the linear rheology of viscoelastic materials (*ie,* polymers); this model could therefore be utilized for selecting polymers that meet the requirements of industrial processing conditions.[1-4] Unlike Newtonian fluids, which undergo a purely viscous response to an applied external force, polymer melts are described as networks of chains that impose a series of topological constraints, also known as "entanglements," upon one another; these constraints causes the bulk polymer melt to respond to an applied external force in a time-dependent manner that increases proportionately with increasing polymer molecular weight. To simulate such a material, a successful and ideal predictive model needs to be able to track the diffusion of an arbitrary chain within a melt (commonly referred to as the "probe chain"), along with each of its entanglements;

unfortunately, however, such a task is computationally expensive. To avoid the detailed physics of capturing the motion of every entanglement imposed upon a probe chain, the model developed by Doi and Edwards utilizes a fictitious tube that represents a mean-field approximation of these confining entanglements; this is why the model has been referenced as the "tube model." When put into practice, the tube model simulates the flow response of a polymer melt by tracking the diffusion or "relaxation" mechanisms that allow the probe chain to escape the confines of its tube of entanglements.

At the time at which the tube model was first established by Doi and Edwards, reptation was the only relaxation physics utilized by the model. As first described in the work of de Gennes,[5] reptation is the longitudinal back-and-forth diffusive motion of the probe chain that is directed along the primitive path of the confining tube. This physics is successful for simulating the flow response of monodisperse polymers with linear architecture; however, the polymers utilized in an industrial setting can be considerably more complex, such as polymers with branched architectures and/or with high polydispersity. To accommodate this increased complexity in both polymer architecture and molecular weight distribution, additional relaxation physics have been added to tube theory over the years such as "contour length fluctuations" (CLF), which describe the fluctuation of the ends of the probe chain, and "constraint release" (CR), which describes the removal of constraints imposed by chains that neighbor the probe chain. Advanced forms of constraint release, dynamic tube dilation (DTD) and Constraint Release-Rouse (CR-Rouse), were specifically introduced to capture the physics of polymers with branched architectures, polydisperse linear polymers, binary blends of linear polymers, and binary blends of linear and star polymers.[6-16] Details concerning DTD and CR-Rouse will be addressed in Sections III.2 and III.3, respectively.

There have been many versions of tube models developed over the years that implement the relaxation physics described above. The most modern tube models include the Branch-on-Branch (BoB) model developed by Das et. al.;[17] the Hierarchical 3.0 model developed by Wang et. al.;[18] and the Time-Marching Algorithm (TMA) that was developed by van Ryumbeke and coworkers.[19] The BoB and Hierarchical models, under the conditions that will be addressed in Chapter 3 of this dissertation, behave similarly in the modeling of basic branched and linear polymeric architectures, including blends of the two architectures. However, a key difference between the BoB and Hierarchical models is that the BoB model, as hinted by its name, can also capture the physics of branch-on-branch structures such as hyperbranched and dendrimer polymers. For a detailed comparison between the Hierarhical and BoB models, please reference Wang et al.[18] All three models (*i.e.*, BoB, TMA and Hierarchical models) are united by the fact that they are implemented by using four material-based parameters: the plateau modulus (G_N^0), entanglement density (M_e), tube-segment frictional Rouse time (τ_e), and the dilution exponent (α). We note that the G_N^0, M_e, and τ_e are dependent on polymer chemistry and solution concentration, but are independent of polymer architecture. In addition, the dilution exponent (α) is typically assigned a value of 4/3 or unity, depending on the polymer system being observed and the tube model utilized.[17-21] Further details concerning the four model parameters will be provided in Section III.1.

II. Successes of Tube Theory

The Hierarchical, TMA and BoB models have shown to be quite successful in predicting the rheology of asymmetric polyisoprene stars,[19, 22] H polymers,[21, 23] pom-pom polymers,[23, 24]

comb polymers,[22, 24, 25] bidisperse linear 1,4-polybutadiene blends,[26] monodisperse star and linear polymers,[19, 24] and metallocene-catalyzed high density polyethylene.[27]

III. Failures of Tube Theory

Despite the successful rheological predictions of the TMA, BoB and Hierarchical models, limitations in tube theory, particularly the BoB and Hierarchical models, have been identified in recent works. In a study conducted by Park et al.,[28] the Hierarchical model was used to predict the linear rheology of 1,4-polybutadiene binary linear blends. For the binary blend dataset that features linears of molecular weights 36.8 kDa and 168 kDa, the Hierarchical model predictions accurately captured the experimental rheology regardless of whether α=1 or α=4/3 is assumed. However, within the same study, only the α=1 assumption resulted in model predictions that accurately captured the rheology data featuring binary blends of 20 kDa and 550 kDa linears. Although the Hierarchical model reasonably predicted the rheology of both binary linear blend cases, the prediction results are somewhat troublesome. There is no clear explanation as to why the model assumption of α=4/3 worked well for predicting the rheology of one blend, but failed for the other blend. This finding calls into question the legitimacy of selecting the value for α.

In another study conducted by Desai et. al.,[29] Hierarchical and BoB model predictions were compared against a freshly prepared 1,4-polybutadiene star-linear blend consisting of a 4-arm star of 24 kDa per arm (referred to here as "24KS," where "K" represents "kDa" and "S" represents star architecture) and a 58 kDa linear (referred to as "58KL," where "K" represents "kDa" and "L" is linear architecture). Also featured in the study are two 1,4-polybutadiene star-linear blends that were taken from literature: the 24.5KS- 7.5KL blend, which was taken from Shivokhin et al.[30] (We note that Desai et al. modeled the Shivokhin et al. data using star arm

and linear molecular weights of 27.4 kDa and 6.9 kDa, respectively, for reasons discussed in their paper.), and the 42.3KS-105KL blend that was taken from Struglinski et. al.[31] We note that both the 24.5KS and the 42.3KS are 3-arm stars. Since all three star-linear blend datasets (*i.e.*, 24KS-58KL, 24.5KS-7.5KL and 42.3KS-105KL) are of nearly identical 1,4-polybutadiene chemistry, the Hierarchical model predictions should capture the rheology of the datasets with consistent use of model parameters; however, this was not the case in practice. The model predicted accurately the rheology of the pure star and pure linear data of each star-linear blend; however, no consistent combination of model assumptions concerning the value of α, CR-Rouse relaxation, and disentanglement mechanisms (details of disentanglement mechanisms are discussed in Larson[24]), all of which were utilized in an ad-hoc manner, were able to produce successful prediction results for all three star-linear blend datasets. In addition, this model failure may be influenced by the shortcomings of dynamic tube dilation (DTD), a key physics that describes the relaxation behavior of branched molecules.

In the wake of the BoB and Hierarchical model failure in predicting the three star-linear blend datasets, Desai et al.[28] showed that a slip-model produced successful predictions of the three blends. This slip-link model, known as the "Clustered-Fixed Slip-Link Model" (CFSM), was developed by Schieber and coworkers,[32-36] and unlike the Hierarchical model, the physics of the CFSM is considered self-consistent by not having to invoke ad-hoc model assumptions to produce accurate predictions. Although, the CFSM was shown to be successful in the Desai et al. study, the model is not without fault. Most notably, the CFSM is computationally expensive since it meticulously tracks the diffusion of constraints imposed on a given polymer probe chain, which is a stark contrast to the less detailed entanglement averaging approach employed by tube models. Due to computation limits, the CFSM experiences difficulty in predicting the rheology

of polymers that have more than 19 entanglements present. Therefore, although the CFSM may be capturing physics of star-linear blends that the BoB and Hierarchical models are missing and/or misrepresenting, there is incentive to make repairs to tube models due to their advantageous computational speed.[28]

Overall, the studies conducted by Park et al.[28] and Desai et al.[29] have primarily indicated three potential aspects of BoB and Hierarchical model failure (and tube theory failure in general), which includes 1) the discrepancy of the of the dilution exponent (α) value; 2) the possible failure of dynamic tube dilation physics; and 3) the uncertainty of CR-Rouse physics. Should any of these three described points of model failure be resolved, tube models would become more robust in predicting accurately an assortment of polymer chemistries, blends and architectures.

III.1. Discrepancy of the Dilution Exponent

As noted previously, tube model simulations are implemented with the use of four material-based parameters: the plateau modulus (G_N^0), the entanglement density (M_e), the tube-segment frictional Rouse time (τ_e), and possibly the dilution exponent (α), although it is normally thought to have a universal value for all polymers. Fortunately, discrepancies concerning G_N^0 can be reasonably addressed through direct analysis of experimental rheological data. As for the M_e value, it cannot be extracted directly from experiments; however, M_e is related to G_N^0 through use of the "G" equation as described below in Eq. 1.[37]

$$G_N^0 = \frac{4\rho RT}{5M_e} \qquad (1)$$

The variables in Eq. 1 included the polymer density (ρ), universal gas constant (R), and temperature (T). Similar to G_N^0, the τ_e parameter can be directly measured from rheology

experiments or self-consistently extrapolated with use of the entanglement density, M_e, when Eq. 2 is implemented.[37]

$$\tau_e = \frac{M_e \zeta b^2}{M_o^2 3\pi^2 kT} \qquad (2)$$

The variables in Eq. 2 are the monomeric friction coefficient (ζ), statistical segment length (b), monomer molecular weight (M_o), Boltzmann constant (k), and temperature (T). Unfortunately, the remaining tube theory parameter, the dilution exponent (α), cannot be extracted from experiments as easily in comparison to the other parameters. Commonly, α is assigned a value of 4/3 or unity, depending on the version of tube theory implemented and/or polymer system to be predicted. Conceptually, when α is 1, the entanglements in a polymer melt are considered binary; experimental evidence suggesting this is found in the work of Tao, H. et al.[38] in a plot featuring polymer volume fraction (ϕ) dependence of the loss modulus maximum (G_m'') for hydrogenated (deuterated) polybutadiene solutions. This work is not considered definitive, however, since the difference between the predictions for α=1 and α=4/3 is not great in this plot and perhaps could be within the uncertainty of the experiments. Colby and Rubinstein,[39] on the other hand, assumed that multiple contacts between multiple chains is required to create a single entanglement, and used scaling relationships to derive a dilution exponent of α=4/3. This argument in favor for α=4/3 was further supported experimentally by the power law correlation arising from a plot of the polymer solution viscosity (η), scaled by the solvent viscosity (η_s) and the molecular weight to the 2/3 power, against polymer concentration, scaled by the overlap concentration (c*), for polybutadiene suspended separately in two different theta solvents: isobutyl acetate and dioxane. In addition, a similar plot featuring scaled η against scaled polymer concentration for polystyrene suspended in cyclohexane, a theta solvent, also resulted in a power law correlation in support for α=4/3. Given that the value of α is not definitive, both values have

been implemented in tube model predictions. For instance, the van Ruymbeke's TMA model[19] and the BoB model from Das et. al.[17] both assume α=1. In contrast, Larson's Hierarchical model may employ α=1 for cases of binary linear blends and monodisperse linear polymers;[28] however, the model utilizes α=4/3 for cases of monodisperse star and star-linear blends.[20, 29] Since α has been heavily influenced by tube model bias, a pathway to establishing a definitive value for α is to conduct a model-independent study.

Fortunately, a few model-independent studies for determining α already exist in literature. Recently, through an extensional flow rheology study involving a series of polystyrene melts suspended in oligomeric styrene solvent at varying concentrations, Huang et al.[40] determined that the G' and G" moduli data scaled with the polymer concentration in accordance to α=1 (*i.e.*, $G_N^0(\phi) = G_{N,o}^0\phi^{1+\alpha}$). In another study conducted by van Ruymbeke and Watanabe,[41, 42] it was shown that the linear rheology of cis-polyisoprene binary linear blends is scaled using α=1 at early relaxation times but then assume an α=4/3 at late times due to a "tension re-equilibration" process. In a sequential study, Shahid et al.[43] investigated further this apparent time-dependent transition of α=1 to α=4/3 by studying the shear rheology of linear monodisperse polymer melts that were carefully diluted by oligomer solvent, of the same chemistry, to obtain a series of concentrations that span both melt and semi-dilute conditions. Ultimately, this study concludes that both the plateau modulus and terminal relaxation time scales with polymer concentration using α=1 when the polymer solutions are considered well-entangled. However, for solution cases where the linear chains are considered weakly entangled (*i.e.*, semi-dilute polymer solutions), an α scaling that's a little higher than 4/3 is preferred due to additional relaxation modes. Shahid et al. did note, however, that a scaling greater than α=1 is

observed when polymer solutions are generated with a small-molecule solvent, even when the long-chain linear is considered well-entangled.

These studies conducted by Huang et. al.,[40] Shahid et. al.[43] and van Ruymbeke and Watanabe[41, 42] have made good progress in determining the value of α for linear polymers; however, such studies have yet to be conducted with branched polymers. As will be discussed in Section III.2, the physics of branched polymers are heavily dependent on the α value, even more so than linear polymers. Thus, there is a need address branched polymers with the same rigor that has been performed for the linear polymers.

III.2. Failure of Dynamic Tube Dilation

Due to the presence of branch points, multi-armed polymers, such as stars, are unable to undergo reptation relaxation like linear polymers. Thus, the relaxation of branched polymers must rely upon a deep contour fluctuation (CLF) process in which the arms of a given branched molecule must retract towards its branch point in order to escape entanglements imposed by neighboring molecules. However, this deep CLF process becomes increasingly isotropically unfavorable as the molecular weight of the arms increase. In a study conducted by Helfand and Pearson,[44] it was determined that deep CLF alone was not enough to capture the relaxation physics of star polymers since the observed model overpredicted the experimental rheology data. Subsequent to this finding, Ball and McLeish[15] developed a theory known as Dynamic Tube Dilation (DTD) that provides a means for accelerating the deep CLF relaxation process of star arms. DTD theory assumes that as the end of a star arm escapes entanglements through CLF, the resulting disentangled segment of the star serves as a solvent and therefore accelerates the CLF of the entangled portion of the arm that is closer to the branch point. The dilution exponent (α),

as described in the previous section, determines the effectiveness of the unentangled arm solvent in accelerating the relaxation of the segments of the star arm that are still yet entangled. When α=1, each entanglement imposed on a given star polymer arm is considered binary, whereas α=4/3 assumes multiple chains can contribute to any given entanglement. Therefore, a star polymer will relax notably faster when α=4/3 is utilized in comparison to α=1.

Unfortunately, the DTD picture is considered artificial and therefore dissimilar to the actual physics observed in branched polymers. After studying the viscoelastic and dielectric relaxation of well-entangled star polyisoprene, Watanabe et al.[45] determined that the assumptions of DTD is unable to yield model predictions that agree with both viscoelastic and dielectric experimental data. Watanabe et. al. noted that a possible source of DTD failure is related to its inability to capture the relaxation of entanglements located near the branch point of star polymers. This constraint release of entanglements near the branch point of star molecules was further explored in slip-link model studies conducted by Shanbhag et al.[46] and Cao et al.[47] Both studies suggest that these long-lived, near-branch-point entanglements are able to shuffle along the star arm towards its free end, which ultimately reduces the CLF distance of the arm for escaping the last remaining entanglements.

Therefore, prior to the failure of the BoB and Hierarchical models to predict the rheology of star-linear blends, as shown in Desai et. al.,[29] DTD physics was already under suspicion. In addition, since DTD physics of branched polymers is not consistent with the physics employed for linear polymers, obtaining reasonably accurate model predictions of star-linear blends is an even harder feat. Thus, a path forward towards correcting tube model predictions of branched polymers would be to establish physics that is both more consistent with existing linear polymer physics and is a closer representation of the branched polymer relaxation process.

III.3. Uncertainty of Constraint Release-Rouse

Originating from the work of Doi et al.[10] and Viovy et al.,[11] and further refined by Milner and McLeish,[16, 48] Larson,[24] and Park et al.,[22] Constraint Release-Rouse (CR-Rouse) was developed to coordinate with DTD for capturing the relaxation physics of binary linear blends, polydisperse linear melts, and star-linear blends. In essence, CR-Rouse describes how the long-lived entanglements of a high molecular weight polymer specie (defined as the "probe chain") are removed after the smaller polymer specie component of a binary blend has finished relaxing. In this situation, the probe chain attempts to relax out of the remaining long-lived entanglements, whose confines on the probe chain are defined by a "fat tube." However, a segment of this probe chain inevitably re-entangles locally with the smaller polymer specie; these new constraints are represented by a "thin tube," whose diameter is on order of the original tube diameter just prior to when the smaller polymer specie initially relaxed out of the system. Once this happens, there are three different CR-Rouse assumptions that can be invoked to describe the diffusion of the newly entangled probe chain segment: "arm frozen," "thin tube," or "fat tube" relaxation. When the "arm frozen" CR-Rouse criterion is assumed, the probe chain segment is unable to diffuse while confined by the thin tube. Localized diffusion of this probe chain segment may only resume after the smaller polymer specie relaxes and therefore dissipates the newly formed thin tube. However, when CR-Rouse "thin tube" is assumed, the probe chain segment is allotted some diffusive motion while confined by the thin tube. Once again, after the smaller polymer specie relaxes and dissipates the thin tube, the probe chain can relax locally. And lastly, the CR-Rouse "fat tube" assumption considers the diffusion of probe chain to be unhindered by the smaller polymer specie. In essence, any newly created entanglements imposed

by the smaller polymer specie will be destroyed at a short enough time scale that the probe chain does not "feel" the constraints of the thin tube. Therefore, the probe chain would be free to relax in the much larger fat tube of entanglements.[37]

Despite the robustness of the current CR-Rouse criteria, there has yet to be established a clear, comprehensive guideline for determining the appropriate assumption to be used for a given polymer system. Thus far, the Graessley "Gr" parameter was established to determine whether the longer polymer specie in a binary linear blend will relax by reptation or by CR-Rouse.[49] The work of Park et al.[28, 50] and Read et al.[51] have sought to further define the specifics of CR-Rouse; however, the Gr parameter can only characterized the physics of polydisperse melts and binary blends of linear architecture. No attempts have been made to expand the Gr parameter to include star-linear blends. Admittedly, the physics of star-linear blends is considerably more complicated since the existing tube theory for describing the relaxation of monodisperse star polymers, namely DTD, is notably different from monodisperse linear polymers. Evidence of this difficulty and lack of CR-Rouse selection criteria for star-linear blends is clearly observed in the work of Desai et al.[29]

Another shortcoming of CR-Rouse is that the current understanding is quite limited. For example, the work of van Ruymbeke and Watanabe[41, 42] identified a new "tension re-equilibration" relaxation process that occurs at late relaxation times for both bidisperse linear blends and polydisperse linear melts. As described in their work, tension re-equilibration defines the physics of how a polymer probe chain escapes the entanglements located near its free ends when the imposed stress in the system induces slack removal along the probe chain. Further evidence of additional CR-Rouse relaxations can be seen in the binary linear blend study conducted by Read et. al.,[52] where the thin tube confining the slow-relaxing, high molecular

weight probe chain is described to undergo contour length fluctuations (CLF) within the confines of the fat tube.

IV. Dissertation Objectives and Outline

As explained in the previous section, there are quite a few shortcomings of tube theory that need to be addressed in order to build more robust models. These shortcomings include the discrepancy in the value of α, the failure of Dynamic Tube Dilation theory, and the uncertainty of CR-Rouse physics. This dissertation attempts to address all three issues with the approaches described in the following two chapters.

In Chapter 2, we experimentally determined that α=1, not $\alpha = 4/3$, by analyzing the linear rheology of three, 1,4-polybutadiene 4-arm stars that were diluted to various concentrations with a sub-entangled linear of the same chemistry, which served as a theta-like solvent. By invoking only the model-independent assumptions of tube theory, we primarily identified α by examining the dependence of terminal crossover frequency ($\omega_{x,t}$), which was extracted from the linear rheology of the diluted 4-arm stars, on entanglement density (M_e) and comparing these results with pure 1,4-polybutadienes featured in the literature. Both $\omega_{x,t}$ and M_e were scaled to account for the star volume fraction for each blend (ϕ_s), the dilution exponent (α), and the reduction in segmental friction due to the linear polymer being sub-entangled. We also observed the influence of α on the dependence of the terminal crossover modulus ($G_{x,t}$) on M_e; however, such measurements proved $G_{x,t}$ to be insensitive to α. This study concludes with comparing Hierarchical 3.0 model predictions with the diluted 4-arm star datasets, providing further validation to the prior experimental determination that α=1. This study is in agreement with the α=1 determination for linear polymers.[40-43]

In Chapter 3, we present the most comprehensive linear rheology datasets of star-linear blends (over 50 star-linear blends are featured), where the difference in terminal relaxation times between the pure star and pure linear components are widely varied. The purpose of this study is to illuminate additional details concerning Dynamic Tube Dilation (DTD) failure and Constraint Release-Rouse (CR-Rouse) physics, as well as to serve as a rigorous benchmark for testing the accuracy of both existing viscoelastic models and models that have yet to be fully developed. For instance, in two cases of star-linear blends, where the pure linear component has a longer relaxation time than the pure star component, the experimental data revealed the presence of non-monotonicity, which features blends having longer relaxation times than both the pure star and the pure linear components. Interestingly, predictions from both the Hierarchical 3.0 model,[18] invoking the assumptions that α=1 and "thin tube" CR-Rouse, and the Branch-on-Branch (BoB) model[17] accurately capture this experimentally observed non-monotonicity. Thus, despite the failings of the Hierarchical and BoB models, particularly identified in Desai et al.,[29] there may be some physics that the current understanding of DTD and CR-Rouse is capturing correctly.

V. References

[1] Doi, M.; Edwards, S. F. Dynamics of Concentrated Polymer Systems Part 1: Brownian Motion in the Equilibrium State. *J. Chem. Soc., Faraday Trans. 2* **1978**, 74, 1789−1801.

[2] Doi, M.; Edwards, S. F. Dynamics of Concentrated Polymer Systems Part 2: Molecular Motion Under Flow. *J. Chem. Soc., Faraday Trans. 2* **1978**, 74, 1802−1817.

[3] Doi, M.; Edwards, S. F. Dynamics of Concentrated Polymer Systems Part 3: The Constitutive Equation. *J. Chem. Soc., Faraday Trans. 2* **1978**, 74, 1818−1832.

[4] Doi, M.; Edwards, S. F. Dynamics of Concentrated Polymer Systems Part 4: Rheological Properties. *J. Chem. Soc., Faraday Trans. 2* **1979**, 75, 38−54.

[5] de Gennes, P. G. Reptation of a Polymer Chain in the Presence of Fixed Obstacles. *J. Chem. Phys.* **1971**, 55, 572.

[6] Rubinstein, M. Discretized Model of Entangled-Polymer Dynamics. *Phys. Rev. Lett.* **1987**, 59 (17), 1946−1949.

[7] O'Connor, N.P.T. and Ball, R.C. Confirmation of the Doi Edwards Model. *Macromolecules* **1992**, 25, 5677-5682

[8] de Gennes, P.G. Dynamics of Entangled Polymer Solutions. II. Inclusion of Hydrodynamic Interactions. *Macromolecules* **1976**, 9 (4), 594-598

[9] de Gennes, P.G. Theory of Polymer Absorption. *J. Phys. (Paris)* **1976**, 37 (12), 1445-1452

[10] Doi, M.; Graessley, W. W.; Helfand, E.; Pearson, D. S. Dynamics of Polymers in Polydisperse Melts. *Macromolecules* **1987**, 20 , 1900−1906.

[11] Viovy, J.; Rubinstein, M.; Colby, R. Constraint Release in Polymer Melts: Tube Reorganization versus Tube Dilation. *Macromolecules* **1991**, 24, 3587−3596.

[12] Marrucci, G. Relaxation by Reptation and Tube Enlargement: A Model for Polydisperse Polymers. *J. Polym. Sci., Polym. Phys. Ed.* **1985**, 23, 159−177.

[13] Klein, J. The Onset of Entangled Behavior in Semidilute and Concentrated Polymer Solutions. *Macromolecules* **1978**, 11 (5), 852− 858.

[14] Daoud, M.; de Gennes, P. G. Some Remarks on the Dynamics of Polymer Melts. *J. Polym.*

Sci., Polym. Phys. Ed. **1979**, 17, 1971− 1981.

[15] Ball, R. C.; McLeish, T. C. B. Dynamic Dilution and the Viscosity of Star-Polymer Melts. *Macromolecules* **1989**, 22, 1911− 1913.

[16] Milner, S.T.; McLeish, T.C.B. Parameter-Free Theory for Stress Relaxation in Star Polymer Melts. *Macromolecules* **1997**, 30, 2159-2166.

[17] Das, C.; Inkson, N. J.; Read, D. J.; Kelmanson, M. A.; McLeish, T. C. B. Computational Linear Rheology of General Branch-on-Branch Polymers. *J. Rheol.* **2006**, 50 (2), 207−234.

[18] Wang, Z.; Chen, X.; Larson, R. G. Comparing Tube Models for Predicting the Linear Rheology of Branched Polymer Melts. *J. Rheol.* **2010**, 54, 223−260.

[19] van Ruymbeke, E.; Keunings, R.; Bailly, C. Prediction of Linear Viscoelastic Properties for Polydisperse Mixtures of Entangled Star and Linear Polymers: Modified Tube-Based Model and Comparison with Experimental Results. *J. Non-Newtonian Fluid Mech.* **2005**, 128, 7-22.

[20] Park, S. J.; Larson, R. G. Dilution Exponent in the Dynamic Dilution Theory for Polymer Melts. *J. Rheol.* **2003**, 47, 199−211.

[21] Milner, S. T.; McLeish, T. C. B.; Young, R. N.; Hakiki, A.; Johnson, J. M. Dynamic Dilution, Constraint-Release, and Star-Linear Blends. *Macromolecules* **1998**, 31, 9345−9353.

[22] Park, S. J.; Shanbhag, S.; Larson, R. G. A Hierarchical Algorithm for Predicting the Linear Viscoelastic Properties of Polymer Melts with Long-Chain Branching. *Rheol. Acta* **2005**, 44, 319−330.

[23] van Ruymbeke, E.; Bailly, C.; Keunings, R.; Vlassopoulos, D. A General Methodology to Predict the Linear Rheology of Branched Polymers. *Macromolecules* **2006**, 39, 6248-6259.

[24] Larson, R. G. Combinatorial Rheology of Branched Polymer Melts. *Macromolecules* **2001**, 34, 4556−4571.

[25] Ahmadi, M.; Bailly, C.; Keunings, R.; Nekoomanesh, M.; Arabi, H.; van Ruymbeke, E. Time Marching Algorithm for predicting the Linear Rheology of Monodisperse Comb Polymer Melts. *Macromolecules* **2011**, 44, 647-659.

[27] Park, S.J. and Larson, R.G. Modeling the Linear Viscoelastic Properties of Metallocene-Catalyzed High Density Polyethylenes with Long-Chain Branching. *J. Rheol.* **2005,** 49, 523-536.

[28] Park, S. J.; Larson, R. G. Tube Dilation and Reptation in Binary Blends of Monodisperse Linear Polymers. *Macromolecules* **2004**, 37, 597 −604.

[29] Desai, P.S.; Kang, B.G.; Katzarova, M.; Hall, R.; Huang, Q.; Lee, S.; Shivokhin, M.; Chang, T.; Venerus, D.C.; Mays, J.; Schieber, J.D.; and Larson, R.G. Challenging Tube and Slip-Link

Models: Predicting the Linear Rheology of Blends of Well-Characterized Sar and Linear 1,4-Polybutadienes. *Macromolecules* **2016**, 49(13), 4964-4977.

[30] Shivokhin, M. E.; van Ruymbeke, E.; Bailly, C.; Kouloumasis, D.; Hadjichristidis, N.; Likhtman, A. E. Understanding Constraint Release in Star/Linear Polymer Blends. *Macromolecules* **2014**, 47 (7), 2451−2463.

[31] Struglinski, M. J.; Graessley, W. W.; Fetters, L. J. Effects of Polydispersity on the Linear Viscoelastic Properties of Entangled Polymers. 3. Experimental Observations on Binary Mixtures of Linear and Star Polybutadienes. *Macromolecules* **1988**, 21, 783−789.

[32] Schieber, J.D. and Andreev, M. Entangled Polymer Dynamics in Equilibrium and Flow Modeled Through Slip Links. *Annu. Rev. Chem. Biomol. Eng.* **2014**, 5, 367-381.

[33] Khaliulin, R.N. and Schieber, J.D. Self-Consistent Modeling of Constraint Release in a Single-Chain Mean-Field Slip-Link Model. *Macromolecules* **2009**, 42 (19), 7504-7517.

[34] Pilyugina, E.; Andreev, M.; and Schieber, J.D. Dielectric Relaxation as an Independent Examination of Relaxation Mechanisms in Entangled Polymers Using the Discrete Slip-Link Model. *Macromolecules* **2012**, 45 (14), 5728-5743.

[35] Andreev, M. and Schieber, J.D. Accessible and Quantitative entangled Polymer Rheology Predictions, Suitable for Complex Flow Calculations. *Macromolecules* **2015**, 48(5), 1606-1613.

[36] Andreev, M.; Feng, H.; and Schieber, J.D. Universality and Speedup in Equilibrium and Nonlinear Rheology Predictions of the Fixed Slip-Link Model. *J. Rheol.* **2014**, 58, 723.

[37] Dealy, J.M.; Larson, R.G. *Structure and Rheology of Molten Polymers: From Structure to Flow Behavior and Back Again;* Hanser Gardner Publications, Inc.: Cincinnati, OH, **2006**.

[38] Tao, H.; Huang, C.; Lodge, T.P. Correlation Length and Entanglment Spacing in Concentrated Hydrogenated Polybutadiene Solutions. *Macromolecules* **1999**, 32, 1212-1217.

[39] Colby, R.H.; Rubinstein, M. Two-Parameter Scaling for Polymers in Θ Solvents. *Macromolecules* **1990**, 23, 2753-2757.

[40] Huang, Q.; Hengeller, L.; Alvarez, N. J.; Hassager, O. Bridging the Gap between Polymer Melts and Solutions in Extensional Rheology. *Macromolecules* **2015**, 48, 4158−4163.

[41] van Ruymbeke, E.; Masubuchi, Y.; Watanabe, H. Effective Value of the Dynamic Dilution Exponent in Bidisperse Linear Polymers: From 1 to 4/3. *Macromolecules* **2012**, 45, 2085−2098

[42] van Ruymbeke, E.; Shchetnikava, V.; Matsumiya, Y.; Watanabe, H. Dynamic Dilution Effect in Binary Blends of Linear Polymers with Well-Separated Molecular Weights. *Macromolecules* **2014**, 47, 7653− 7665.

[43] Shahid, T.; Huang, Q.; Oosterlinck, F.; Clasen, C.; van Ruymbeke, E. Dynamic Dilution Exponent in Monodisperse Entangled Polymer Solutions. *Soft Matter* **2017**, 13, 269−282.

[44] Pearson, D.S.; Helfand, E. Viscoelastic Properties of Star-Shaped Polymers. *Macromolecules* **1984**, 17, 888-895.

[45] Watanabe, H.; Matsumiya, Y.; Inoue, T. Dielectric and Viscoelastic Relaxation of Highly Entangled Star Polyisoprene: Quantitative Test of Tube Dilation Model. *Macromolecules* **2002**, 35, 2339-2357.

[46] Shanbhag, S.; Larson, R.G.; Takimoto, J.; Doi, M. Deviations from Dynamic Dilution in the Terminal Relaxation of Star Polymers. *Phy Rev. Lett.* **2001**, 87 (19), 199502(1) – 199502(4).

[47] Cao, J.; Wang, Z.; Likhtman, A.E. Determining Tube Theory Parameters by Slip-Spring Model Simulations of Entangled Star Polymers in Fixed Networks. *Polymers* **2019**, 11, 496-522.

[48] Milner, S.T.; McLeish, T.C.B. Reptation and Contour-Length Fluctuations in Melts of Linear Polymers. *Phys. Rev. Lett.* **1998**, 81, 725-728.

[49] Struglinski, M.J.; Graessley, W.W. Effects of Polydispersity on the Linear Viscoelastic Properties of Entangled Polymers. 1. Experimental Observations for Binary Mixtures of Linear Polybutadiene. *Macromolecules* **1985**, 18(12), 2630-2643.

[50] Park, S. J., and R. G. Larson, "Long-chain dynamics in binary blends of monodisperse linear polymers," J. Rheol. 50, 21–39 (2006).

[51] Read, D.J.; Shivokhin, M.E.; Likhtman, A.E. Contour Length Flucturations and Constraint Release in in Entangled Polymers: Slip-Spring Simulations and their Implications for binary Blend Rheology. *J. Rheol* **2018**, 62 (4), 1017-1036.

[52] Read, D.J.; Jagannathan, K.; Sukumaran, S.K.; Auhl, D. A Full-chain Constitutive Model for Bidisperse Blends of Linear Polymers. *J. Rheol.* **2012**, 56, 823-873.

Chapter 2: Determining the Dilution Exponent for Entangled 1,4-Polybutadienes Using Blends of Near-Monodisperse Star with Unentangled, Low Molecular Weight Linear Polymers

Disclosure: Text and figures in this chapter are reprinted from the manuscript- Hall, R.; Kang, B.-G.; Lee, S.; Chang, T.; Venerus, D.C.; Hadjichristidis, N.; Mays, J.; Larson, R.G. *Macromolecules* **2019**, 52 (4), 1757-1771.

I. Introduction

The 1978-1979 publications by Doi and Edwards, "Dynamics of Concentrated Polymer Systems," laid the groundwork for the "tube theory," which, with some modifications, is still commonly used to predict the viscoelastic relaxation of polymer melts. As described in that series of papers,[1-4] polymer melt relaxation is described by a representative chain (the "probe chain") escaping the entanglements with neighboring chains. These entanglements are accounted for by a mean-field "tube" confining the probe chain. A variety of mechanisms have been identified to describe the relaxation of the probe chain out of its confining tube, in particular reptation, contour length fluctuations (CLF), and constraint release (CR) by dynamic tube dilation (DTD) and by constraint release Rouse (CR-Rouse) motion. This paper focuses on dynamic tube dilation, specifically on determining the value of the so-called "dilution exponent," α. Details regarding the other relaxation mechanisms can be found elsewhere.[5-15]

DTD describes the widening of the diameter of the tube confining the probe chain as the time-dependent entanglement constraints defining this tube at some initial time disappear by motion of surrounding chains. The DTD concept was originally applied to near monodisperse

linear polymers by Marrucci[16] and then to near monodisperse star polymers by Ball and McLeish.[17] It was later incorporated into a theory for blends of near monodisperse stars with near monodisperse linear polymers (both species entangled) by Milner and McLeish[18] and then used as a crucial element in general theories for polydisperse mixtures of linear and branched chains by Larson and coworkers,[19-21] by Das et al.,[22] and by van Ruymbeke and coworkers.[23] As applied to linear bidisperse and linear polydisperse polymers, DTD occurs in response to the relaxation of lower molecular weight chains, allowing the tube containing the unrelaxed long chains to gradually explore a larger-diameter tube comprised of longer-lived constraints imposed by the higher molecular weight chains.[10, 24-26] DTD has also been used to describe the relaxation of branched polymers, including star polymers, as described by Ball and McLeish.[17] Monodisperse star polymers are unable to undergo reptation due to the extremely limited mobility of the branch point. Thus, star arms must relax by deep CLF, and this produces a very wide range of relaxation rates for highly entangled arms, with the parts of the arm closer to its free end relaxing orders of magnitude more quickly than those parts near the branch point. The fast-relaxing parts of surrounding arms move so quickly that they act as diluents for the unrelaxed portions of the test chain. Over increasing time scales, more and more of the surrounding entanglements become "diluent" for the test chain, gradually expanding the tube diameter, until the star molecule is fully relaxed.

To employ the DTD theory, the dependence of the dilution of the entanglement density on the molecular weight between entanglements $M_e(\phi_s)$ must be quantified, where ϕ_s is the fraction of the original entanglements that are still active after relaxation has rendered the rest of them diluents. Once $M_e(\phi_s)$ is specified, the plateau modulus $G_N^0(\phi_s) = \frac{4\rho RT}{5M_e(\phi_s)}\phi_s = G_{N,o}^0 {\phi_s}^{1+\alpha}$ is determined, where $G_{N,0}^0$ is the plateau modulus prior to dilution, as is the tube diameter $a(\phi_s)$ =

$a_0 M_e^{1/2}(\phi_s)$. The scaling of $M_e(\phi_s)$ with the dilution exponent, α, has been widely debated throughout literature. In general, it is believed to be given by a power law, $M_e(\phi_s) = M_{e,o}/{\phi_s}^{\alpha}$. Some sources suggest that α should be 1,[17, 27] which is consistent with viewing entanglements as discrete, mutually constraining, interactions between two chains. However, others have argued that α should be 4/3, by viewing entanglement restraints as multi-chain interactions within an entanglement volume.[28, 29] Both values of the dilution exponent α have been widely used in tube theories, with better agreement being obtained with experimental data in some cases when one takes α = 1, whereas other cases favor α = 4/3.

For example, by using the value α = 4/3, the general "Hierarchical model" deployed by Park and Larson accurately matched the experimental linear rheology of single-site catalyzed high density polyethylene;[30] as well as some 1,4-polybutadiene samples: bidispersed linear blends,[31] a nearly monodisperse star, and star-linear blends.[20, 32] However, the experimental data for a mixture of linear polymers with a very large difference in molecular weight, namely 20kDa- 550kDa 1,4-polybutadiene linear blends, required α = 1, not 4/3, to yield acceptable agreement.[31] More generally, the literature indicates that in cases of binary blends of long and short linear chains, the value α = 1 provides predictions in agreement with experiment;[31] however, if one wishes to predict the linear rheology of both nearly monodisperse linear polymers and nearly monodisperse stars for a given polymer chemistry using the same set of model parameters, one typically must use α = 4/3.[32] The inconsistency in choice of the value of α, with different values used by different researchers and even by the same researchers at different times, has for 20 years remained one of the most irksome problems in tube theory.[17, 18, 22, 31, 32, 33-37]

In recent years, progress has been made towards resolving this issue. In particular, Huang et al.[27] have found that the moduli G' and G'' of melts diluted with oligomer of the same chemistry as the melt scale with polymer concentration in a manner consistent with $\alpha = 1$. In addition, van Ruymbeke and Watanabe[38, 39] found that for binary linear blends, $\alpha = 1$ at early relaxation times, but that the *effective* value of α shifts to $\alpha = 4/3$ at late times due to "tension re-equilibration," which enables the longer chains to escape long-lived entanglements via a combination of constraint release and contour length fluctuations. This shift from α=1 to an effective dilution exponent value of $\alpha = 4/3$ was investigated further by Shahid et al.,[40] who considered long linear polystyrenes diluted with polystyrene oligomers to determine the scaling of the plateau modulus and the terminal relaxation time. They determined that good fits to the G' and G" data were provided by a version of the tube model (the time-marching algorithm, TMA) which contained both constraint release and contour length fluctuations, when using $\alpha = 1$. The apparent rubbery modulus G_δ extracted directly from the data scaled with the concentration c of long chains as c^2, in accord with the scaling expected for $\alpha = 1$ when the number Z_2 of entanglements of a long chain with other long chains exceeded around 12, but scaled as $c^{8/3}$, in accord with $\alpha = 4/3$ for $Z_2 < 12$. Since the TMA tube model predicted both regimes correctly using a fixed value of $\alpha = 1$, the apparent transition from $\alpha = 1$ to $\alpha = 4/3$ at low Z_2 could be taken to be a consequence of tension re-equilibration. A similar transition was observed in the scaling of the terminal relaxation time from that predicted using an effective dilution exponent of $\alpha = 1$ to a higher value of α at $Z_2 < 20$. The conclusion of these studies is that, at least for long linear chains mixed with their unentangled oligomers, fundamentally the dilution exponent is $\alpha = 1$; but when long chains are not highly self-entangled, additional relaxations lead to changes in *apparent* scaling laws consistent with a slightly higher value of $\alpha = 4/3$. Interestingly, Shahid et

al.[40] also observed that when mixed with a small-molecule solvent rather than an oligomer, an apparent value of α higher than unity is found even for highly self-entangled polymers.

At the same time, new light has been shed on the proper value of α for branched architectures. In a study described in Desai et al.,[41] the "Hierarchical" version of the tube model successfully predicted the relaxation behavior of a pure 24kDa star (24KS) and pure 58kDa linear (58KL) polymer using α = 4/3, but predicted very poorly the behavior of the 24KS-58KL blends. Modifications of tube theory entailing combinations of different CR-Rouse treatments, dilution exponents (α = 4/3 or 1), and entanglement thresholds did not yield consistently accurate predictions of these and other star/linear blends, using either the Hierarchical model, or another general-purpose model, the branch-on-branch "BoB" model developed by Das et al.[22] On the other hand, it was shown in Desai et al. that the "clustered fixed slip-link model" (CFSM), developed by Schieber et al.,[42] gave very good predictions of the 24KS-58KL blends, which could be attributed to its handling of constraint release dynamics. Details of the CFSM are discussed elsewhere.[42-47] For our purposes, the important point is that since the CFSM takes an entanglement to be a binary interaction between a pair of chains, the accurate predictions by the CFSM of the pure 24KS, pure 58KL, and 24KS-58KL blends suggests that the dilution exponent, α, should be unity for star polymers, linears, and blends. However, the failure of the most advanced versions of the tube model, using $\alpha = 1 \text{ or } 4/3$, to predict correctly the rheology of the blends, suggests that the tube model is not yet accurate enough to trust the fitting of its predictions to experimental data to determine unambiguously the value of α.

Thus, the value of α has remained controversial largely because it is typically assigned based on agreement of the tube model with experimental data. This confounds the accuracy (or lack thereof) of tube model physics with the value of the dilution exponent. This problem is

particularly acute for branched polymers, where existing tube models seem to be less accurate than for linear polymers. In principle, however, the dilution exponent can be measured directly by diluting the entangled polymer with a solvent that does not alter chain configurations of the entangled polymer. This can be accomplished by using either a theta solvent or a solvent that is close enough to being a theta solvent for the polymer concentration used, that the excluded volume "correlation blob" size is smaller than the "thermal blob" size.[48, 49] If this is achieved, one could in principle determine α in a "model-free" way by plotting the plateau modulus $G_N^0(\phi_s)$ against the concentration ϕ_s of entangled polymer, which should yield a power law with exponent 1+ α. Such a plot has been made,[36] but the values α = 1 or 4/3, respectively corresponding to exponents 2.0 and 2.33 for $G_N^0(\phi_s)$, are hard to distinguish with confidence in such a plot.

A property that is much more sensitive to α is the terminal time for relaxation of a star polymer. The relaxation time of a star arm is expected, and observed, to be exponentially dependent on the number of entanglements per arm, $M_a/M_e(\phi_s) \propto M_a/\phi_s^{-\alpha}$ where M_a is the arm molecular weight. Thus, if one blends a monodispersed star with an isofrictional theta-like solvent to dilute the density of entanglements, the resulting diluted star should possess nearly the same terminal time (to within a prefactor that depends weakly on molecular weight) of a lower molecular weight, non-diluted star of the same chemistry, with the same value of $M_a/M_e(\phi_s) = M_a/(M_{e,0}\phi_s^{-\alpha})$. Since the terminal relaxation time is exponentially dependent on $M_a/(M_e\phi_s^{-\alpha})$, this putative "self-similarity" or matching of terminal relaxation time will be much more sensitive to the dilution exponent α than is the modulus, which scales only as a power law $G_N^0(\phi_s) \propto \phi_s^{1+\alpha}$. However, four important caveats arise. First, one needs a theta-like solvent, in which the replacement of some of the polymer chains by the solvent does not alter the

configurations of the remaining chains. The second caveat for attainment of an equality in relaxation time is that the solvent is "isofrictional" with the polymer, so that the monomeric drag coefficient acting on the polymer is not changed by replacement of polymer with solvent. This "isofrictional" criterion is hard to meet; however, there is no need to fulfill this requirement if the change in friction produced by the addition of solvent can be accounted with reasonable accuracy. The third caveat is that the prefactor of the exponential dependence of relaxation time on $M_a/(M_e\phi_s^{-\alpha})$ be properly accounted for. The fourth caveat is that the terminal relaxation time, *or its equivalent*, be properly measured at sufficiently low frequencies where rheological data can become noisy or sensitive to small contributions from high-molecular-weight tails. The second and third caveats both deal with the frictional prefactor of the exponential dependence of relaxation time on $M_a/(M_e\phi^{-\alpha})$ and so results are not as sensitive to the accuracy with which they are accounted for, as they are to the value of α.

We propose here to determine the α value by performing a series of dilutions of star polymers with sub-entangled linear polymer of the same chemistry, where the sub-entangled linear polymer serves as an approximately isofrictional theta-like solvent, as described above. Since the "solvent" used here is itself 1,4-polybutadiene, with chemistry nearly identical to the entangled star polymers (although with slight differences in 1,2 content), this "solvent" should be approximately a theta solvent as well as approximately isofrictional. We qualify this remark by the word "approximately" because, although the monomers are chemically nearly identical to that of the star, the small size of the linear chain implies that it might have some osmotic swelling power with respect to the much larger star polymer; and the linear chain might have somewhat smaller monomeric friction coefficient, owing to a dependence of the glass transition on molecular weight, which is quite weak for well entangled polymers, but becomes more

pronounced for smaller chains. As to the swelling power of the short linear chain, we remark that our blends all contain at least 20% by volume star polymer, implying that the correlation "blob" size is quite small, likely smaller than the size of the "thermal blob." Without getting into details here, we simply note that when this is the case, the high molecular weight star chain is ideal on all length scales, and the solvent is then effectively a theta solvent even if it is not perfectly so at low star polymer concentration. This is called the "concentrated" regime, to distinguish it from the "semi-dilute" regime in which swelling of the long polymer chain occurs over length scales between that of the thermal blob and the correlation (or excluded-volume) blob. In studies of small-molecule solvents with polystyrene,[48] Heo and Larson showed that a transition from semi-dilute to concentrated solutions occurred once the concentration was raised to 20% polymer or so for a good solvent (tricresylphosphate) for polystyrene. Hence, for short 1,4-polybutadiene chains, which should have weaker swelling power for long 1,4-polybutadiene than small-molecule tricresylphosphate has for polystyrene, we expect that long polymers at concentrations of 20% or more should have nearly ideal (i.e., non-swollen) conformations.

A more important concern is the change in monomeric friction coefficient produced by dilution of the long star chains with much shorter linear chains. To evaluate such changes in friction, it is important to gather data at high frequency for a variety of temperatures, where frictional effects are most clearly distinguished from the confounding effects of entanglement dynamics. The change in the monomeric friction, along with the known scaling of the Rouse relaxation time of an entanglement segment with M_e, namely $\tau_e(\phi_s) \propto {M_e}^2 \propto \phi_s^{-2\alpha}$, allows for the effect of added solvent on the fundamental time constant of the tube model, $\tau_e(\phi_s)$, to be accounted for in a model-insensitive way.

Motivated by this background, here we present linear rheology measurements of three symmetric approximately 4-armed 1,4-polybutadiene stars diluted with a 1,000 Dalton linear 1,4-polybutadiene. These stars have arm molecular weights M_a of approximately 48 kDa, 61.5kDa and 70.1kDa, hereby referred to as StarA, StarB and StarC, respectively. Details of synthesis will be discussed below, as well as characterization using gel permeation chromatography (GPC) and temperature gradient interaction chromatography (TGIC). The quality of these star polymers is further evaluated via rheological measurements which are compared to established trends in the literature for star 1,4-polybutadiene polymers. Each of these stars is blended with nearly monodispersed 1 kDa linear 1,4-polybutadiene, hereby referred to as 1KL obtained from Polymer Source; its quality is verified via GPC and rheology. Following the preparation of the star-1KL blends, these samples are subjected to a series of small amplitude oscillatory shear rheology tests over a range of temperatures to produce viscoelastic G' and G" master curves, which are compiled using time-temperature superposition.

To determine the value of the dilution exponent α from these curves without relying on a specific tube model, and its various assumptions, and to avoid difficulties in the accurate determination of the terminal relaxation time (i.e., the fourth caveat mentioned above), we extract the low-frequency cross-over modulus, $G_{x,t}$, and frequency, $\omega_{x,t}$, from these data and plot them in properly scaled form against entanglement density $M_a/M_e(\phi_s)$ on "universal" plots for both α = 1 and α = 4/3. The validity of using the cross-over frequency $\omega_{x,t}$, rather than the terminal relaxation time, to assess the dilution exponent rests on the dependence of all tube model (and slip link model) predictions on only three non-universal parameters: a frictional time constant (such as the equilibration time τ_e), a modulus scale (such as the plateau modulus G_N^0), and the number of entanglements per chain Z. The first two of these constants set the frequency

and modulus scales of the rheology and can be removed in dimensionless plots. The parameter Z determines not only the terminal relaxation time, *but in principle also the shape* of the relaxation function (e.g., G' or G'' against frequency ω). Thus, both a rescaled terminal time τ_t/τ_e and a rescaled terminal cross-over frequency $\omega_{x,t}\tau_e$ should be a universal function of Z for any polymer architecture (such as a monodisperse star). But this universal function will depend on the value of the dilution exponent α, and, for stars diluted with a theta-like solvent, even the value of Z itself depends on α. Nevertheless, if we guess a value of α, and compute the values of Z for a series of diluted stars, the dependence of $\omega_{x,t}\tau_e$ on Z should be the same for the diluted stars as for a series of undiluted stars of various molecule weights *if we have guessed the right value of* α. We carry out this exercise in what follows for both α = 1 and α = 4/3. The results show that the α = 1 scaling of star-1KL data within the $\omega_{x,t}$ vs. $M_a/M_e(\phi_s)$ plot are in agreement with data for pure stars, whereas the α = 4/3 scaling fails. The data in the plot of $G_{x,t}$ vs. $M_a/M_e(\phi_s)$ are, not surprisingly, inconclusive due to the plot's lack of sensitivity of $G_{x,t}$ to the value of α. While our procedure requires us to perform many experiments to determine the dependence of $\omega_{x,t}\tau_e$ on Z for a variety of star concentrations, this procedure is advantageous in greatly increasing the robustness of our conclusion, since it is insensitive to random errors in characterization or rheology of individual samples, and averages out such errors. Establishing the value of α without invoking model specifics is critical considering the that the dynamic dilution theory of the tube model has had difficulty in describing simultaneously both mechanical and dielectric data for star polymers, as summarized by McLeish.[50] These results suggest that we cannot rely on good agreement between tube model predictions and star polymer rheological data to determine the appropriate value of α. After establishing the correct value of α experimentally, we also predict the blend rheological data

using the Hierarchical model, leading to reasonably good agreement with the experimental datasets for $\alpha = 1$.

II. Materials and Experimental Methods

II.1. Materials and Preparation

The three nominally 4-arm 1,4-polybutadiene star polymers (StarA, StarB and StarC) featured in this study were carefully synthesized and characterized via temperature gradient interaction chromatography (TGIC) and gel permeation chromatography (GPC) to ensure that they are nearly monodisperse, or at least that they are entirely star polymers with nearly monodisperse arm length and no linear contaminants. Details regarding the synthesis and molecular weight characterization of these 1,4-polybutadiene samples can be found below and in the Supporting Information. As an added level of inspection, the molecular weights of the star samples were further verified by fitting rheological predictions from the Hierarchical 3.0 model with experimental data resulting from small amplitude oscillatory shear (SAOS) rheological measurement. Since previous studies have shown that this model predicts the rheological response of pure star molecules well, the model can help confirm the accuracy of the molecular weight assignments from GPC and TGIC.

The linear 1,4-polybutadiene in this study has a molecular weight of approximately 1 kDa, hereby referenced as 1KL; with "K" indicating the molecular weight in kDa and "L" the linear architecture. Since the entanglement molecular weight for 1,4-polybutadiene is $M_{e,o}$ = 1.62 kDa (using the so-called "G definition"[51] of M_e), and the cross-over molecular weight to the entangled regime is 2-3 times higher than this, the 1KL sample in this study is well within the unentangled regime. This linear polymer was obtained from Polymer Source, which reported the

polydispersity as 1.1. Since this material acts as a diluent, its precise molecular weight (and molecular weight distribution) is unimportant, as long as it is unentangled with itself and we account experimentally for this linear polymer's effect on the monomeric friction coefficient of the blend.

Blends of star and 1KL samples were prepared in accordance to the procedure detailed in Desai et al.[41] The StarA-1KL blend series contains star volume fractions ϕ_s of 1, 0.6, 0.4, 0.2, and 0. The StarB-1KL series has ϕ_s of 1, 0.5, 0.4, 0.2, and 0. And finally, the StarC-1KL series has ϕ_s of 1, 0.6, 0.5, 0.4, 0.2, and 0.

II.2. Synthesis

All three 4-arm 1,4-polybutadiene stars were synthesized via anionic polymerization, high vacuum techniques and chlorosilane chemistry, using custom-made glass reactors equipped with break-seals for the addition of reagents and constrictions for removal of aliquots.[52] The synthetic procedure is given in Scheme 2.1. A non-polar solvent (benzene) was used to ensure the highest 1,4 microstructure of PBds and a linking agent (1,2-bis(dichloromethylsilyl)ethane, BMDCSE) having two chlorines instead of four ($SiCl_4$) per silicon atom, to ensure complete replacement of the chlorines by 1,4-polybutadiene chains.[53, 54] Details of the synthesis are given in the Supporting Information.

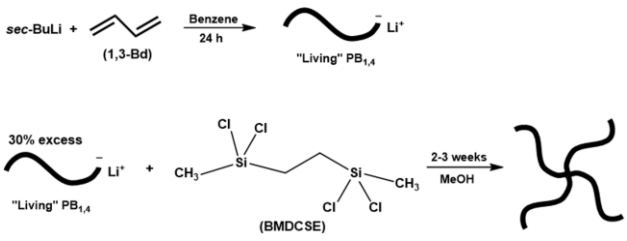

Scheme 2.1. General reactions for the synthesis of 4-arm stars 1,4-polybutadiene **(Scheme provided by Nikos Hadjichristidis)**

II.3. Characterization

The 1,4-polybutadiene stars featured in this study were characterized via gel permeation chromatography (GPC) and temperature gradient interaction chromatography (TGIC). For further verification of the arm molecular weights reported by GPC and TGIC, two separate predictions from the Hierarchical 3.0 model were generated for comparison with linear viscoelastic shear rheological data of each of the pure stars. One prediction was obtained by implementing the model with the "Park" parameter set,[20] and the other prediction was generated by utilizing the "Das" parameter set.[22] The key difference between these two parameter sets (which are given later in this paper) is that the Park parameter set utilizes a dilution exponent of $\alpha = 4/3$, while for the Das set, $\alpha = 1$. As mentioned previously in this paper, α is a parameter that characterizes Dynamic Tube Dilation, which is crucial for capturing the relaxation behavior of branched polymer architectures. Further details of the Hierarchical model and its parameter sets are given in the results and discussion section. We simply note here that for monodisperse star polymers, both the Hierarchical model and the "Bob" model are equivalent to the Milner-McLeish theory for star polymers.[33]

All three stars were intended to contain four arms, which is consistent with GPC, TGIC, and rheological characterization for StarB and StarC. However, both GPC and TGIC data for the post-fractionated StarA, shown in Figure 2.1, indicate that it is polydisperse in the number of arms per molecule. The TGIC chromatogram shows two distinct peaks, which likely correspond to stars possessing 4 to 8 arms per molecule. The associated GPC plot in Figure 2.1, which displays a broad peak indicating polydispersity, is consistent with the TGIC chromatogram. Due

to the ambiguity in the number of branches in StarA, we report in Table 2.1 the molecular weight determinations of the linear precursor arms of StarA, which are 47 kDa from GPC and 49.1 kDa from TGIC, and nearly monodisperse. We note that it is only the molecular weight of the arm that matters, not the number of arms, since both experiments and theory show that the rheology is independent of the number of star branches and of polydispersity in the number of branches, as long as there are no linear contaminants nor star species with more than 10 arms. Of this we can be confident, based not only on the TGIC and GPC chromatograms, but also on the rheological data themselves, as we shall soon see.

Shown in Figures 2.2 and 2.3 are the GPC and TGIC results for StarB and StarC, respectively. For StarB, Figure 2.2 shows that the linear precursor is almost entirely gone after fractionation. Prior to fractionation, TGIC and GPC reported for the linear precursor a molecular weight of 68 kDa. Dividing this into the molecular weight of the main peak (260k for GPC and 280k for TGIC) gives very close to four for the number of arms. No direct data on the arm molecular weight for StarC are available. But according to Figure 2.3, when we divide the molecular weight of the main peak (285k for GPC and 290k for TGIC), assuming four arms per molecule, we obtain arm molecular weights of 71.3k for GPC and 72.5k for TGIC for StarC. Note the presence of substantial side peaks in the TGIC trace for StarA in Figure 2.1 and their absence for StarB and StarC in Figures 2.2 and 2.3, respectively. Both StarB and StarC show a narrow molecular weight distribution (M_w/M_n = 1.01 to 1.03) and very little presence of side peaks, indicating a nearly pure four-arm star in each case.

In addition to these characterizations, we can estimate the arm molecular weights from application of the tube model, which has been found to fit well the rheology of pure star for a variety of 1,4-polybutadiene stars of various molecular weights.[19-21,32,41] Thus, we can also

assign the arm molecular weights of all three stars according to predictions from the Hierarchical model, using both Das and Park parameters. This gives us four ways to determine arm molecular weight: GPC, TGIC, and tube model fittings using both Das and Park parameters. As will be seen, results are very similar for all four methods of determining molecular weight.

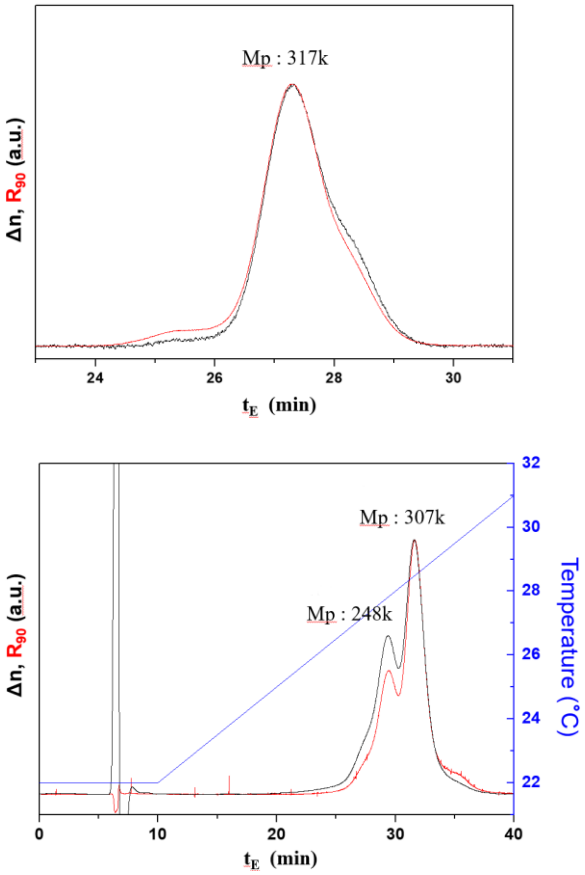

Figure 2.1: Elution profiles from gel permeation chromatagraphy (top) and temperature gradient interaction chromatography (bottom) for StarA. The y-axes are the differential refractive index (Δn), which is represented by the black line, and the light scattering intensity determined at 90° angle (R_{90}), represented by the red line. **(Figure provided by Sanghoon Lee)**

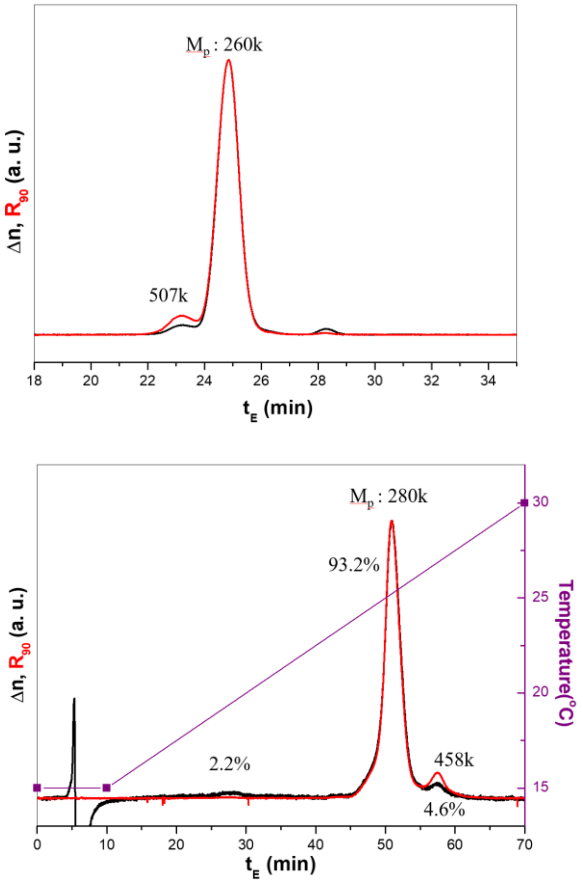

Figure 2.2: The same as Figure 2.1, but for StarB. **(Figure provided by Sanghoon Lee)**

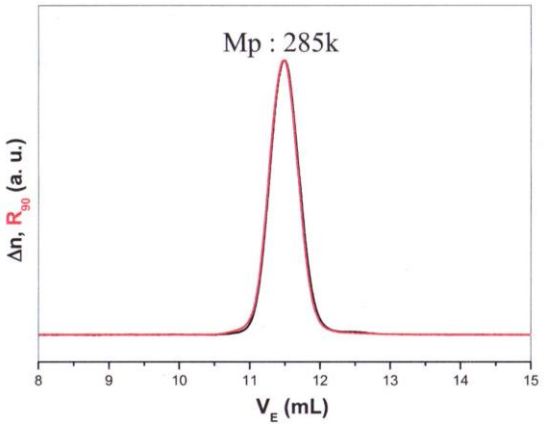

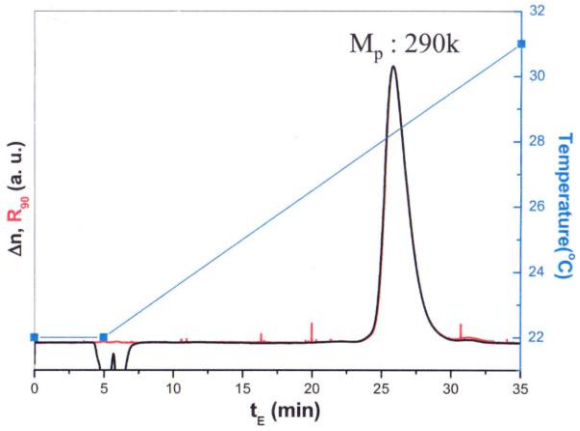

Figure 2.3: The same as Figure 2.1 but for StarC. **(Figure provided by Sanghoon Lee)**

Table 2.1 gives the star arm molecular weights reported by GPC and TGIC of our three stars, along with the arm molecular weights obtained from fitting Hierarchical model predictions, using both Park and Das parameters, to the rheology of these melts. The Hierarchical model fit for StarB will be shown below, while those for StarA and StarC are given in the Appendix. For StarA, the GPC and TGIC results are taken from the molecular weight of the precursor arm, while for StarB and StarC, the molecular weight of the star was divided by four to obtain the arm molecular weight. Table 2.1 indicates differences of up to 9 kDa among the arm molecular weights derived from GPC, TGIC and tube-model predictions. These uncertainties in molecular weight have in previous work generally limited the confidence with which such data can be used to test model predictions, especially for stars, whose rheology is extremely sensitive to arm molecular weight. Thus, to mitigate these uncertainties, here we will test our conclusions using all four of the molecular weights given in Table 1 for each polymer and will not rely on fits of the tube model predictions to rheological data to get a "best" value of α. Instead, we will use the low frequency cross-over frequency of G' and G'' and its scaling with molecular weight and dilution with low molecular weight linear polymer, for multiple star polymers, to derive a robust

conclusion regarding the exponent α that is not sensitive to the uncertainty in molecular weight of the arm.

Table 2.1: Star arm molecular weights derived from GPC and TGIC star peak for StarB and StarC and from the arm peak for StarA, as well as through fits by the Hierarchical model by using both Das and Park parameters.

	GPC (kDa per arm)	**TGIC (kDa per arm)**	**Hierarchical Park (kDa per arm)**	**Hierarchical Das (kDa per arm)**
StarA	47	49.1	50.4	48
StarB	65*	70*	65.5	61.5
StarC	71.3*	72.5*	76	70.1

* The MW was calculated by dividing the star MW by 4.

II.4. Rheology

Small amplitude oscillatory shear (SAOS) rheological measurements were performed on ARES-LS and RMS 800 rheometers to obtain linear viscoelastic G' and G" data. Tests were conducted using 25mm and 8mm parallel plates. Strain-controlled frequency sweeps, ranging from 0.1 to 100 rad/s, were performed at various temperatures from 50^{o}C to -105^{o}C. The TA Orchestrator software was implemented for analyzing the rheological data and generating master curves. A horizontal shift factor, a_T, at each temperature was obtained via the Williams- Landel-Ferry equation. A vertical shift, b_T, was implemented to account for changes in temperature only; the density of the 1,4-polybutadiene was taken as constant. The resulting master curves all have a reference temperature of 25^{o}C. The shift factors for the StarB-1KL blend series can been seen in Figure 2.5. The shift factors for the StarA-1KL and StarC-1KL blend series, along with "van Gurp-Palmen" plots that reveal the quality of the shifting, can be viewed in the Supporting Information. These plots indicate very good superposition at all temperatures except the lowest (below -85^{o}C).

III. Results and Discussion

We report in Figure 2.4 the WLF horizontal shift factors obtained through time-temperature superposition of G' and G" linear rheology data for the 1,4-polybutadiene pure StarB, StarC and 1KL (symbols). (We note that StarA is not included because this sample was depleted prior to rheological testing at temperatures below 25°C.) As discussed in Park et al.,[55] we can estimate roughly the 1,2-vinyl content of our pure stars through comparison of horizontal shift factors with those of other 1,4-polybutadienes, with varying 1,2-vinyl content, found throughout literature. The larger the 1,2 content, the higher is the low-temperature shift factor. The vinyl content of these literature 1,4-polybutadienes are shown in parentheses within the legend, along with their respective backbone architectures. In this plot, we observe the shift factors of the pure StarB superpose closely with the shift factors of a 11% 1,2-vinyl content linear reported by Palade et al.[56] Based on this observation, we estimate that the 1,2-vinyl content for the pure StarB is approximately 11- 12%. On the other hand, we observe the shift factors of pure StarC at low temperature are close to those reported by Colby et al.,[57] which report 1,2-vinyl contents of around 10%, and not far from those of Li et al.,[58] who report 5% 1,2-vinyl content . Therefore, the 1,2-vinyl content of our StarC polymer is between around 5% and 10%. Lastly, we observe a notable difference in shift factors between the pure 1KL and that of the other 1,4-polybutadienes featured in Figure 2.4, as can be expected. The pure 1KL is sub-entangled; thus, its monomeric friction coefficient is lower than the well-entangled melts, which ultimately contributes to this observed difference in shift factors. Due to this difference in the monomeric friction coefficient between the pure 1KL and well-entangled melts featured in Figure 2.4, we are unable to estimate the 1,2-vinyl content of the 1KL. However, having explicit

knowledge of the 1,2-vinyl content of the 1KL is not necessary for this study, as can be seen in what follows.

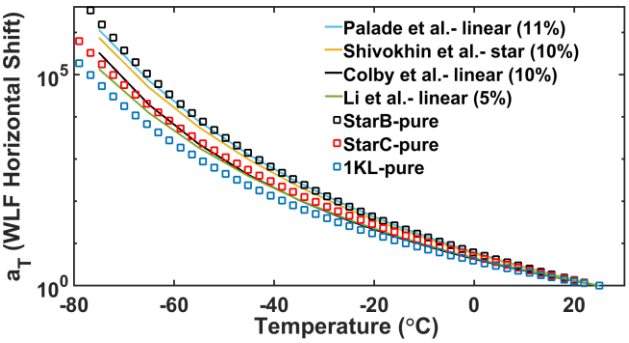

Figure 2.4: Shift factors plotted with respect to temperature given by the WLF equation with C_1 and C_2 time-temperature superposition constants reported for each of the materials. The pure stars of 1,4-polybutadiene chemistry explored in this study (symbols) are compared with other 1,4-polybutadiene polymers (lines), of varying 1,2-vinyl content, found throughout literature[55-59]. The backbone architecture (star or linear) is noted in the legend, along with their respective 1,2-vinyl content shown in parentheses. The reference temperature for this and all subsequent figures following (except for fig. 7) is 25°C.

Figure 2.5 plots the shift factors obtained through the time-temperature superposition of the StarB-1KL blend series. StarB experiences a reduction in its monomeric friction coefficient with increasing concentration of 1KL, presumably due to a reduction in the glass transition temperature, owing to the increasing number of chain ends. The effect of this becomes large at low temperatures. For instance, the horizontal shift factor for the pure StarB at -95°C is about two orders of magnitude larger than the horizontal shift factor for the pure 1KL at the same temperature.

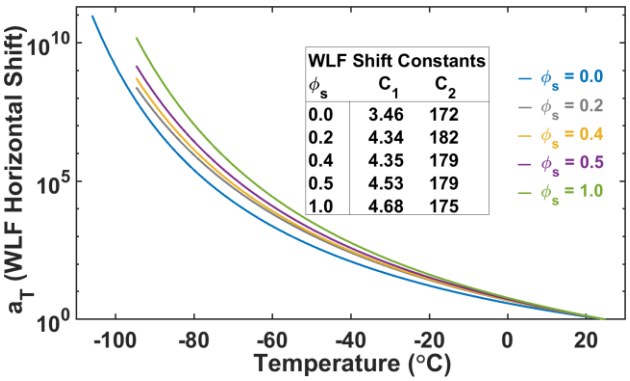

Figure 2.5: Shift factors obtained from time-temperature superposition of G' and G'' for StarB-1KL blends with various star volume fractions, ϕ_s.

Appearing in Figure 2.6 are the linear viscoelastic G' and G'' curves of the StarB-1KL blend series produced by time-temperature superposition. The presence of the 1 kDa linear chain significantly shortens the terminal relaxation time of StarB. Although the full terminal relaxation behavior for the pure StarB is not experimentally captured due to the low frequencies required to do so, the plot does capture the terminal G'/ G" frequency cross-over (ω_x), whose inverse (ω_x^{-1}) can be taken as an estimate of the terminal relaxation time. The value of ω_x increases with increasing 1KL content, with ω_x for ϕ_s = 0.5 exceeding ω_x for the pure StarB by three orders of magnitude. Also evident in Figure 2.6 is the effect of the 1KL diluent on the plateau modulus (G_N^0) of the StarB. Since it is unentangled, the short linear 1 kDa chain reduces the number of effective entanglements of the star arm by increasing the molecular weight between entanglements (M_e) following the equation: $G_N^0 = \frac{4\phi_s \rho RT}{5M_e}$, where we are here using the so-called "G" definition for M_e.[50] Note also that the pure StarB passes from the transition region to the rubbery plateau region at a higher frequency than do the StarB-1KL blends, due to the larger tube diameter of the blends and consequent larger range of frequencies over which local Rouse modes dominate the response.

The insert within Figure 2.6 features G' in the transition region to the glassy plateau, which indicates a shift to higher frequencies of the pure 1KL polymer and of the blends relative to the pure StarB as a result of the shift in the glass transition temperature alluded to above. The shifting along the frequency axis of the G' curves is roughly monotonic with star content; however, the G' curves of all blends, from ϕ_s = 0.2 to ϕ_s = 0.5, are almost coincident, although they are well separated from the curve for the pure star and, to a lesser extent, from that for the pure short linear polymer. One possible reason for the lack of a greater spread among the curves for these blends with composition in the range ϕ_s = 0.2 to ϕ_s = 0.5 might be accuracy limitations of the rheometer, which arises from two possible sources. First, the moduli values of these 1,4-polybutadiene samples near the glassy plateau are closer to the elastic modulus for the rheological tooling, which is made of steel (the elastic modulus for steel is roughly 200 GPa); thus, the tooling may experience some compliance if the strain posed on the samples is too large, which results in a reduction in G* as determined by the rheometer (although we minimized this by using 8 mm diameter plates). Second, the response of the 1,4-polybutadiene samples becomes increasingly elastic near the glassy plateau, and there is a chance that the rheological tooling may experience wall-slip with the samples. Note that testing samples near their glassy plateau requires the use of strains as low as 0.16% to help reduce wall-slip. Errors from these possible sources seem to be modest, however, since there were no obvious anomalies in the frequency-dependence of the data, other than the near overlap of data for the blends. Also, as described in the SI, the other two sets of star/linear blends show almost identical high-frequency behavior. Thus, it seems unlikely that there is any unsystematic error in our data, as might be caused by sporadic slip phenomena.

We also note here an analogous study of a 61-armed 1,4-polybutadiene star with an arm molecular weight of 47.5 kDa, hereby referred to as 47.5KS ("K" represents "kDa" and "S" represents star architecture), blended with a 1 kDa linear by Miros et al.[59] Featured in Figure 2.7 are some G' curves from their blend series, showing that blending of the 1 kDa linear polymer with the pure 47.5KS caused significant shifts of the G' curve from ϕ_s = 1.0 to ϕ_s = 0.8 to ϕ_s = 0.5, which indicates a notable change of the free volume available at the chain ends. However, increased 1KL concentration beyond ϕ_s = 0.5 did not produce significant shifts in the G' behavior. Our results are somewhat analogous to the results from Miros et. al., since we also see little shift between ϕ_s = 0.5 and ϕ_s = 0.2; however, we do see a small shift when the star volume fraction drops from 0.2 to zero, which Miros et al.[60] did not see.

From these observations, we can judge that the high-frequency data for our blends are likely quite accurate, despite some suspicions due to the near identity of the high frequency data over the composition range ϕ_s = 0.2 to ϕ_s = 0.5. Since the curves shift along the frequency axis by a total of a factor of three over the entire composition range from ϕ_s = 0 to ϕ_s = 1, we can, in all probability, assess that any error is significantly less than a factor of two shift along the frequency axis. While the behavior of the polymer in this glassy region is not the focus of this study, we will use the high-frequency cross-over of G' and G'' to correct for changes in monomeric friction coefficient in our analysis of the composition dependence of the terminal frequency cross-over below. Hence, we take note here of the magnitude of possible error in the high-frequency rheology and show below that a possible error of a factor of two would not change the conclusions of our work.

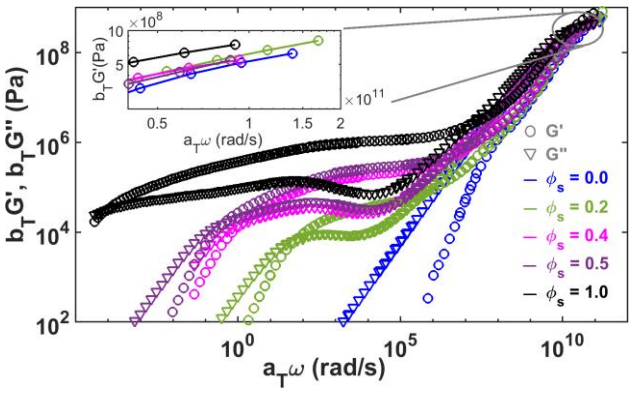

Figure 2.6: G' and G" for the StarB-1KL blend series, obtained via time-temperature superposition. The insert expands the high frequency region for G'.

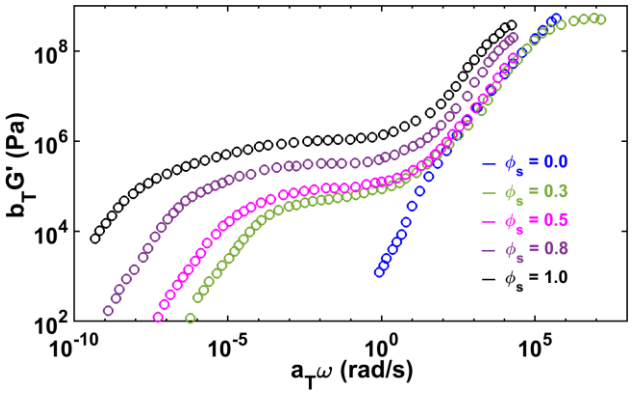

Figure 2.7: Experimental G' curves for the 47.5KS-1KL blend series at a reference temperature of -83°C, obtained from Miros et al.[60]

We now seek to use the data of Figure 2.6 and the analogous data for the two other blend series to determine the dilution exponent independently of details specific to a particular tube model. To do so, we focus on the scaling of the terminal regime with entanglement density, tuned by a combination of arm molecular weight and star volume fraction. To avoid invoking modeling details, we use only the scaling of the three tube parameters with star concentration, namely the plateau modulus (G_N^0), the entanglement molecular weight (M_e), and the equilibration time (τ_e). As a metric of the horizontal and vertical shifting of the terminal regime, we take the low-frequency cross-over modulus $G_{x,t}$ and frequency $\omega_{x,t}$ at which the G' and G'' curves

intersect in onset of the terminal regime. While it is expected that the inverse of the terminal relaxation time $1/\tau_1$ differs from $\omega_{x,t}$ to a degree that depends on the molecular weight and concentration of polymer, tube theories generally imply that the product $\omega_{x,t}\tau_1$ depends only on the number of entanglements per chain Z, whether this is reduced by reducing molecular weight or concentration of the polymer. Hence, our method of scaling described below should in principle apply equally well to either $\omega_{x,t}$ or to τ_1. Note that this conclusions rests on the assumption that the only three material-dependent parameters controlling the linear rheology are G_N^0, τ_e, and Z. The possibility that this might not be the case is discussed at the end of the paper. As noted previously, since the 1KL is sub-entangled and shares the same chemistry as the pure StarB, the 1KL is here treated as a theta solvent, which means that we can simply scale the tube model parameters, using the dilution exponent, according to equations 1-3 below.

$$G_N^0(\phi_s) = G_{N,o}^0 \phi_s^{1+\alpha} \quad (1)$$

$$G_N^0(\phi_s) = G_{N,o}^0 \phi_s^{1+\alpha} \quad (1) M_e(\phi_s) = \frac{4\phi_s \rho RT}{5G_N^0(\phi_s)} \propto \phi_s^{-\alpha} \quad (2)$$

$$\tau_e(\phi_s) = \frac{M_e(\phi_s)^2 \zeta(\phi_s) b^2}{M_o^2 3\pi^2 kT} \propto \frac{\zeta(\phi_s)}{\zeta_0} \phi_s^{-2\alpha} \propto [\omega_{x,g,0}/\omega_{x,g}(\phi_s)]\phi_s^{-2\alpha} \propto \phi_s^{-2\alpha}/\Omega_{x,g,ratio} \quad (3)$$

The variables in Eq. 2 are the entanglement molecular weight (M_e), polymer density (ρ), gas constant (R), temperature (T), and the plateau modulus (G_N^0), which is given in Eq. 1. Once Eq. 2 has been solved, the resulting entanglement molecular weight can be used in Eq. 3 to solve for the equilibration time (τ_e), which also involves the monomeric friction coefficient (ζ), statistical segment length (b), monomer molecular weight (M_o), Boltzmann constant (k), and temperature (T). After rescaling the equilibration time of the melt to account for the star volume fraction using the factor $\phi_s^{-2\alpha}$, an additional correction must be applied to account for changes in

the monomeric friction coefficient due to the presence of the 1KL. As can be seen in Figure 2.6, the presence of the 1 kDa linear chain horizontally shifts the experimental G' of the blends to higher frequencies due to the reduced monomeric friction coefficient. Therefore, in addition to rescaling the melt equilibration time by the factor $\phi_s^{-2\alpha}$, it must also be multiplied by the ratio of monomeric friction coefficients of the solution to the melt $\frac{\zeta(\phi_s)}{\zeta_0}$, as shown in Eq. 3. Since the high-frequency cross-over frequency should be proportional to the inverse of the monomeric friction coefficient, to obtain the equilibration time of the blend from that of the pure star, we must divide the latter by the glassy frequency cross-over ratio, $\Omega_{x,g,ratio} \equiv \omega_{x,g}(\phi_s)/\omega_{x,g,o}$ which is the ratio of the glassy cross-over frequency of the respective star-1KL blend to that of the pure star. This scaling allows us to horizontally shift experimental data to correct for changes in monomeric friction coefficient, owing to dilution with the 1KL linear polymer.

We note that there is an alternative to using the high-frequency cross-over frequency to determine the shift in the rheological curves due to the effect of dilution with 1KL linear polymer. We could instead use the curve of shift factor versus temperature near the reference temperature to determine an "isofrictional temperature," and plot data shifted to this temperature for each blend. That is, we can use WLF plots of the shift factor versus temperature for each blend, and find the shift in temperature "ΔTg" needed for each blend to map the blend shift factor plot onto that of the pure star. This, in principle allows us to shift data for each blend to a temperature that is theoretically the same distance from the glass transition temperature as for the pure star. This should correct for the change in Tg produced by the blending with 1KL linear polymer, for each blend, without needing the high-frequency data to determine the shift. This "isofrictional" temperature shifting is especially useful for high-Tg polymers, such as polystyrene, for which a single master curve, extending into the glassy region, is not possible.

Such as method was used, for example, by Wagner.[61] We carry out a similar analysis here, presented in the Appendix, and find, again, that superposition of terminal frequency $\omega_{x,t}$ is achieved for α= 1, and not for α = 4/3. The similarity of the result obtained using an isofrictional temperature analysis to that obtained by shifting using the high-frequency cross-over is not surprising since 1,4-polybutadiene obeys time-temperature superposition much better across a wide range of frequencies into the glassy region than does polystyrene, for example.

Figure 2.8 plots the terminal cross-over modulus ($G_{x,t}$) vs. the effective number of entanglements per star arm, scaled in accordance with Eq. 1 to account for the dilution effects of the 1KL polymer. The arm molecular weights of the new stars featured in this study are taken from fitting the Hierarchical model implemented using Das parameters, as mentioned earlier and given in Table 2.1. Use of the other molecular weights in Table 2.1 yield similar plots. Along the x-axis, the effective number of entanglements is obtained by scaling $M_{e,o}$, which is the entanglement molecular weight of the pure star, with $\phi_s^{-\alpha}$ and taking $M_{e,o}$ = 1.62 kDa. The scaling was done for both α = 1 and α = 4/3, with solid lines in Figure 2.8 linking the data scaled using α = 1 and dashed lines for those scaled using α = 4/3. There is of course no need to apply any scaling for data sets for the pure stars (given by solid symbols) from our work and from the literature.[35, 41, 59, 62-64] From Figure 2.8, the data for the blends (open symbols) favor either of the α values, α = 1 and α = 4/3, approximately equally. Therefore, we conclude that the dependence of $G_{x,t}$ on M_e does not provide enough sensitivity to the small difference in α values to determine which value is preferred. Although not shown, plots generated from star arm molecular weights reported from GPC, TGIC and the Hierarchical model Park parameters prediction, as given in Table 2.1, lead to the same conclusion.

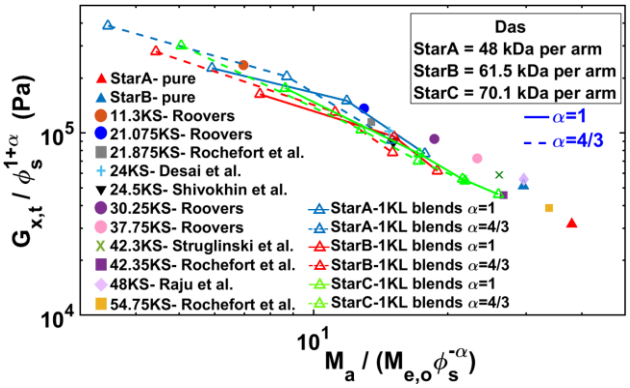

Figure 2.8: Terminal cross-over modulus plotted against the effective number of entanglements per star arm, with both axes scaled appropriately for the concentration of star ϕ_s, taken from the experimental data for the star-1KL blends featured in this paper (open symbols), as well as from pure 1,4-polybutadiene stars (ϕ_s= 1) from our work and from the literature (closed symbols).[35, 41, 59, 62-64] For each polymer, the arm molecular weight is given by the numerical value in the legend. The pure-star arm molecular weights of the new stars in our study (StarA, StarB, StarC) are given by fits to predictions made with the Hierarchical model implemented with Das parameters. For the blends, two versions of each data point are given; the points obtained using α = 1 are connected by solid lines, while those for α = 4/3 are connected by dashed lines. The number of entanglements is obtained by dividing the arm molecular weight by the entanglement molecular weight, which for pure stars is taken as $M_{e,o}$ = 1.62 kDa.

The ambiguity in determining α from the composition dependence of $G_{x,t}$ motivates examining the dependence of terminal cross-over frequency, $\omega_{x,t}$, on the effective number of entanglements per star arm, which is featured in Figure 2.9. This plot is generated using star arm molecular weights defined by fits of the Hierarchical model using Das parameters. Figures 2.10-2.12 are similar plots developed based on the other estimates of molecular weight given in Table 1. (Readers who prefer to rely on experimental characterization of molecular weight should feel free to ignore results in Figures 2.9 and 2.10, which are based on fits to the tube model.) Also, the effective number of entanglements is scaled in the same way as in Figures 2.8, where $M_{e,o}$ is taken as 1.62 kDa. To properly scale the vertical axis, $\omega_{x,t}$ must be adjusted to account for the reduction in the monomeric coefficient caused by the presence of the 1KL in the star-1KL blends. As shown in Figure 2.6, the presence of the 1KL causes the glassy plateau cross-over for

the StarB-1KL blends to shift to roughly three-fold higher frequencies with respect to the pure star. Therefore, in Figure 2.9, the terminal cross-over frequency of each blend is divided by the ratio of the cross-over frequency near the glassy plateau of a given blend to that of a pure star, $\Omega_{x,g,ratio}$, as discussed earlier; see Eq. 3. In addition, as described above, $\omega_{x,t}$ needs to be corrected for changes in τ_e due to the dilution effects of the 1KL in the star-1KL blends, again according to Eq. 3. With these corrections, unlike the results in Figure 2.8, Figure 2.9 displays a clear distinction (a decade difference along the y-axis) in the star-1KL blend scaling between α = 1 vs. α = 4/3, with the blend data clearly superimposing better onto the pure star data when α = 1 (solid lines) than when α = 4/3 (dashed lines). We note that these results are robust. Even if we do not account for changes in the monomeric friction coefficient through the use of $\Omega_{x,g,ratio}$ for the scaling of the terminal cross-over frequency, the conclusion that α = 1 coalesces the data better than does α = 4/3 would still stand. We also note that each of the three blend series, those involving StarA, StarB, and StarC, show the same clear superiority of α = 1 over α = 4/3. Thus, if the blue open symbols in Figure 2.9, which are data from StarA, whose characterization might be questioned (as discussed above) are ignored, the conclusion that α = 1 provides the clear best fit remains solid. We note that there is substantial scatter in the data in Figures 2.9- 2.12, substantially exceeding the estimated maximum error (factor of two) in the value of $\Omega_{x,g,ratio}$. This additional scatter is likely due to random errors in characterization, some impurities in the sample, and/or errors in rheometry. However, such errors, if random, do not undermine the conclusion we draw here, since we only rely on the overall superposition of blend data on top of pure star data to establish the correct value of α. Deviations of results for individual samples are averaged out by our procedure, again showing the robustness of our method.

Thus, plotting the rescaled terminal cross-over frequency against entanglement length clearly establishes $\alpha = 1$ as the only value of the dilution exponent consistent with any version of the tube model. This conclusion is independent of the particular tube model chosen, since any such model has behavior that is universal when plateau modulus and entanglement time are used to scale the modulus and time scales with the number of entanglements per chain as a sole parameter. Not only does Figure 2.9 establish the correct dilution exponent for the tube model (at least when applied to star polymers), but the value $\alpha = 1$ also is the only value consistent with slip-link models that treat slip-links as entanglement interactions between two chains. Thus, had our results for blends not coalesced with those for pure stars when using $\alpha = 1$, then our blend data would not be consistent with typical slip-link models.

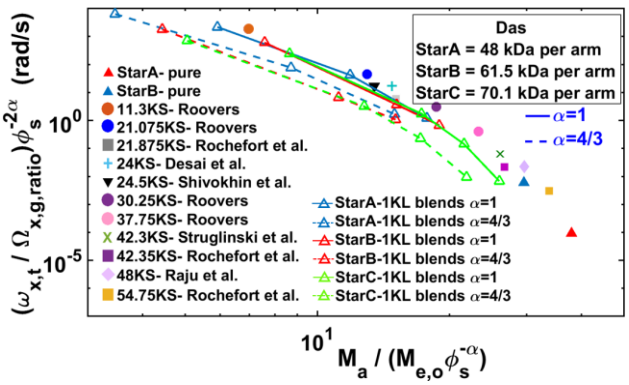

Figure 2.9: The rescaled terminal cross-over frequency vs. the effective number entanglements of experimental star-linear data using the molecular weights determined by fitting of the Hierarchical model with Das parameters to the pure melt data for StarA, StarB, and StarC. In addition to rescaling to account for the concentration of star, the change in friction due to the short linear chain is scaled out using the ratio $\Omega_{x,g,ratio}$ of the cross-over frequencies near the glassy plateau of the blend to that of the pure star, as discussed in the text. Other details are the same as in Figure 2.8.

To test the sensitivity of our conclusion to characterization errors, we replot in Figures 2.10- 2.12 our star-1KL blend data from Figure 2.9, using arm molecular weights of the pure

stars resulting from TGIC, GPC and Hierarchical model predictions implemented with Park parameters, as given in Table 2.1. For each Figure 2.9- 2.12, we observe that α = 1 gives clearly the superior agreement with melt data. Thus, our conclusion is independent of the uncertainties in the arm molecular weights reported by our characterization approaches. Moreover, any one of the three star blend series suffices to draw the same conclusion, and hence the ambiguities and uncertainties in our characterizations are very unlikely to undermine the conclusion that only α = 1 can properly account for the dilution effect.

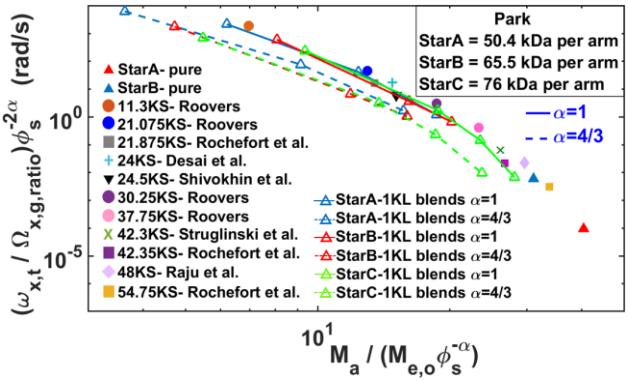

Figure 2.10: The same as in Figure 2.9 except that the molecular weight assignments for Stars A, B, and C were obtained from fits of the pure melt data to the Hierarchical model with Park parameters.

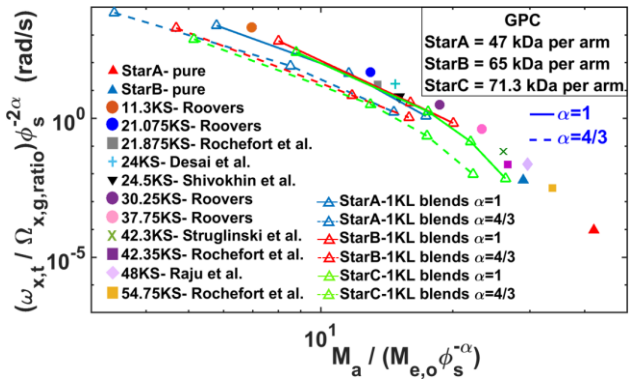

Figure 2.11: The same as in Figure 2.9 except that the molecular weight assignments for Stars A, B, and C were obtained from GPC analysis.

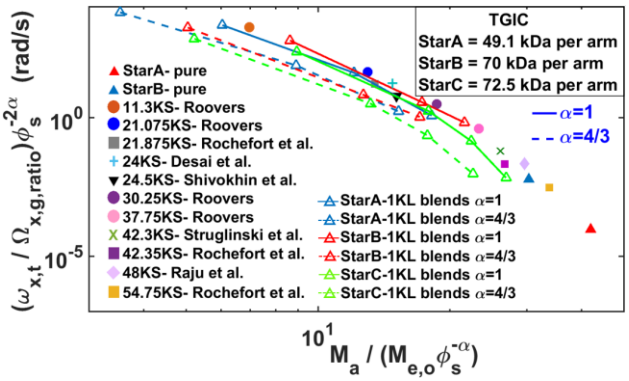

Figure 2.12: The same as in Figure 2.9 except that the molecular weight assignments for Stars A, B, and C were obtained from TGIC analysis.

As additional evidence that α = 1 provides the correct scaling, we compare in Figure 2.13 the scaled G' and G'' curves for the blend StarB-1KL ϕ_s = 0.4, which are represented as red lines, with those for a pure 30.25KS that are shown as symbols. This 30.25KS, which was taken from Roovers,[62] has almost the same value of number of entanglements per star arm as in the StarB-1KL blend with ϕ_s = 0.4, if α = 1. Figure 2.13 shows agreement in both the terminal and plateau regions between the pure 30.25KS and the StarB-1KL blend data scaled using α = 1. Note that the high-frequency upturn in G'' occurs at lower frequency in the blend than in the pure 30.25KS because the linear polymer present in the blend (but absent in the pure star) begins to contribute to the rheology in this regime. We show some evidence of this by subtracting away the 1KL contribution to the blend, as indicated by the grey line. The 1KL subtraction yields negligible difference in the profile of the StarB blend in the terminal regime and at lower frequencies of the plateau region. However, as we approach frequencies at which Rouse modes begin to dominate the relaxation, we observe a deviation between the original G" data for the blend and that with the 1KL data subtracted. While we cannot use the pure star to prepare an analogous plot using α = 4/3, since the entanglement molecular weight would not agree with that

of the blend if α = 4/3, we will show below other plots that indicate the failure of α = 4/3 to provide agreement between Hierarchical model predictions and the linear rheological data.

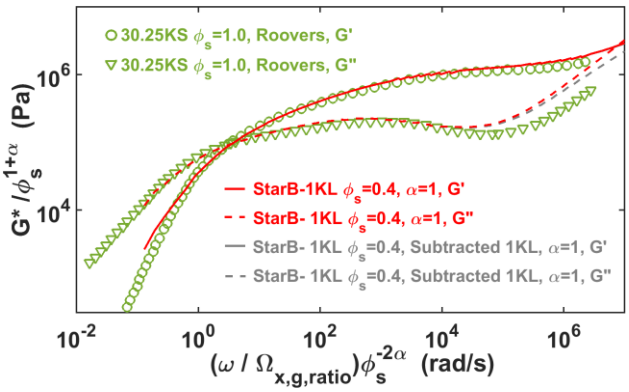

Figure 2.13: G' and G'' curves for the StarB-1KL ϕ_s=0.4 blend scaled using α=1 (red lines). Contributions from the 1KL are subtracted (gray lines) from the scaled StarB blend for comparison. Also featured are unscaled data for a pure 30.25KS (light blue symbols) of Roovers.[62] The y and x axes for the blend are scaled in accordance to Eqs. 1 and 3, respectively.

We now compare our experimental results with viscoelastic predictions of the Hierarchical 3.0 model for one of the three sets of blends. These comparisons will show that, while the model does not give perfect agreement with the data, the terminal behavior of the blends are generally fitted significantly better using α = 1 than using α = 4/3, consistent with the findings reported above. There are two parameter sets commonly used within the Hierarchical and other tube models for 1,4-polybutadiene melts at 25°C: those of Park et al.[20] and of Das et al.[22] Each parameter set is comprised of four key variables: the equilibration time (τ_e), the plateau modulus (G_N^0), the entanglement molecular weight (M_e), and the dilution exponent (α). For details concerning the origin of the Park and Das parameters, please consult Wang et al.[21] The Park parameter set uses α = 4/3, whereas that of Das uses α = 1. The density values for 1,4-polybutadiene needed to obtain the corresponding Park and Das entanglement molecular weights

from the plateau moduli using $G_N^0 = \frac{4\rho RT}{5M_e}$ differ slightly: 894 kg/m^3 for Park parameters and 899 kg/m^3 when solving for Das parameters. The Park equilibration time requires that the value for the monomeric friction coefficient to be 5.08e-11 kg/s, whereas for the Das parameters it is ζ = 2.94e-11 kg/s. Note that for both Park and Das parameters, the equilibration time was determined by fitting rheology data for linear or star 1,4-polybutadienes, and the friction coefficients are not available other than by backing them out from Eq. 3, using the fitted τ_e.

Featured in Figure 2.14 are the rheological data for the pure 1 kDa linear polymer along with a comparison of Hierarchical model predictions (lines) of the pure StarB sample with the experimental rheological data for this star (symbols). The legend within the figure lists the Park and Das parameters for a pure star. We observe that both the Das and Park parameters are able to capture the terminal relaxation of the pure star; however, the molecular weights were adjusted to obtain these fits in each case. The Park parameters require an arm molecular weight of 65.5 kDa, whereas the Das parameters require 61.5 kDa. These Das and Park molecular weights are the values given in Table 1 and were used in Figures 2.9 and 2.10. This difference in these molecular weights is primarily caused by the dilution exponent used: the Park parameters uses α = 4/3, whereas the Das parameters uses α = 1. We utilize these two different molecular weights to fit the rheological data for the pure StarB in order to have an unbiased basis for assessing the accuracy of the predictions for each value of α when unentangled linears are blended with the pure star. We note that the fits using the Das and the Park parameters are almost equally good for the pure star and that the difference in the Das and Park molecular weights required for these fits is only 4 kDa, which is within the error of the characterization of these stars. This comparison in Figure 2.14 illustrates well the futility of trying to ascertain the value of α from fits of tube model predictions to one or even several different polymers: small differences in molecular

weight, that are well within experimental uncertainty, can easily skew the conclusion regarding the proper value of α. Thus, the conclusion drawn from directly diluting the melt is much superior to that obtained by fitting a particular tube model to the data for pure melts. The latter depends on the accuracy of the molecular weight assignment and the accuracy of the particular tube model used, while the former only depends on scaling laws for the tube parameters and not on model details, or even on the precise value of the molecular weight. Lastly, we want to mention that no Hierarchical predictions were made for the pure 1KL in Figure 2.14 because the Hierarchical model fails to account for the combination of Rouse and glassy modes that dominates the relaxation of such low molecular weight melts.

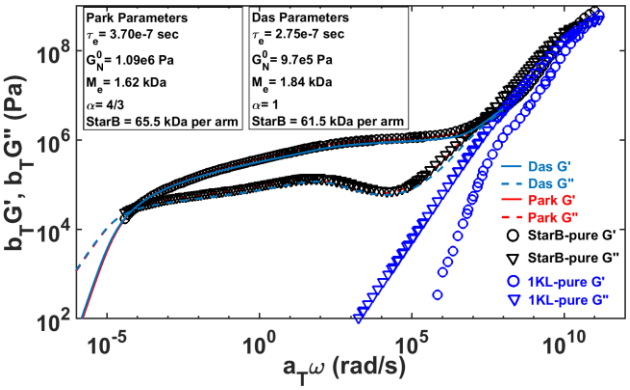

Figure 2.14: Hierarchical model predictions of Park (red lines) and Das (blue lines) of pure StarB data (black symbols). The inserted legend lists the Das and Park parameters of the pure star. Also plotted are the viscoelastic curves of pure 1KL data (blue symbols).

Featured in Figures 2.15- 2.17 are predictions and data for StarB-1KL blends of star volume fractions (ϕ_s) 0.5, 0.4, and 0.2, respectively. The comparison of Hierarchical predictions with experimental data for the StarA-1KL and StarC-1KL blends can be found in the Supporting Information. These figures, including Figures 2.15- 2.17 and those in the SI, show that the terminal cross-over frequency for the blends is always better predicted when using the Das data

set with α = 1 than when using α = 4/3. Also shown in Figures 2.15- 2.17 are experimental data with the influence of 1KL subtracted out. This is done to assess the experimental data independently of the 1KL contribution to the Rouse and glassy modes. As mentioned earlier, the Hierarchical model is unable to predict the relaxation behavior of the 1KL melt or its contribution to the rheology of the star polymers because the model does not account for the combination of Rouse and glassy modes, which is a dominating feature of the 1KL. The 1KL is removed from a given StarB-1KL blend by first horizontally shifting the 1KL relaxation moduli so that the high-frequency glassy cross-over superimposes on that of the StarB-1KL blend in question. Then, the 1KL moduli are multiplied by the volume fraction of 1 KL linear polymer comprising the StarB-1KL blend in question. The resulting 1KL relaxation moduli are then subtracted from the respective StarB-1KL blend data. The same procedure was used for Figure 2.13, discussed earlier.

In Figure 2.15, the rheological data after subtracting the 1KL contributions deviates from the original experimental data in the region near the onset to the glassy plateau, where the subtraction produces a factor of two shift in the G' and G" moduli along the y-axis. The difference between the data with the 1KL rheology subtracted and those of the uncorrected StarB-1KL blend becomes minimal at frequencies below that of the middle cross-over of G' and G'', where the Rouse modes gain dominance over the glassy modes with decreasing frequency. Upon entering the plateau region, there is no difference between the subtracted 1KL and the blend data. Also in Figure 2.15, the Hierarchical model with Das parameters yields predictions that are in reasonable agreement with the experimental StarB-1KL ϕ_s = 0.5 data in the terminal and plateau regions and also captures the Rouse modes of the experimental data after the influence of the 1KL is subtracted out. However, there is some discrepancy between predictions

with the Das parameters and the experimental data in the plateau region. The Park parameters give no better predictions in this region and under-predict the terminal relaxation time by almost an order of magnitude. The Das and Park parameters used in Figures 2.15- 2.17 are obtained from the values for the melt, given in Figure 2.14, by applying to these melt values the scaling formulas in Eqs. 1-3, with the appropriate value of α, including the adjustment for change in friction, yielding the values given in the legends in Figures 2.15- 2.17.

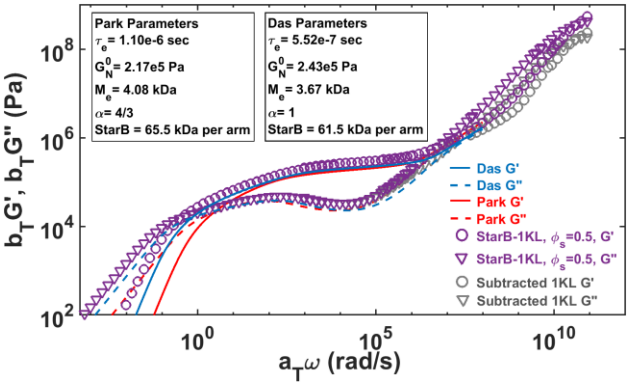

Figure 2.15: Scaled Hierarchical model predictions using Park (red lines) and Das (blue lines) parameters compared to data (symbols) for 50% StarB with 1KL. Predictions use scaled parameters given in the legends, with plateau modulus $G_N^0(\phi)$, entanglement molecular weight $M_e(\phi)$ and equilibration time $\tau_e(\phi)$ obtained from Eqs. 1-3, with α = 4/3 for Park parameters and α = 1 for Das parameters, and the parameters for the pure melt given in the legend to Figure 2.14. Also featured are experimental results with the influence of the 1KL linear subtracted from the original experimental data, as described in the text (gray symbols).

Similarly to Figure 2.15, Figure 2.16 shows that the difference between the data with 1KL contribution subtracted and the original StarB-1KL ϕ_s = 0.4 blend data is most notable in the Rouse and glassy mode regions, with a difference slightly greater than a factor of two near the glassy cross-over. This deviation between the two sets of curves extends over a larger frequency range than in Figure 15, which is due to the increased volume fraction of the 1KL in the ϕ_s = 0.4 blend.

For neither the Das nor Park parameters do the Hierarchical predictions in Figure 2.16 agree well with the experimental data. However, in the terminal regime, the Park predictions deviate from experimental terminal data by at least one order of magnitude along the x-axis, while for the Das parameters, the deviation is significantly less than this. The plateau modulus for both predictions is too low. Both predictions within the plateau region deviate from experimental data by roughly 30% along the y-axis. However, predictions for both Park and Das parameters are in reasonably good agreement within the Rouse region near the intermediate cross-over with the data for which the 1KL contribution has been subtracted.

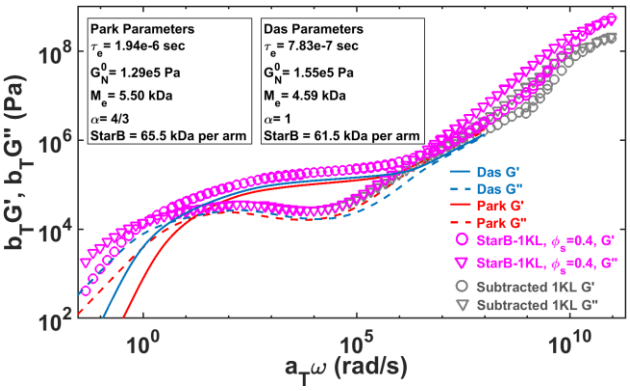

Figure 2.16: The same as in Figure 2.15, except for the 40%S-60%L blend.

Since the volume fraction of linear polymer for the StarB-1KL blend series is largest for the ϕ_s=0.2 blend, the difference between the subtracted 1KL plot and the ϕ_s = 0.2 is more notable in Figure 2.17 than for the blends featured in Figures 2.15 and 2.16. Near the glassy plateau, the data with 1KL rheology subtracted deviate from the original blend by at least a factor of three along the y-axis. In addition, the frequency range over which these two data deviate from each other is notably larger than in Figures 2.15 and 2.16. The predictions using Das parameters are in better agreement with the experimental data for which the 1KL data were

subtracted both in the regime dominated by local Rouse modes and in the terminal regime. Predictions using the Park parameters, on the other hand, capture the Rouse modes but fail to capture the terminal relaxation and show a horizontal shift of almost a decade along the x-axis in the terminal region. Note that these comparisons between the predictions using α = 1 and α = 4/3 are "fair" comparisons since the molecular weight of the star arm was adjusted for each value of α, so that equally good predictions were obtained for the pure stars, as shown in Figure 2.14. Given equal chances to succeed, the value α = 4/3 fails notably when the best-fit value of molecular weight is taken for each value of α in the melt. Figures 2.15- 2.17, along with Figures 2.9- 2.13, strongly suggest that the Das parameters, with α = 1, provide better predictions in the terminal regime than do the Park parameters, for which α = 4/3. However, neither prediction is perfect, owing to either imperfect synthesis or characterization, and/or deficiencies in the tube model used for the predictions. These deficiencies only serve to emphasize once again the importance of the use of the scaling plots in Figures 2.9- 2.12, which provide a robust test of the value of α. Best-fits of tube model predictions to one or a few sets of star or linear rheological data cannot overcome the uncertainties introduced by unavoidable limitations in synthesis and characterization, the parameter values, and the tube model itself.

One might argue that the proper dilution exponent to use when the dilution is gradual, or "dynamic," as envisioned in the original theory, is different from that for "static" dilution as we have explored here, where the diluting effect is due to addition of an unentangled species. A hint that this might be the case can be found in Matsumiya et al.,[64] who showed (in the Appendix) that there are differences in the ratio of constraint-release time to terminal time of linear polystyrene and linear polyisoprene at fixed number of entanglements Z. This implies that the three parameters G_N^0, τ_e, and Z are not the only material-dependent parameters controlling

relaxation of entangled polymers, but that the constraint-release dynamics are governed by an additional material-dependent property. Conceivably, this non-universal additional parameter might affect dynamic dilution and its exponent while leaving the static dilution exponent at □ = 1. Based on the work of Shahid et. al.[40] discussed in the Introduction, we acknowledge that the *effective* value of α as measured by the height of the modulus may increase from α = 1 to α = 4/3 if the entanglement densities of linear architectures are reduced by dilution to low enough values. This shift in the effective dilution exponent is attributed by Shahid et al. to relaxation mechanisms that reduce the modulus when the chains have limited numbers of entanglements, and not to any deviation in the true value of α from α = 1. Thus, in the work of Shahid et al., the shift in scaling of modulus to that corresponding to an effective value of α = 4/3 appears at a critical number of entanglements per chain, not at a critical dilution level. Because we plot our cross-over frequencies $\omega_{x,t}$ against the diluted number of entanglements per arm $M_a/(M_e\phi^{-\alpha})$, such a change in the *effective* α from unity would not cause any failure in superposition of the data, but only in the dependence of $\omega_{x,t}$ on $M_a/(M_e\phi^{-\alpha})$. More research into branched polymer relaxation, and an improved tube model for star polymers, is likely needed to determine if there is a shift in the *effective* dilution exponent from α=1 to α=4/3 for star polymers at low entanglement densities, as there is for linear ones.

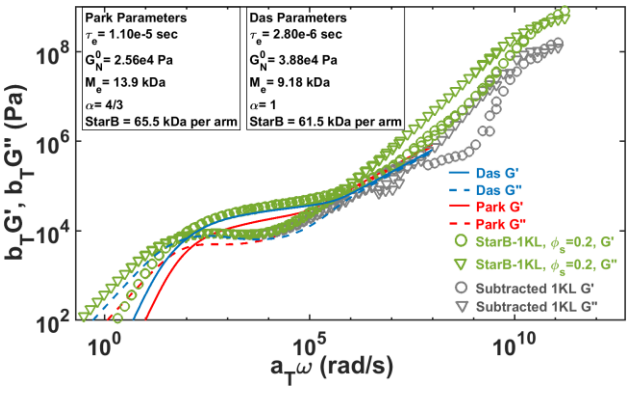

Figure 2.17: The same as in Figure 2.15, except for the 20%S-80%L blend.

IV. Conclusions

Using well characterized symmetric, 4-arm 1,4-polybutadiene star polymers of arm molecular weights of around 48 kDa, 61.5 kDa, and 70.1 kDa, blended with unentangled 1,4-polybutadiene linear polymer of molecular weight 1 kDa, only a dilution exponent of $\alpha = 1$, and not 4/3, correctly scales the change in terminal cross-over frequency with dilution. In addition, the Hierarchical model using the Das parameter set with $\alpha = 1$ generally gives quite good agreement (i.e., terminal time within a factor of 2-3) with the experimental data for most (but not all) of the blends. The better agreement given by $\alpha = 4/3$ for some pure star and pure linear melt data throughout literature seems to have arisen because some error in the tube model is counteracted by using $\alpha = 4/3$ or perhaps becomes of errors in characterization of the molecular weight of the polymers. Such errors are neutralized by the methods employed here, which use the concentration scaling of the cross-over frequency of a series of blends of three star polymers with an unentangled linear molecule to avoid dependence on a particular tube model, and use of four different estimates of molecular weight for three different stars, which ensures robustness of our conclusion to synthesis and characterization errors. Further confidence is provided by including in our master plots of cross-over frequency versus entanglement density data for all 1,4-polybutadiene stars available in the literature. We note that it has been known for some time that for a number of blends of short and long (both self-entangled) linear polymers, the value $\alpha = 1$ is necessary to give a good fit. While it remains possible that for other mixtures of entangled polymers a dilution exponent of $\alpha = 4/3$ will provide a better model of polymer rheology, the results presented here seem to be the clearest demonstration that the value $\alpha = 1$ is most

consistent with the most basic underlying assumptions of both the idea of a tube and with other entanglement paradigms, such as slip link models.

V. Appendix

Complementary to the StarB-1KL blend data featured in the main text of this chapter, we present here data for the remaining 1,4-polybutadiene, 4-armed star-1KL blends referenced in this study: StarA and StarC. The StarA polymer was blended with the 1KL to produce blends of star volume fractions ϕ_s = 1.0, 0.6, 0.4, 0.2 and 0. The StarC-1KL blend series features ϕ_s = 1.0, 0.6, 0.5, 0.4, 0.2 and 0. Consistent with the StarB-1KL blends featured in the main paper, small amplitude oscillatory shear (SAOS) rheology experiments were also performed with the StarA-1KL and StarC-1KL blends over a range of temperatures, and master curves were generated using time-temperature superposition. We then compared Hierarchical model predictions, which were scaled in accordance to the dilution exponent α, with linear rheology data to ascertain whether α = 1 or α = 4/3 would provide a better fit. The analysis presented here corroborates the evidence presented in the main paper, which indicates that α=1 is the desired value for scaling model predictions, not α = 4/3. To add robustness to the conclusion of α=1, we also derive plots of the terminal frequency cross-over as a function entanglement density, analogous to Figures 2.9- 2.12 presented in the main paper, but without the aid of the glassy frequency cross-over ratio ($\Omega_{x,g,ratio}$). Instead of using shifts in the high-frequency cross-over $\Omega_{x,g,ratio}$ to correct for changes in the glass transition temperature through addition of low-molecular-weight linear polymer, as we do in the main text, here we instead shift each set of Star-1KL blend data to an isofrictional reference temperature based on an analysis of the horizontal shift factors that originate from the WLF equation. The linear rheological data for each blend, and therefore the low-frequency cross-over, are then shifted to a reference temperature that produces the same

friction as in the pure star at the standard reference temperature of 25°C. We find, as described below, that this "isofrictional temperature" correction of the terminal cross-over frequencies plotted against entanglement density leads to a collapse of data for α=1, not α=4/3. This is the same conclusion as was reached when the high-frequency ratio $\Omega_{x,g,ratio}$ was used to shift the data to correct for changes in friction. Also featured in this appendix are details concerning the synthesis of our 4-armed 1,4-polybutadiene stars; the influence of thermorheological complexity in the application of time-temperature superposition; and a cross-comparison of Star-1KL linear rheology of equal star volume fractions.

The contents of this abstract are presented in the following order. First, we highlight details regarding the materials and methods used for synthesizing and characterizing our 4-armed 1,4-polybutadiene stars. Second, we investigate thermorheological complexity with the use of van Gurp-Palmen plots of phase angle against the complex modulus. Third, we disclose the WLF horizontal shift parameters of the StarA-1KL and StarC-1KL blends. Fourth, we discuss the scaled Park and Das implementations of the hierarchical model for the StarA and StarC blends. Fifth, we re-evaluate star-1KL data using isofrictional shifting of temperature. Then, we conclude this document by comparing the linear rheology of Star-1KL blends with different stars at the same star volume fractions.

V.1 Details of the Synthesis and Characterization of 4-Armed 1,4-Polybutdiene Stars

V.1.i. StarA and StarC Synthetic Description (Hadjichristidis Lab)

All chemicals were purified according to the standards required for anionic polymerization using well-established high-vacuum procedures.[52] 1,3-Butadiene (Sigma-Aldrich, 99%) was purified *via* repeated distillations over *n*-BuLi, at -10 ^{o}C (ice/salt bath).

Benzene (Sigma-Aldrich, 99.8%) was purified by distillation over CaH_2 and stored in a round bottom flask under high vacuum over polystyryllithium. *sec*-Butyllithium (*s*-BuLi, 1.4 M in cyclohexane, Sigma-Aldrich) was used without purification after dilution with dry n-hexane. 1,2-bis(dichloromethylsilyl)ethane (Gelest, 95%) was purified by crystallization from *n*-hexane, followed by three crystallizations from the bulk, diluted in *n*-hexane and stored under high vacuum at -30 ^{o}C. Methanol (Sigma-Aldrich, 99.8%) (terminating agent) was stored under high vacuum and used as received.

A typical procedure for the synthesis of the 1,4-polybutadiene 4-arm StarA and StarC is as follows. 10 g of 1,3-butadiene was polymerized at room temperature, using 0.13 mmol of *sec*-butyllithium in benzene. The mixture was left to react for 1 day, and then an aliquot was taken by heat-sealing the corresponding constriction tube for molecular characterization. The rest of the living polymer solution was reacted with 0.024 mmol of 1,2-bis(dichloromethylsilyl)ethane (BMDCSE). The linking reaction was monitored by GPC and lasted, depending on the sample, 2-3 weeks. After the completion of the reaction, the excess of the living chains was terminated by addition of degassed methanol, and the solution precipitated in methanol. The 4-arm star 1,4-polybutadiene was purified from the unreacted linear chains by repeated solvent/non-solvent (toluene/methanol) fractionations.

V.1.ii. StarB Synthetic Description (Mays Lab)

1,3-Butadiene (Bd) (Aldrich, 99%), benzene (Aldrich, 99.8%), and methanol (terminating agent, Aldrich, 99%) were purified according to experimental techniques common in high-vacuum anionic polymerization[66]. 1,2-Bis(methyldichlorosilyl)ethane (BMDCSE) (linking agent, Gelest, 95%) was distilled several times over CaH_2 on a vacuum line. *s*-Butyllithium (*s*-

BuLi, 1.4 M in cyclohexane, Aldrich) was used without purification and was diluted with dry *n*-hexane. The diluted reagents were stored at –30 °C in ampules equipped with break-seals before use. The polymerization and linking reaction were performed under high vacuum condition in the sealed all-glass reactors equipped with break-seals. The reactors were pre-washed with *n*-BuLi solution after sealing off from the vacuum line.

Synthesis of Living PBd. The polymerization of Bd (10 g) was performed using *s*-BuLi (0.16 mmol) in benzene at room temperature for 24 h. Then, a small portion of living PBdLi was sampled by heat-sealing the constriction for characterization. The rest of living polymer solution was subsequently gathered in a pre-calibrated ampule equipped with break-seals for the linking reaction with BMDCSE. The resulting PBd was characterized by GPC, giving PBd (M_n(obsd) = 68 kg/mol, M_w/M_n = 1.01).

Synthesis *of 4-arm star PBd.* The linking reaction of a benzene solution of living PBd (StarB, 0.14 mmol) with the linking agent BMDCSE (0.03 mmol) was performed in benzene (500 mL) at room temperature for 4 weeks with vigorous stirring to form well-defined 4-arm star PBd. The reaction was monitored by sampling a small amount of reaction solution via constrictions for GPC characterization. After terminating the linking solution with degassed methanol, the polymer solution was stabilized with butylated hydroxytoluene (BHT) and then poured into a large excess of methanol to precipitate the polymers. The fractional precipitation was repeated using toluene/MeOH to isolate highly pure 4-arm star PBd. The fractionated star polymer was further precipitated in methanol and dried under high vacuum condition for characterization. The resulting 4-arm star PBd was characterized by GPC, giving star B (M_n(obsd) = 290 kg/mol, M_w/M_n = 1.03).

V.1.iii. StarB GPC and TGIC (Chang lab) Characterization Details

Gel Permeation Chromatography (GPC). Size exclusion chromatography/two-angle laser light scattering (GPC-TALLS) connected with a refractive index (RI) detector and Viscotek differential viscometer was used to characterize the star arm, PBd, and 4-arm star PBd, starB. Tetrahydrofuran (THF) was used as the mobile phase at a flow rate of 1.0 mL/min at 40 °C. This system features a Waters 1525 high-pressure pump, Waters Ultrastyragel columns (HR-2, HR-4, HR-5E, HR-5E, and HR-6E with pore sizes 10^3, 10^4, and 10^5 Å), a Waters 2410 differential refractometer detector (at 680 nm), a Precision Detectors PD-2040 two-angle (15°, 90°) light scattering detector, and a Viscotek differential viscometer. The Precision Detectors software "Discovery 32" was utilized to calculate the M_w values from GPC-TALLS data. The refractive index increment (dn/dc) value was measured on a Wyatt Optilab DSP detector at a wavelength of 690 nm and temperature of 40 °C in THF. After dn/dc was measured for five different concentrations of each sample, the average value 0.130 mL/g was used.

Temperature Gradient Interaction Chromatography (TGIC). TGIC is an HPLC technique controlling the interaction strength of the analytes with the stationary phase by changing the temperature of the column[67, 68]. TGIC experiments were carried out with a typical HPLC system equipped with a C18 bonded silica column (Nucleosil C18, 250 × 4.6 (i.d.) mm, 500 Å, 7 μm particle size). The eluent was 1,4-dioxane (Samchun, HPLC grade) at a flow rate of 0.4 mL/min. The temperature of the column was controlled by circulating a fluid from a programmable bath/circulator (Thermo-Haake, C26P) through a homemade column jacket. All TGIC analyses were done with a linear temperature gradient as shown in the plots. (0.25 °C/min). Sample solutions in 1,4–dioxane (~3 mg/mL, dn/dc = 0.104 mL/g) were prepared by dissolving the polymers in a small volume of the eluting solvent and the injection volume was 100 μL[69]. The

TGIC chromatograms were recorded with a differential refractometer (RI) detector (Shodex, RI-101) and a light scattering (LS) detector (Wyatt, miniDawn).[67]

V.2. Results and Discussion of the Rheology of Star-1KL 1,4-Polybutadiene Blends

V.2.i Analysis of Thermorheological Complexity in Star-1KL Blends

We analyze the influence of thermorheological complexity in the time-temperature superposition of our Star-1KL blends by plotting the phase angle (δ) with respect to the absolute value of the complex modulus (|G*|), which was obtained through linear rheology measurements over a range of temperatures. As described in the original work of van Gurp and Palmen[70], these δ vs. |G*|plots (we hereafter refer to these plots as vGP plots) test time-temperature superposition without the horizontal and/or vertical shifting that is needed for generating linear rheology master curves. For a thermorheologically simple fluid (i.e., one for which time-temperature superposition is valid), the δ vs. |G*| plot should show a nearly continuous, smooth line that connects the segments of linear rheology data obtained over a range of temperatures; although some small gaps may exist along the |G*| axis because of a weak temperature dependence of the modulus scale. An example of a thermorheologically simple fluid is seen in Figure 2.A1 in the van Gurp and Palmen paper[70], which showcases a vGP plot.

In direct contrast to the case of thermorheological simplicity, the presence of thermorheological complexity indicates failure of time-temperature superposition to horizontally shift G' and G" linear rheology data. Furthermore, this "failure" of time-temperature superposition visually manifests in the inability of the phase angles featured in the vGP plot to superpose into a continuous line. Figure 2.A1, which was taken from the van Gurp and Palmen paper[70], shows the thermorheological complexity present in a long-chain branched polymer of

ethylene propylene diene monomer (EPDM) chemistry. There is clear discontinuity in the value phase angle values among different linear rheology measurement temperatures. For instance, the phase angle within the range of log(G/Pa) between 4 and 5.5 at 250^{o}C is differs by a factor of up to 1.23 from the phase angles over the same range of log(G/Pa) at 100^{o}C. This thermorheological complexity in branched polymer melts is not uncommon, and can be correlated with factors such as chemistry, inhomogeneous branching distribution, the dependency of entanglement spacing on temperature, and the temperature coefficient of chain dimensions, which contributes to the activation energy for arm diffusion[70, 71, 72]. However, we must also note that not all branched melts have thermorheologically complex behavior; examples of thermorheologically simple behavior in branched melts can be found in Trinkle, S. et al.[73]

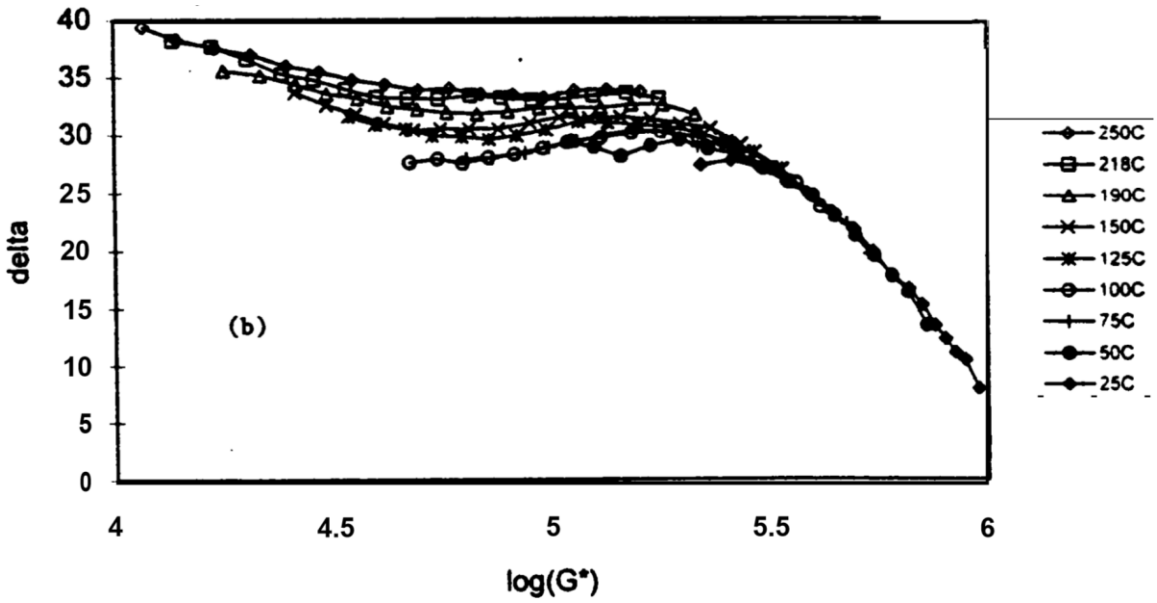

Figure 2.A1: From the work of van Gurp and Palmen[70], phase angle versus complex modulus obtained through linear rheological measurements at temperatures ranging from 25-250^{o}C. The polymer is ethylene propylene diene monomer (EPDM).

Given examples of thermorheological complexity in branched melts, we might suspect its presence in the Star-1KL blends featured in this study. Figure 2.A2 features vGP plots of the StarB-1KL blend series, where subfigures A-D respectively represent star volume fractions (ϕ_s) of 1, 0.5, 0.4, and 0.2. We note that each of the subfigures displays some thermorheological complexity. Although not presented here, we observe similar levels of thermorheological complexity in vGP plots of StarA-1KL and StarC-1KL blends. In Figure 2.A2-A we observe only a slight discontinuity in phase angles associated with complex moduli below 10^6 Pa for the pure StarB. These slight mismatches can be largely corrected by shifts along the modulus axis in the vGP plot, which correspond to normal vertical shifts along the modulus axis in the plots of G' and G" against frequency. At complex moduli ranging from 10^6 Pa to approximately 10^8 Pa, the phase angles superpose very well with each other. Thus, time-temperature superposition is quite accurate if applied to this range of complex moduli. Unfortunately, this accuracy in time-temperature superposition appears to diminish at temperatures of -90^{o}C and -95^{o}C, as indicated by the discontinuity the phase angles between these two temperatures. However, since the phase angles collected at -90^{o}C and -95^{o}C would superpose quite well if the data in Figure 2.A2-A are horizontally shifted along the x-axis, time-temperature superposition can be reasonably applied to the pure StarB linear rheology dataset if normal temperature-dependent vertical shifting is applied to the G' and G" curves.

vGP plots of the StarB-1KL blends (Figure 2.A2-B, C & D) are quite similar to that of the pure star in Figure 2.A2-A. At complex moduli values below 10^6 Pa, the phase angles are either minimally discontinuous or superpose nearly perfectly, indicating the dominance of thermorheological simplicity, which is consistent with the successful application of time-temperature superposition with minimal aid of vertical shifting. However, for complex moduli

above 10^6 Pa, thermorheological complexity becomes readily apparent. In particular, we note in Figure 2.A2-D, which is for star volume fraction ϕ_s = 0.2, a factor of 1.1 discontinuity between the phase angles collected at temperatures of -85°C and those at -95°C. The increased volume fraction of sub-entangled linear polymer in this StarB-1KL(ϕ_s = 0.2) blend seems to have amplified the thermorheological complexity. However, although not perfect, the combined use of temperature-dependent vertical shifting and horizontal time-temperature superposition has yielded a reasonable linear rheology master curve, even for the StarB-1KL(ϕ_s = 0.2) blend (and of the other Star-1KL blends featured in this work; see Figures 2.A26- A29). Fortunately, any errors incurred by using in the shifting of our Star-1KL G' and G" data are likely modest, since the difference in the glassy cross-over frequency of the pure star and that of the lowest-concentration star is only a factor of two, as stated in the main paper. Thus, even a complete neglect of the difference in the monomeric friction coefficient among the samples would not change the conclusion that should be α = 1, not α = 4/3.

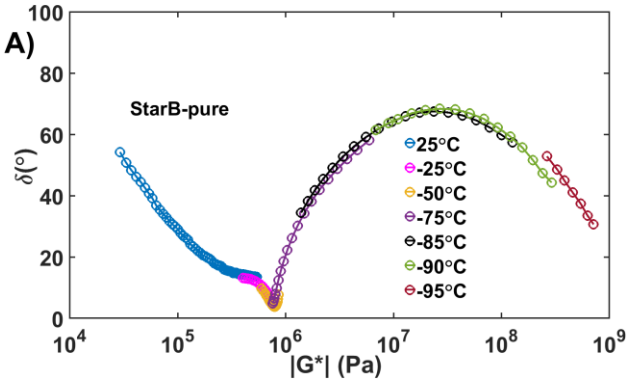

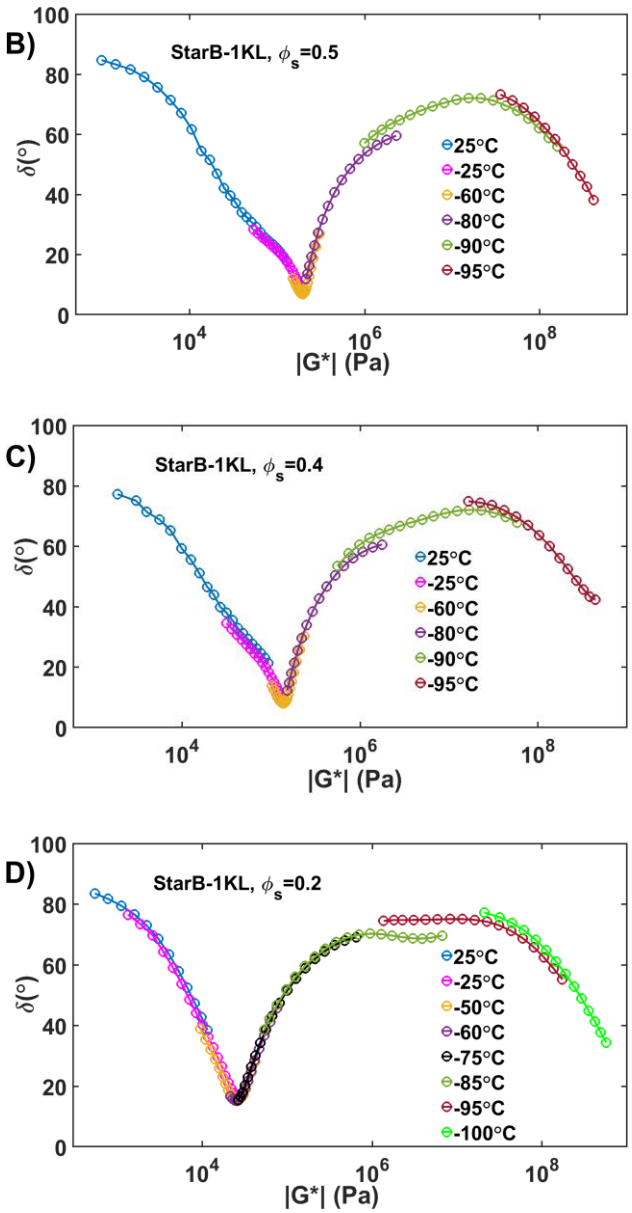

Figure 2.A2: Phase angle plotted against complex modulus from linear rheological data at temperatures ranging from 25°C to -105°C for the StarB-1KL blend series at star volume fractions (ϕ_s) of A) 1.0 (i.e., pure Star), B) 0.5, C) 0.4, and D) 0.2.

V.2.ii. WLF Shift Factors of the Star-1KL Blends

The WLF horizontal temperature shift factors (a_T) for the StarA-1KL series are given in Figure 2.A3 and for the StarC-1KL series in Figure 2.A4. For both Figures 2.A3 and 2.A4, the horizontal shift factors were calculated from the time-temperature superposition of linear

rheology data gathered at temperatures ranging from 50°C to -105°C. The reference temperature for both plots is 25°C. Shift factors for StarB-1KL series are given in the main text.

In Figure 2.A3, the horizontal shift factors for the pure StarA are absent because this pure star sample was consumed prior to rheological testing at temperatures below 25°C. Despite the missing a_T for pure StarA, we still observe the effects on the monomeric friction coefficient contributed by the blending with the pure 1KL. For instance, when the temperature is decreased to -95°C, the difference in a_T between the blends and the pure linear polymer spans half of an order of magnitude. The a_T curves of the StarA-1KL ϕ_s = 0.2, 0.4, and 0.6, however, appear to superpose on one another nearly perfectly, although they differ from the curve for the pure 1KL. Figure 2.5 in the main text shows that the a_T values are also quite similar for the StarB-1KL blends with ϕ_s = 0.2, 0.4, and 0.5, while being distinctly different from that of the pure StarB. Presumably the same is true for the pure StarA.

Figure 2.A4 gives a complete set of WLF horizontal shift factors for the StarC-1KL blend series. Similarly to Figure 2.A3, the difference between a_T grows with decreasing temperature in Figure 2.A4. The most distinct contrast between the a_T values of the pure 1KL and that of the pure StarC polymer occurs at T= -95°C, where the difference in the reported a_T spans roughly half of an order of magnitude and is monotonic in the volume fraction of 1KL, as expected.

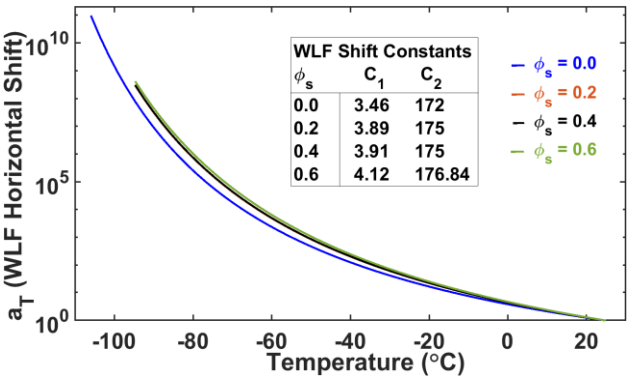

Figure 2.A3: WLF Horizontal Shift factors as a function of temperature from time-temperature superposition of linear rheology data for StarA-1KL blends at temperatures ranging from 25°C to -105°C. The reference temperature is 25°C.

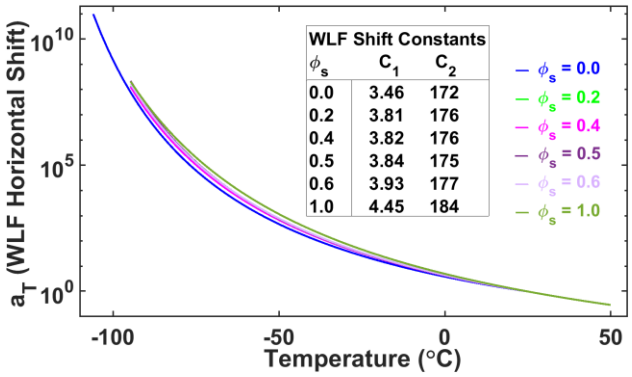

Figure 2.A4: The same as Figure 2.A3 except for the StarC-1KL blend series and temperatures range from 50°C to -105°C.

V.2.iii. Hierarchical Model Analysis of the StarA-1KL Blend Series

We show in Figure 2.A5 the linear rheology of the StarA-1KL blend series generated using time-temperature superposition. The individual rheology data at each temperature were horizontally and vertically shifted in the same manner as defined in the main paper. As a reminder, we note that we do not have the complete linear rheology of the pure StarA polymer because the material was depleted prior to further rheological measurements at temperatures below 25°C. However, we do have the terminal regime of the pure StarA, from which we obtain the inverse frequency (ω^{-1}) at the G' / G" cross-over located to the left of the plateau region. Similar to the StarB-1KL blend series featured in Figure 2.6 of the main paper, we observe drastic changes in the shape of the StarA linear rheology as increased quantities of 1KL are blended with the star. For instance, the terminal relaxation time of the pure star is reduced by three orders of magnitude when the star volume fraction ϕ_s decreases from unity to 0.6, and by an additional order of magnitude when ϕ_s is further reduced to ϕ_s = 0.4. We also observe roughly a one order-of-magnitude reduction in the plateau modulus upon reduction from ϕ_s =

0.6 to ϕ_s = 0.2 in the StarA-1KL blend. In addition, the intermediate G'/G" cross-over frequency ($\omega_{x,i}$), which is located just to the right of the plateau region, differs by roughly one order of magnitude between the ϕ_s = 0.6 and the ϕ_s = 0.2 blends involving StarA.

Since we do not have data for the pure StarA, we cannot capture completely the change in monomeric friction coefficient of the pure linear relative to that of the pure star. Nevertheless, the insert within Figure 2.A5 shows a noticeable shift in the pure 1KL G' profile with respect to that of the StarA-1KL blends where the latter nearly superpose upon each other, similar to, but more precisely than what we observed for the StarB-1KL blends in Figure 2.6 of the main text. This suggests that the inclusion of 1KL has minimal impact on the monomeric friction coefficient of StarA at star volume fractions of ϕ_s = 0.6 through 0.2.

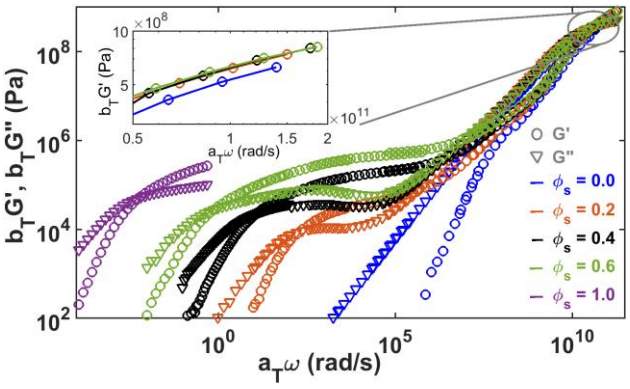

Figure 2.A5: G' and G" master curves for the StarA-1KL blend series. Each blend is listed according to star volume fraction (ϕ_s). The plot insert features a close-up of the G' curves for each blend component near the glassy plateau. Here, and in subsequent Figures, the reference temperature is 25°C.

Figure 2.A6 compares the pure StarA data (symbols with Hierarchical model fits implemented with Das parameters (blue lines) and Park parameters (red lines), with arm molecular weight used as the fitting parameter. The Das and Park parameters values given in the legend are identical to those used for other pure 1,4-polybutadiene stars at 25°C. We note that the

arm molecular weight assignments for the Das and Park parameters differ slightly, as expected, and this was discussed for StarB in the main text. As explained in the main text, allowing the molecular weights to differ for the Park and Das parameters puts both sets on equal footing for predictions of the rheology of the blends. The Das and Park behaviors in the terminal regime superpose quite well with each other, but there are some slight differences in the G' and G" moduli values throughout the plateau region; this discrepancy arises from the slight differences in the plateau modulus (G_N^0) assigned, with the Park value being larger than the Das value of G_N^0.

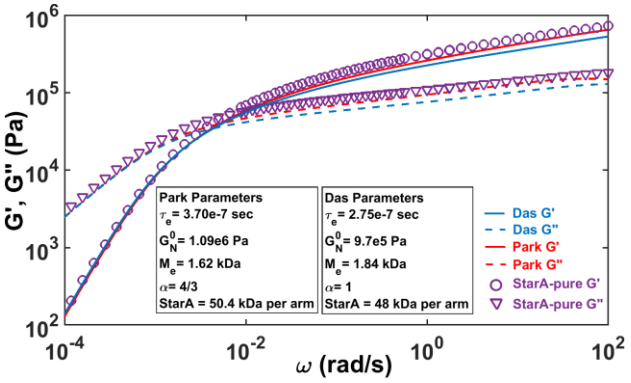

Figure 2.A6: Linear rheology data of the pure StarA (symbols) compared with Hierarchical predictions implemented separately with "Das" parameters (blue lines) and "Park" parameters (red lines), as reported in the legend.

Using these molecular weights for the undiluted StarA polymer, the parameters governing model predictions are scaled in accordance to the volume fraction of star in a given blend (ϕ_s) and the dilution exponent (α) following Eqs. 1-3 in the main paper, as discussed there for blends with StarB. As indicated in Fig. S5, we do not possess the G'/G" glassy plateau cross-over frequency ($\omega_{x,g}$) for the pure StarA, which is one of the essentials for scaling the Hierarchical parameters. Fortunately, we have high frequency (low temperature) data, above 100 rad/s, for both the pure StarB and pure StarC, as shown in Figure 2.A7, showing good

superposition at these higher frequencies. Considering that StarA, StarB and StarC share the same chemistry; that StarA and StarC were synthesized by the same laboratory; and that all three stars are well-entangled and undiluted, there is good reason to suggest that the high-frequency linear rheology of the pure StarA should also superpose with those for the pure StarB and pure StarC shown in Figure 2.A7. Thus, instead of using the actual $\omega_{x,g,0}$ value for the pure StarA (which we lack), we assigned to StarA the average of the $\omega_{x,g,0}$ values of the pure StarB and pure StarC samples, which differ from each other by only a factor of 1.02. With this value of $\omega_{x,g,0}$ identified for the pure StarA, we were able to scale the Hierarchical model parameters using Eqs. 1-3 featured in the main paper.

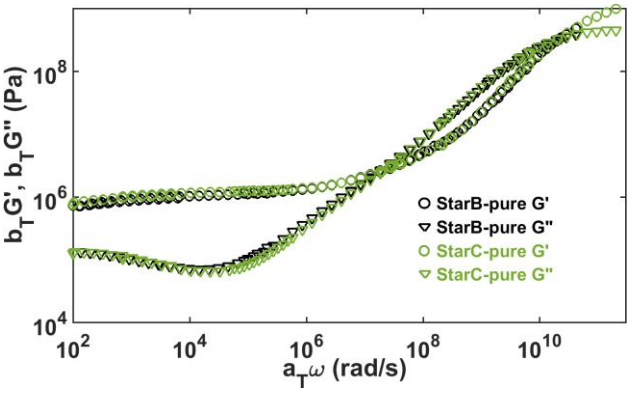

Figure 2.A7: Linear rheology of the pure StarB and pure StarC 1,4-polybutadienes in the plateau and high frequency regions.

Featured in Figures 2.A8- 2.A10 are the scaled hierarchical predictions, implemented with Das parameters (blue lines) and Park parameters (red lines), compared with the linear rheology measurements of StarA-1KL blends (symbols) with star volume fractions ϕ_s = 0.6, 0.4, and 0.2. Also shown in these plots are the StarA-1KL linear rheology data with the contribution of the pure 1KL subtracted out, again following the procedure described in the main text. These figures show that the Hierarchical model implemented with Das parameters outperforms the Park

parameters due to the use of α = 1 in the Das scaling, which is consistent with the findings for the StarB-1KL blends featured in the main paper. For instance, in Figure 2.A8, the model with both the Das and Park parameters partially captures the Rouse behavior of the StarA-1KL(ϕ_s = 0.6) blend after the 1KL contribution has been subtracted out. Although neither prediction perfectly captures the terminal relaxation of the ϕ_s = 0.6 blend, the Das parameter predictions, which were scaled using α = 1, are in closer agreement with the experimental data in the terminal region than are the predictions using the Park parameters, which uses α = 4/3.

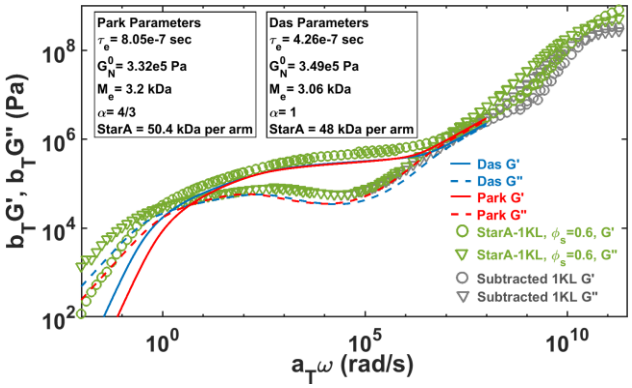

Figure 2.A8: linear rheology of the StarA-1KL blend composed of 0.6 star volume fraction (green symbols). The grey symbols give the data with the contribution of the linear polymer subtracted out as discussed in the text. The Hierarchical model Das (blue lines) and Park (red lines) predictions, are scaled from the pure StarA parameters featured in Figure 2.A6.

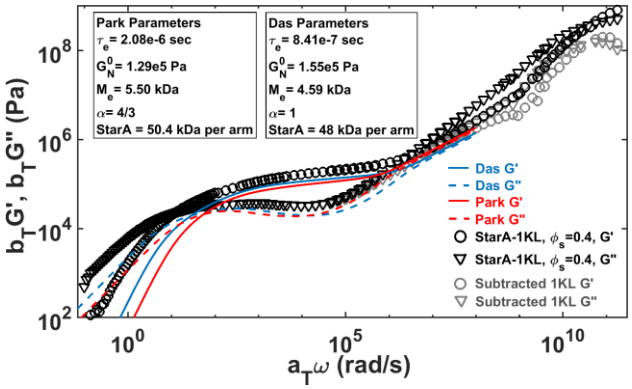

Figure 2.A9: The same as Figure 2.A8, except with 0.4 star volume fraction.

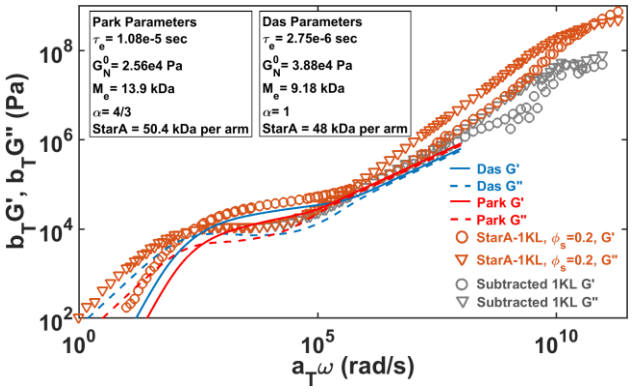

Figure 2.A10: The same as Figure 2.A8, except for 0.2 star volume fraction

V.2.iv. Hierarchical Model Analysis of the StarC-1KL Blend Series

We present in Figure 2.A11 the linear rheology measurements of the StarC-1KL blends generated from time-temperature superposition. Similar to Figure 2.A5, the plateau modulus of the StarC-1KL ϕ_s = 0.2 blend is more than an order of magnitude lower than that of the pure star. Also, the terminal relaxation time of the StarC-1KL(ϕ_s = 0.6) blend differs by three orders of magnitude from that of the ϕ_s = 0.2 blend. The insert in Figure 2.A11 shows a monotonic horizontal shift in the G' data with star volume fraction near the glassy plateau, similar to that seen in Figure 2.A5 for the StarA-1KL blend series and in Figure 2.5 within the main paper for the StarB-1KL blends. Since the pure StarC in Figure 2.A11 has such a low terminal cross-over frequency, we attempted to obtain the star's terminal relaxation by increasing the testing temperature from 25°C to 50°C and invoking time-temperature superposition. However, this effort was halted due to the occurrence of cross-linking within the sample at prolonged testing times.

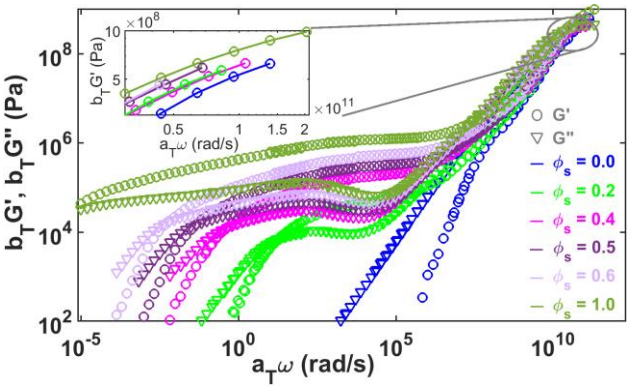

Figure 2.A11: The same as Figure 2.A5 except for the StarC-1KL blend series.

Thus, the lack of a clear terminal region for the pure StarC complicates the rheological determination of its arm molecular weight (although its molecular weight values from GPC and TGIC are available and given in the main text in Table 2.1). Fortunately, the Hierarchical parameter values of G_N^0, M_e, and τ_e for StarC at the reference temperature of 25°C should be the same as for other 1,4-polybutadiene samples. [19-21, 31, 32, 41] Lacking StarC terminal data, we thus might still obtain the arm molecular weight from the G' and G" measurements that we do have, which might reach closely enough to the terminal relaxation to enable a reasonable estimate of the arm molecular weights by fitting the Hierarchical model with the Das and Park parameters, as we have done with data for which the terminal region is present. In Figure 2.A12, we analyze the near-terminal G' and G" measurements of the pure StarC by first recording the ratio, G'/G" = 1.34 (black line in Figure 2.A12), at the lowest frequency, ω = 1.01e-5 rad/s, for which rheology was measured. We then run both the Hierarchical Das and Park predictions using a range of star arm molecular weights and recorded the G'/G" ratios of the predictions at ω= 1.01e-5 rad/s. By plotting these ratios against the arm molecular weight in Figure 2.A12, we are able to estimate the most reasonable star arm molecular weight for the "Das" and "Park" parameters that best matched the G'/G" ratio of the pure StarC linear rheology, namely 70.1kDa for the Das

parameters and 76kDa for the Park parameters. As given in the main paper, GPC and TGIC StarC arm molecular weights are 71.3 kDa and 72.5 kDa, respectively. Thus, the near-terminal G'/G" ratio appears to yield reasonable arm molecular weights from Hierarchical model predictions.

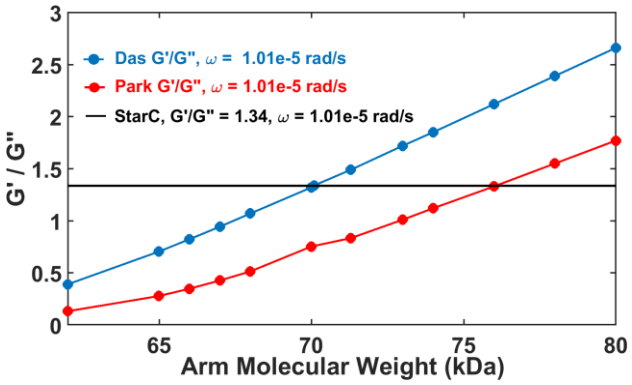

Figure 2.A12: G'/G" at ω=1.01e-5 rad/s from StarC rheological data (black line) compared with G'/G" predicted by the Hierarchical model with Das (blue line) and Park (red line) parameters, also at ω=1.01e-5 rad/s.

We can estimate the error in this approach by carrying out the same analysis with the pure StarA and StarB polymers, for which terminal data exist and reliance on the "near terminal G'/G'' ratio is not needed. Also included in this error analysis is a pure, 1,4-polybutadiene, 4-armed star with an arm molecular weight of 24 kDa, hereby referred to as "24KS", taken from the work of Desai et al.[41] We reference this 24KS because it shares the same chemistry as the new stars reported here in this work, and this star was synthesized by the same laboratory as StarB. In the analyses featured below in Figure 2.A13, we identified the frequencies at which pure StarA, pure StarB, and pure 24KS show a G'/G" ratio of 1.34, which is the value at which the analysis was performed for pure StarC, and assess the Hierarchical model predictions of G'/G'' at this frequency for StarA, StarB and 24KS. The near-terminal analysis for StarA,

featured in Figure 2.A13-A, yields star arm molecular weights of 46.3kDa and 49.2kDa for the Das and Park parameters, respectively. As shown in Figure 2.A13-A, the arm molecular weights obtained from fitting the terminal regime of the pure StarA are 48kDa and 50.4kDa for the "Das" and "Park" parameters, respectively. Thus, for the StarA polymer, the error associated with analyzing only the near-terminal G'/G" ratio, rather than fitting over the terminal range, is less than 2 kDa for the Das parameters and roughly 1 kDa for the Park Parameters. For StarB, we see in Figure 2.A13-B that the corresponding molecular weights obtained in the near-terminal region for the Das and Park parameters are respectively 59.9kDa and 64.5kDa, while the values obtained by fitting the terminal regime are 61.5kDa and 65.5kDa, respectively. Thus, the error associated with analyzing the near-terminal G'/G" ratio for StarB is less than 2 kDa for the Das predictions and 1 kDa for the Park predictions. Lastly, the 24KS analysis featured in Figure 2.A13-C indicates that the 1.34 G' / G" ratio is best fitted using star arm molecular weights of 23.5 kDa and 23.3 kDa for the Hierarchical Park and Das, respectively. As reported in the paper by Desai and colleagues[41], the 24KS terminal data was fitted assuming an arm molecular weight of 24 kDa by both the Hierarchical Das and Park parameters, which indicates that error associated with obtaining the arm molecular weight using the near-terminal G'/G" ratio is less than 1 kDa for either modelling parameter approach. Overall, in consideration of the evidence presented in Figure 2.A13, we can reasonably expect that the star arm molecular weight determined from the G'/G" analysis for StarC is within 3 kDa of its true arm molecular weight.

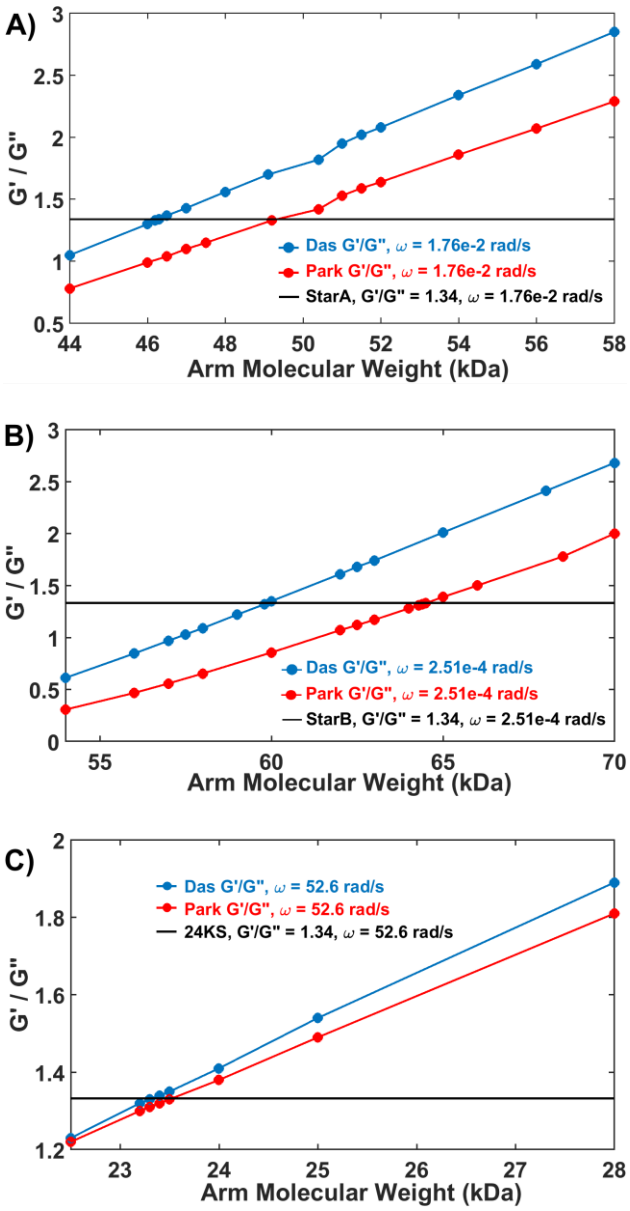

Figure 2.A13: Similar to Figure 2.A12, but for A) StarA and B) StarB that are featured in this work and C) a similar star, 24KS, as reported in Desai et al.[41]

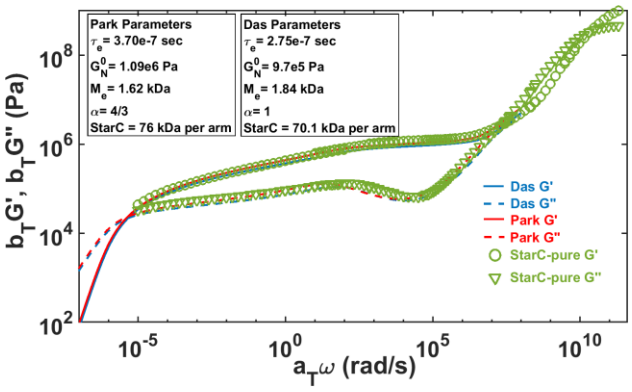

Figure 2.A14: Linear rheological measurements of pure StarC (symbols) compared with Hierarchical predictions using the Das (blue lines) and Park (red lines) parameters.

With the pure StarC molecular weights established for the Das and Park parameters, as shown above in Figure 2.A14, we use Eqs. 1-3 in the main paper to obtain the scaled parameters needed to predict the rheology of the blends with ϕ_s = 0.6, 0.5, 0.4 and 0.2, in Figures 2.A15-2.A18, respectively. Predictions made with the Das parameters (with α = 1) are represented by the blue lines, and the Park predictions (with α = 4/3) are the red lines; the experimental data are shown as symbols. Also featured are the experimental data with the 1KL contribution to the Rouse modes subtracted out, which are represented by the grey symbols. We also report in the legend the Hierarchical Das and Park parameters used for each blend prediction. As was true for the StarA-1KL and StarB-1KL linear rheological data, the Hierarchical model predictions implemented with Das parameters, which utilizes α=1, outperforms the α=4/3 dilution exponent value used in the predictions with the Park parameters. Deviations from the experimental data can be partly attributed to the uncertainty in the pure StarC arm molecular weight. However, despite this shortcoming, the Das parameter predictions are in closer proximity to the data in the terminal relaxation regime than are the Park parameter predictions.

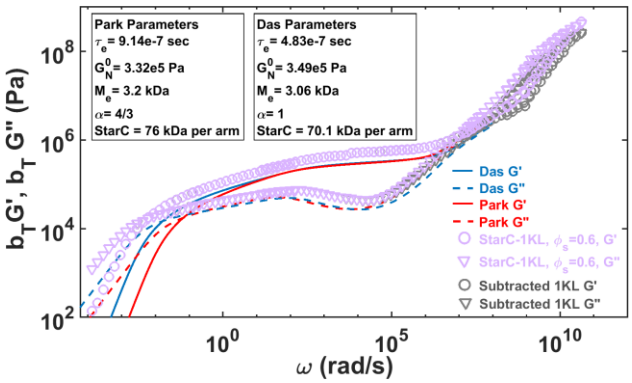

Figure 2.A15: Linear rheology of the StarC-1KL blend composed of 0.6 star volume fraction (symbols). The predictions of the Hierarchical model with Das (blue lines) and Park (red lines) parameters, scaled from the corresponding pure StarC parameters, are given.

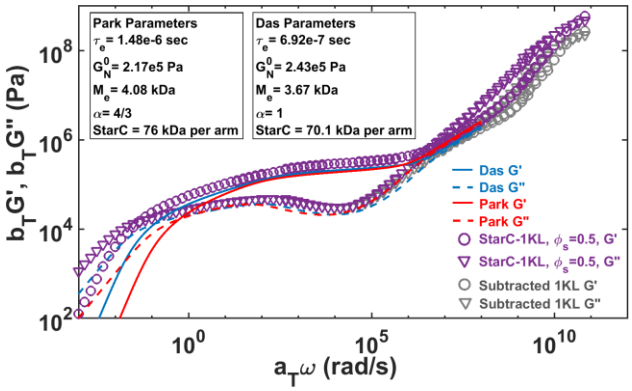

Figure 2.A16: The same as Figure 2.A15, except for 0.5 star volume fraction.

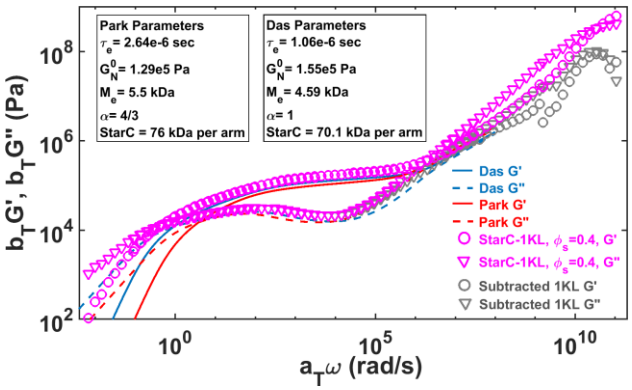

Figure 2.A17: The same as Figure 2.A15, except for 0.4 star volume fraction.

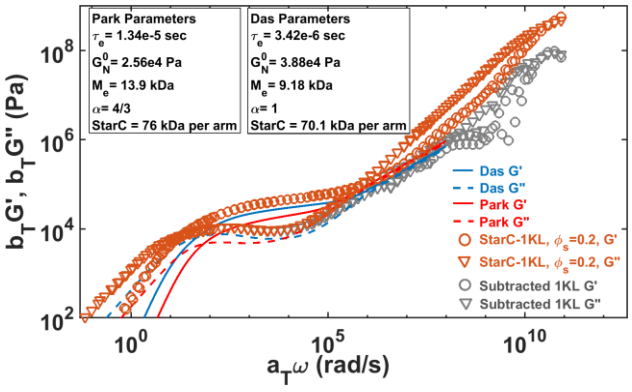

Figure 2.A18: The same as Figure 2.A15, except for 0.2 star volume fraction

V.2.v. Isofrictional Temperature Analysis of Star-1KL Blends

As mentioned in the main text, as an alternative to the analyses presented in Figures 2.9-2.12 in the main paper, we re-evaluate the star-1KL blend data without using the glassy frequency cross-over ratio ($\omega_{x,g,ratio}$) to account for changes in segmental friction of each star-1KL blends with respect to the pure star. To do so, we must first determine the shift in reference temperature needed to counteract the changes in segmental friction caused by blending with 1KL linear chains. This is done by superposing the horizontal shift factors of each star-1KL blend with that of the pure star, using a method demonstrated by Wagner for polystyrene blends with oligomeric polystyrene[61]; we hereby refer to this approach as the "isofrictional temperature method." This shifting of the blend shift factor curve by a temperature difference ΔT_g allows one to compute augmentation of the frequency shift factor a_{Tg} due to the change in glass transition temperature; this is given by $\log_{10} a_{Tg} = -c_1 \Delta T_g/(c_2 + \Delta T_g)$, where the c_1 and c_2 coefficients are those for the pure star. Using the appropriate ΔT_g and a_{Tg}, we superpose the blend shift factor curves onto that of the pure star, as shown in Figure 2.A19 for StarB-1KL blends. The value of a_{Tg} determined in this way is then multiplied by the terminal cross-over frequency $\omega_{x,t}$ to correct it for the change in glass transition temperature produced by blending with the 1KL linear

polymer. This use of the change in shift factor to achieve an "isofrictional condition" allows us to avoid errors that may arise from linear rheology testing at high frequencies, or from failures of time-temperature superposition that may occur at these high frequencies. The isofrictional temperature method only requires that the WLF constant c_1 be roughly the same for the pure star and all its blends, which holds reasonably closely for our samples.

In Figures 2.A19- 2.A22, we report scaled WLF plots that apply this isofrictional temperature method to the starB-1KL, starC-1KL and starA-1KL blends, respectively. Along the y-axis, we observe two horizontal shift factors: a_T and a_{Tg}. The a_T represents the horizontal shift factors arising from the time-temperature superimposed linear rheology data, whereas, a_{Tg} is the augmenting shift factor allowing superposition of the star-1KL a_T data onto the pure star a_T to account for differences in the glass transition temperature. Also reported in the Figures 2.A19-2.A22 are the time-temperature superposition coefficients, c_1 and c_2, of the pure star and the relative changes in T_g of each star-1KL blend with respect to its pure star component.

In Figure 2.A19, we observe that the starB-1KL blends (symbols) superpose quite well with the pure StarB (solid line). We note that the change in the T_g with respect to the pure star becomes larger as the linear content of the star-1KL blends increases, reaching a maximum T_g difference of 10^{o}C between the pure 1KL and the pure StarB. The results of the starC-1KL blends featured in Figure 2.A20 are similar to Figure 2.A19; however, we note that the T_g of the pure StarC is notably more closer to the T_g pure 1KL, since the T_g difference is roughly 4.6^{o}C.

As noted in a previous section, we do not have linear rheology data of the pure StarA sample below 25^{o}C due to a supply shortage. Thus, we estimate the c_1 coefficient of the pure starA by averaging the c_1 values of the pure StarB and pure StarC samples. And likewise, we perform the same estimate for the c_2 coefficient of the pure StarA using the c_2 values of the pure

StarB and pure StarC. Despite having to estimate the c_1 and c_2 values for the pure StarC, we are able to obtain reasonable superposition of horizontal shift factors from the StarA-1KL blends upon that for the pure StarA.

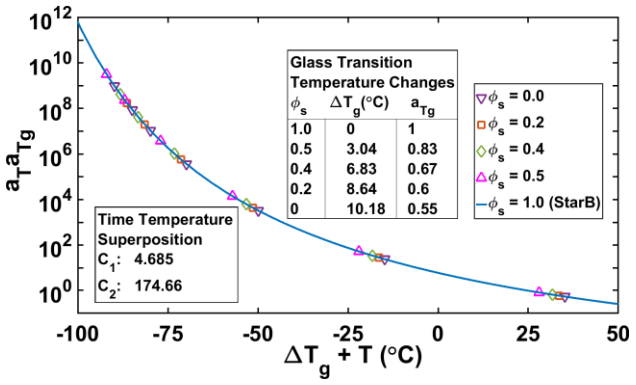

Figure 2.A19: Horizontal shift factors, scaled by a_{Tg}, of StarB-1KL blends (symbols) and pure StarB (solid line) plotted against temperature shifted by ΔT_g; both a_{Tg} and ΔT_g are given in the legend. Also reported in the legend are the time-temperature superposition coefficients, c_1 and c_2, of the pure starB.

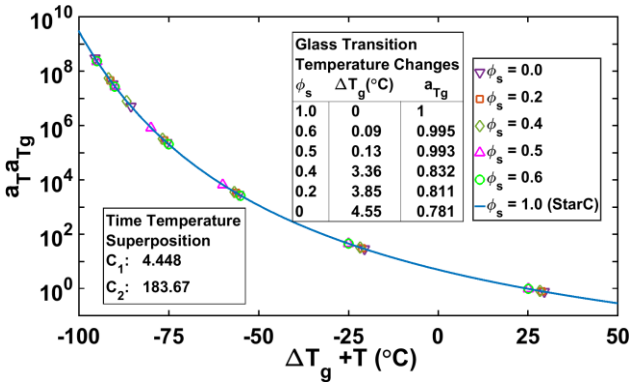

Figure 2.A20: Same as Figure 2.A19, except for the StarC-1KL blends.

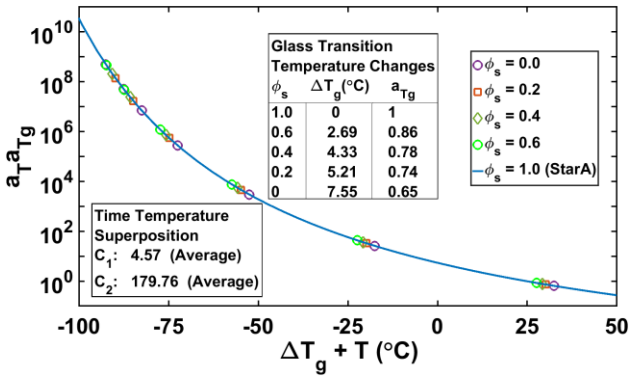

Figure 2.A21: Same as Figure 2.A19, but with the StarA-1KL blends.

By using the horizontal shift factor that corrects for changes in segmental friction (a_{Tg}) in Figures 2.A19- 2.A21, we can construct new linear rheology master curves of the star-1KL blends that remove the influence on low-frequency cross-over of the change in segmental friction due to the addition of the 1KL linear. Similar to Figures 2.9- 2.12 in the main text, we ascertain the value of the dilution exponent, α, in Figures 2.A22- 2.A25 by plotting the terminal frequency cross-over ($\omega_{x,t}$), multiplied by a_{Tg}, against the number of entanglements per star arm ($M_a/ M_{e,o}$), where M_e is 1620 Da. Both $\omega_{x,t}$ and the number of entanglements are scaled to account for changes in star volume fraction, ϕ_s.

Figures 2.A22- 2.A25 plot the $\omega_{x,t}$ scaled using the isofrictional temperature method vs. entanglement density using molecular weights for the pure StarA, StarB, and StarC obtained in the four ways discussed in the main text. As in the corresponding Figures 2.9- 2.12 in the main text, we again observe that the star-1KL experimental data using α=1 superposes well the blend data with the pure stars from literature, whereas α=4/3 does not, irrespective of the method of obtaining the arm molecular weights. Thus, two different approaches for correcting for segmental friction among the star-1KL blends, namely using the ratio of high-frequency cross-

over frequencies $\Omega_{x,g,ratio}$ described in the main text and adjusting to isofrictional temperature conditions via WLF analysis, both lead to the conclusion that α=1, not α=4/3.

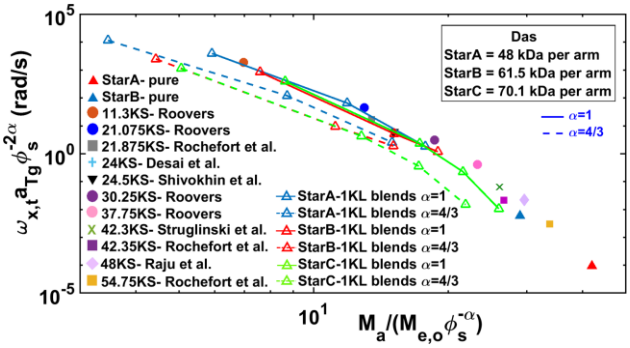

Figure 2.A22: The same as Figure 2.9 in the main text, except that the terminal cross-over frequency is adjusted to isofrictional temperature conditions. The star-1KL blends (open symbols) are compared with the pure StarA and StarB, as well as with a variety of pure stars obtained from literature (closed symbols).[41, 59, 62-64] In this Figure, the star arm molecular weights of the pure StarA, StarB, and StarC were determined by fitting the Hierarchical model with Das parameters. The pure stars were obtained from literature.

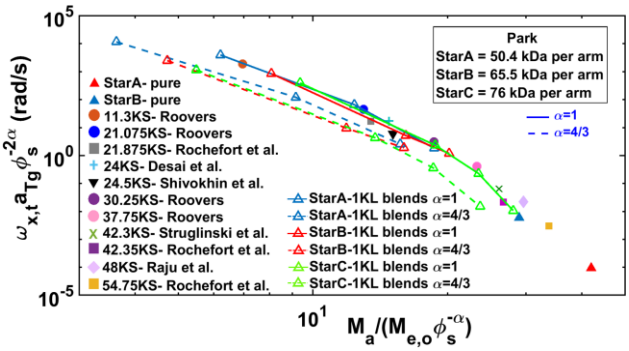

Figure 2.A23: The same as Figure 2.A22, except the molecular weights of the pure StarA, StarB, and StarC were obtained from Hierarchical model fits using the Park parameters.

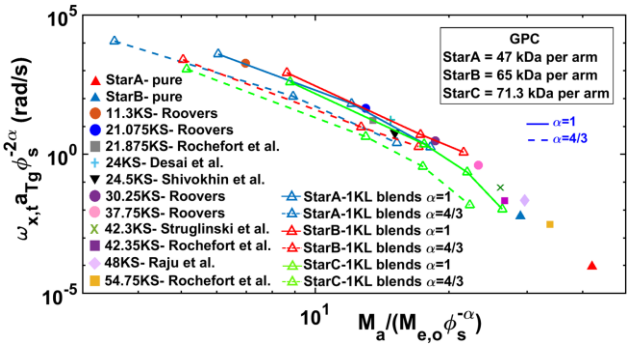

Figure 2.A24: The same as Figure 2.A22, except the molecular weights of the pure StarA, StarB, and StarC were obtained from GPC analysis.

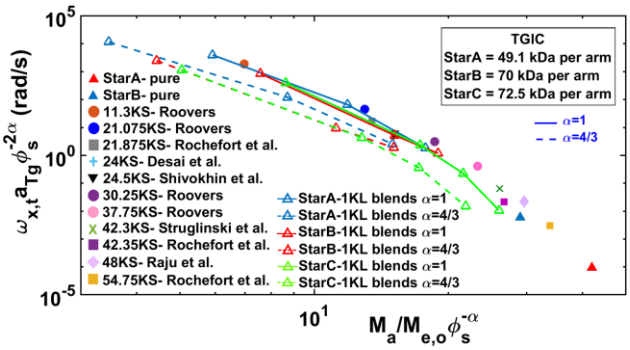

Figure 2.A25: The same as Figure 2.A22, except the molecular weights of the pure StarA, StarB, and StarC were obtained from TGIC analysis.

V.2.vi Cross-Comparison of Star-1KL Blends

Figures 2.A26- 2.A29 features data for blends with different star polymers at star volume fraction (ϕ_s) of 0.6, 0.5, 0.4, and 0.2, respectively. By restricting each plot to a single star volume fraction (ϕ_s), data on each of these figures should share the same plateau modulus (G_N^o), entanglement spacing (M_e) and the equilibration time (τ_e), as defined by Eq. 1-3 in the main paper. Consistent with this, we observe in Figure 2.A26 near perfect superposition of data in the glass transition region and in the plateau region at frequencies near the intermediate G' /G" cross-over in blends of StarA-1KL and StarC-1KL with star volume fraction ϕ_s = 0.6. The close superposition of linear rheological data in the glassy and plateau regions shows that the rheology is nearly independent star arm molecular weight, as expected. The influence of arm molecular weight only becomes apparent at lower frequencies, as can be seen from the deviation of the StarA-1KL(ϕ_s = 0.6) and StarB-1KL(ϕ_s = 0.6) linear rheology at frequencies below 10^5 rad/s in Figure 2.A26. These observations in Figure 2.A26 can also be seen in subsequent plots featured in Figures 2.A27- 2.A29. As a final note, the close superposition of the glass transition region

among Star-1KL blends of equal star volume fractions is also an indication of reasonably valid horizontal and vertical shifting of G' and G" linear rheology over a range of temperatures.

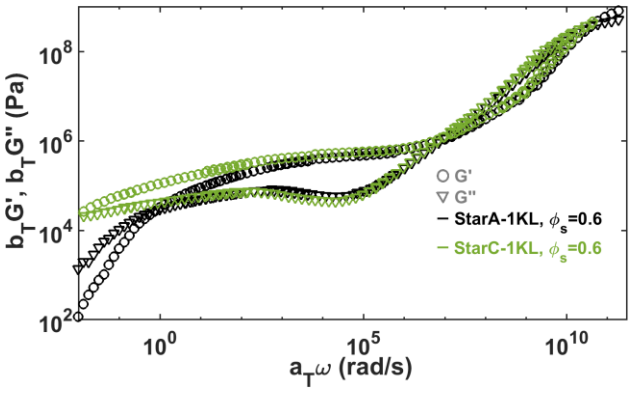

Figure 2.A26: G' and G" linear rheology for blends of StarA and StarC with 1KL linear at star volume fraction ϕ_s = 0.6.

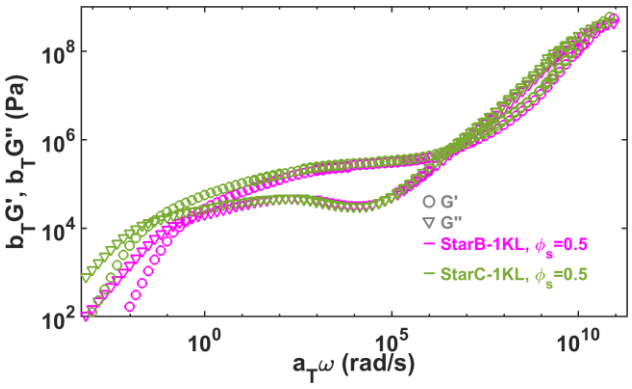

Figure 2.A27: The same as Figure 2.A26, but for StarB and StarC at star volume fraction ϕ_s= 0.5

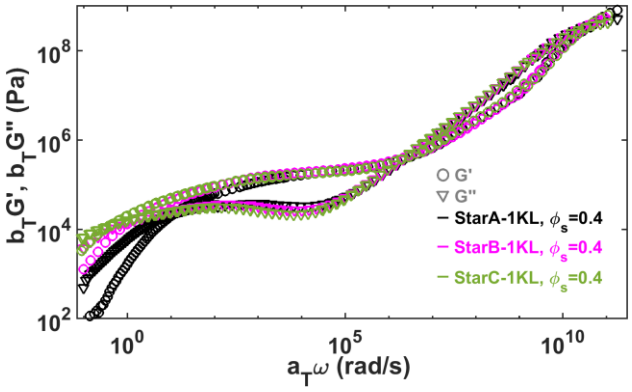

Figure 2.A28: The same as Figure 2.A26, but for all three stars at star volume fraction ϕ_s= 0.4

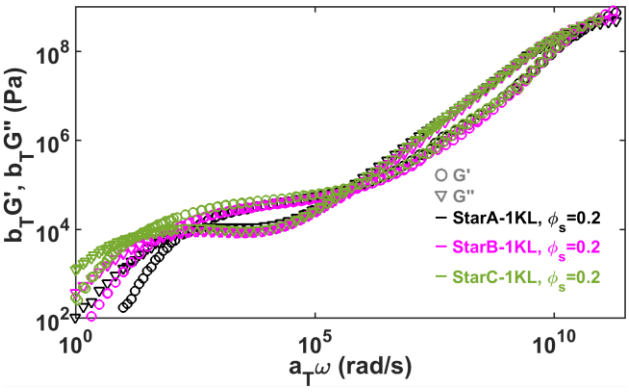

Figure 2.A29: The same as Figure 2.A26, but for all three stars at star volume fraction ϕ_s = 0.2

VI. References

[1] Doi, M.; Edwards, SF. Dynamics of Concentrated Polymer Systems Part 1: Brownian Motion in the Equilibrium State. *J. Chem Soc., Faraday Trans. 2* **1978**, 74, 1789-1801

[2] Doi, M.; Edwards, SF. Dynamics of Concentrated Polymer Systems Part 2: Molecular Motion Under Flow. *J. Chem Soc., Faraday Trans. 2* **1978**, 74, 1802-1817

[3] Doi, M.; Edwards, SF. Dynamics of Concentrated Polymer Systems Part 3: The Constitutive Equation. *J. Chem Soc., Faraday Trans. 2* **1978**, 74, 1818-1832

[4] Doi, M.; Edwards, SF. Dynamics of Concentrated Polymer Systems Part 4: Rheological Properties. *J. Chem Soc., Faraday Trans. 2* **1979**, 73, 38-54

[5] de Gennes, P.G. Reptation of a Polymer Chain in the Presence of Fixed Obstacles. *J. Chem. Phys.* **1971**, 55, 572

[6] Tuminello, W.H. Molecular Weight and Molecular Weight Distribution from Dynamic Measurements of Polymer Melts. *Polym. Eng. Sci.* **1986**, 26, 1339-1347

[7] Tsenoglou, C. Viscoelasticity of Binary Homopolymer Blends. *ACS Polym. Prepr.* **1987**, 8, 185-186

[8] des Cloizeaux, J. Double Reptation vs. Simple Reptation in Polymer Melts. *Europhys. Lett.* **1988**, 6 (5), 437-442

[9] Klein, J. The Onset of Entangled Behavior in Semidilute and Concentrated Polymer Solutions. *Macromolecules* **1978**, 11 (5), 852-858

[10] Viovy, J.; Rubinstein, M.; Colby, R. Constraint Release in Polymer Melts: Tube Reorganization versus Tube Dilation. *Macromolecules* **1991**, 24, 3587-3596

[11] Daoud, M.; de Gennes, P.G. Some Remarks on the Dynamics of Polymer Melts. *J. Polym. Sci.: Polym. Phys. Ed.* **1979**, 17, 1971-1981

[12] de Gennes, P.G. Scaling Theory of Polymer Absorption. *Journal de Physique* **1976**, 37 (12), 1445-1452

[13] de Gennes, P.G. Dynamics of Entangled Polymer Solutions. II. Inclusion of Hydrodynamic Interactions. *Macromolecules* **1976**, 9 (4), 594- 598

[14] O'Connor, N.P.T.; Ball, R.C. Confirmation of the Doi-Edwards Model. *Macromolecules* **1992**, 25, 5677-5682

[15] Rubinstein, M. Discretized Model of Entangled-Polymer Dynamics. *Phys. Rev. Lett.* **1987**, 59 (17), 1946-1949

[16] Marrucci, G. Relaxation by Reptation and Tube Enlargement: A Model for Polydisperse Polymers. *J. of Polym. Sci.: Polym. Phys. Ed.* **1985**, 23, 159-177

[17] Ball, R.C.; McLeish, T.C.B. Dynamic Dilution and the Viscosity of Star-Polymer Melts. *Macromolecules* **1989**, 22, 1911-1913

[18] Milner, S.T.; McLeish, T.C.B.; Young, R.N.; Hakiki, A.; Johnson, J.M. Dynamic Dilution, Constraint-Release, and Star-Linear Blends. *Macromolecules* **1998**, 31, 9345-9353

[19] Larson, R.G. Combinatorial Rheology of Branched Polymer Melts. *Macromolecules* **2001**, 34, 4556-4571

[20] Park, S.J.; Sachin, S.; Larson, R.G. A Hierarchical Algorithm for Predicting the Linear Viscoelastic Properties of Polymer Melts with Long-Chain Branching. *Rheol Acta* **2005**, 44, 319-330

[21] Wang, Z.; Xue, C.; and Larson, R.G. Comparing Tube Models for Predicting the Linear Rheology of Branched Polymer Melts. *J. Rheol* **2010**, 54, 223-260

[22] Das, C.; Inkson, N.J.; Read, D.J.; Kelmanson, M.A.; McLeish, T.C.B. Computational Linear Rheology of General Branch-on-Branch Polymers. *J. Rheol* **2006**, 50 (2), 207-234

[23] Ebrahimi, T.; Taghipour, H.; Grießl, D.; Mehrkhodavandi, P.; Hatzikiriakos, S.G; van Ruymbeke, E. Binary Blends of Entangled Star and Linear Poly(hydroxybutyrate): Effect of Constraint Release and Dynamic Tube Dilation. *Macromolecules* **2017**, 50, 2535-2546

[24] Doi, M.; Graessley, W.W.; Helfand, E.; Pearson, D.S. Dynamics of Polymers in Polydisperse Melts. *Macromolecules* **1987**, 20, 1900-1906

[25] Watanabe, H.; Ishida, S.; Matsumiya, Y.; Inoue, T. Viscoelastic and Dielectric Behavior of Entangled Blends of Linear Polyisoprenes having Widely Separated Molecular Weights. *Macromolecules* **2004**, 37, 1937-1951

[26] Watanabe, H.; Ishida, S., Matsumiya, Y.; and Inoue, T. Test of Full and Partial Tube Dilation Pictures in Entangled Blends of Linear Polyisoprenes. *Macromolecules* **2004**, 37, 6619-6631

[27] Huang, Q.; Hengeller, L.; Alvarez, N.J.; Hassager, O. Bridging the Gap between Polymer Melts and Solutions in Extensional Rheology. *Macromolecules* **2015**, 48, 4158-4163

[28] Milner, S.T. Predicting the Tube Diameter in Melts and Solutions. *Macromolecules* **2005**, 38, 4929-4939

[29] Colby, R.H.; Rubinstein, M. Two-Parameter Scaling for Polymers in Θ Solvents. *Macromolecules* **1990**, 23, 2733-2737

[30] Park, S.J.; Larson, R.G. Modeling the Linear Viscoelastic Properties of Metallocene-Catalyzed High Density Polyethylenes with Long-Chain Branching. *J. Rheol.* **2005**, 49, 523-536

[31] Park, S.J.; Larson, R.G. Tube Dilation and Reptation in Binary Blends of Monodisperse Linear Polymers. *Macromolecules* **2004**, 37, 597-604

[32] Park, S.J.; Larson, R.G. Dilution Exponent in the Dynamic Dilution Theory for Polymer Melts. *J. Rheol.* **2003**, 47, 199-211

[33] Milner, S.T.; McLeish, T.C.B. Parameter-Free Theory for Stress Relaxation in Star Polymer Melts. *Macromolecules* **1997**, 30, 2159-2166

[34] Daniels, D.R.; McLeish, T.C.B.; Kant, R.; Crosby, B.J.; Young, R.N.; Pryke, A.; Allgaier, J.; Groves, D.J.; Hawkins, R.J. Linear Rheology of Diluted Linear, Star and Model Long Chain Branched Polymer Melts. *Rheol. Acta* **2001**, 40, 403-415

[35] Raju, V.R.; Menezes, E.V.; Marin, G.; Graessley, W.W.; Fetters, L.J. Concentration and Molecular Weight Dependence of Viscoelastic Properties in Linear and Star Polymers. *Macromolecules* **1981**, 14, 1668-1676

[36] Tao, H.; Huang, C.; Lodge, T.P. Correlation Length and Entanglement Spacing in Concentrated Hydrogenated Polybutadiene Solutions. *Macromolecules* **1999**, 32, 1212-1217

[37] Brochard, F.; de Gennes, P.G. Dynamical Scaling for Polymers in Theta Solvents. *Macromolecules* **1977**, 10 (5), 1157-1161

[38] van Ruymbeke, E.; Masubuchi, Y.; Watanabe, H. Effective Value of the Dynamic Dilution Exponent in Bidisperse Linear Polymers: From 1 to 4/3. *Macromolecules* **2012**, 45, 2085-2098

[39] van Ruymbeke, E.; Shchetnikava, V.; Matsumiya, Y.; Watanabe, H. Dynamic Dilution Effect in Binary Blends of Linear Polymers with Well-Separated Molecular Weights. *Macromolecules* **2014**, 47, 7653-7665

[40] Shahid, T.; Huang, Q.; Oosterlinck, F.; Clasen, C.; van Ruymbeke, E. Dynamic Dilution Exponent in Monodisperse Entangled Polymer Solutions. *Soft Matter* **2017**, 13, 269-282

[41] Desai, P.S.; Kang B; Katzarova, M.; Hall, R.; Huang, Q.; Lee, S.; Shivokhin, M.; Chang, T.; Venerus, D.C.; Mays, J.; Schieber, J.D.; Larson, R.G. Challenging Tube and Slip-Link Models: predicting the Linear Rheology of Blends of Well-Characterized Star and Linear 1,4-Polybutadienes. *Macromolecules* **2016**, 49 (13), 4964-4977

[42] Andreev, M; Khaliullin, R.N.; Steenbakkers, R.J.; Schieber, J.D. Approximations of the Discrete Slip-Link Model and their Effect on Nonlinear Rheology Predictions. *J. Rheol.* **2013**, 57, 535-557

[43] Schieber, J.D. Fluctuations in Entanglements of Polymer Liquids. *J. Chem. Phys.* **2003**, 5162-5166

[44] Khaliullin, R.N.; Schieber J.D. Self-Consistent Modeling of Constraint Release in a Single-Chain Mean-Field Slip-Link Model. *Macromolecules* **2009**, 42 (19), 7304-7317

[45] Neergaard, J.; Schieber, J.D. A Full-Chain Network Model with Sliplinks and Binary Constraint Release. *Proc. XIIIth Intl. Cong. Rheol.* **2000**

[46] Schieber, J.D; Neergaard, J.; Gupta, S. A Full-Chain, Temporary Network Model with Sliplinks, Chain-Length Fluctuations, Chain Connectivity and Chain Stretching. *J. Rheol.* **2003**, 47, 213-233

[47] Schieber, J.D. GENERIC Compliance of a Temporary Network Model with Sliplinks, Chain-Length Fluctuations, Segment-Connectivity and Constraint Release. *J. Non-Equilib. Thermodyn.* **2003**, 28, 179-188

[48] Heo, Y.; Larson, R.G. The Scaling of Zero-Shear Viscosities of Semidilute Polymer Solutions with Concentration. *J. Rheol* **2005**, 49, 1117-1128

[49] Lipson, J.E.G.; Milner, S.T. Multiple Glass Transitions and Local Composition Effects on Polymer Solvent Mixtures. *J. Poly Sci: Part B: Polym Phys* **2006**, 44, 3528-3545

[50] McLeish, T. Tube Theory of entangled Polymer Dynamics. *J. Adv. Phys.* **2002**, 51 (6), 1379-1527

[51] Larson, R.G.; Sridhar, T.; Leal, L.G.; McKinley, G.H.; Likhtman, A.E.; McLeish, T.C.B. Definitions of Entanglement Spacing and Time Constants in the Tube Model. *Rheol* **2003**, 47, 809-818

[52] Hadjichristidis, N.; Iatrou, H.; Pispas, S.; Pitsikalis, M. Anionic Polymerization: High Vacuum Techniques. *J. Polym Sci A: Polym. Chem.* **2000,** *38*, 3211

[53] Hadjichristidis, N; Roovers, J. Linear Viscoelastic Properties of Mixtures of 3- and 4-arm Polybutadiene Stars. *Polymer*, **1985,** 26, 1087

[54] Polymeropoulos, G.; Zapsas, G.; Ntetsikas, K.; Bilalis, P.; Gnanou, Y.; and Hadjichristidis, N. 50th Anniversary perspective: Polymers with Complex Architectures. *Macromolecules* **2017**, 50, 1253

[55] Park, S.J.; Desai, P.S.; Chen, X.; Larson, R.G. Universal Relaxation Behavior of Entangled 1,4-Polybutadiene Melts in the Transition Frequency Region. *Macromolecules* **2015**, 48, 4122-4131

[56] Palade, L.I.; Verney, V.; Attané, P. Time-Temperature Superposition and Linear Viscoelasticity of Polybutadienes. *Macromolecules* **1995**, 28, 7051-7057

[57] Colby, R.H.; Fetters, L.J.; Graessley, W.W. The Melt Viscosity-Molecular Weight Relationship for Linear Polymers. *Macromolecules* **1987,** 20 (9), 2226-2237

[58] Li, S.W.; Park, H.E.; Dealy, J.M. Evaluation of Molecular Linear Viscoelastic Models for Polydisperse H Polybutadienes. *J. Rheol.* **2011**, 55 (6), 1341-1373

[59] Shivokhin, M.E.; van Ruymbeke, E.; Bailly, C.; Kouloumasis, D.; Hadjichristidis, N.; Likhtman, A.E. Understanding Constraint Release in Star/Linear Polymer Blends. *Macromolecules* **2014**, 47 (7), 2451-2463

[60] Miros, A.; Vlassopoulos, D.; Likhtman, A.E.; and Roovers, J. Linear Rheology of Multiarm Star Polymers Diluted with Short Linear Chains. *J. Rheol.* **2003**, 47 (1), 163-176

[61] Wagner, M.H. Scaling Relations for Elongational Flow of Polystyrene Melts and Concentrated Solutions of Polystyrene in Oligomeric Styrene. *Rheological Acta* **2014,** 53, 765-777.

[62] Roovers, J. Properties of the Plateau Zone of Star-branched Polybutadienes and Polystyrenes. *Polymer* **1985**, 26, 1091-1095

[63] Rochefort, W.E.; Smith, G.G.; Rachapudy, H.; Raju, V.R.; Graessley, W.W. Properties of Amorphous and Crystallizable Hydrocarbon Polymers. II. Rheology of Linear and Star-Branched Polybutadiene. *J. Poly Sci.* **1979**, 17, 1197-1210

[64] Struglinski, M.J.; Graessley, W.W.; Fetters, L.J. Effects of Polydispersity on the Linear Viscoelastic Properties of Entangled Polymers. 3. Experimental Observations on Binary Mixtures of Linear and Star Polybutadienes. *Macromolecules* **1988**, 21, 783-789

[65] Matsumiya, Y.; Kumazawa, K.; Nagao, M.; Urakawa, O.; Watanabe, H. Dielectric relaxation of Monodisperse Linear Polyisoprene: Contribution of Constraint Release. *Macromolecules* **2013**, 46, 6067-6080

[66] Uhrig, D.; Mays, J.W. Experimental Techniques in High-Vacuum Anionic Polymerization. *J Polym Sci Part A: Polym Chem* **2005**, 43, 6179–6222

[67] Chang, T. Polymer Characterization by Interaction Chromatography. *J. Polym. Sci. Part B: Polym. Phys*. **2005**, 43, 1591

[68] Ryu, J.; Chang, T. Thermodynamic Prediction of Polymer Retention in Temperature-Programmed HPLC. *Anal. Chem*. **2005**, 77, 6347

[69] Lee, W.; Park, S.; Chang, T. Liquid Chromatography at the Critical Condition for Polyisoprene using a Single Solvent. *Anal. Chem*. **2001**, 73, 3884

[70] van Gurp, M.; Palmen, J. Time-Temperature Superposition for Polymeric Blends. *Rheol Bull*. **1998**, 67, 5-8

[71] Graessley, W.W. Effect of Long Branches on the Temperature Dependence of Viscoelastic Properties in Polymer Melts. *Macromolecules* **1982**, 15, 1164-1167

[72] Levine, A.J.; Milner, S.T. Star Polymers and the Failure of Time-Temperature Superposition. *Macromolecules* **1998**, 31, 8623-8637

[73] Trinkle, S.; Walter, P.; Friedrich, C. Van Gurp-Palmen Plot II-Classification of Long Chain Branched Polymers by their Topology. *Rheol Acta* **2002**, 41, 103-113.

Chapter 3: Assessing the Range of Validity of Current Tube Models Through Analysis of a Comprehensive Set of Star-Linear 1,4-Polybutadiene Polymer Blends

Disclosure: Text and figures in this chapter are reprinted from the manuscript- Hall, R.; Desai, P.S.; Kang, B.-G.; Huang, Q.; Lee, S.; Chang, T.; Venerus, D.C.; Mays, J.; Ntetsikas, K.; Polymeropoulos, G.; Hadjichristidis, N.; Larson, R.G. *Macromolecules* (under review)

I. Introduction

The well-known tube model is able to describe nearly quantitatively the relaxation of nearly monodisperse linear polymers using a combination of reptation and contour-length fluctuations.[1-7] These relaxation processes involve sliding motions, namely reptation and contour-length fluctuations (CLFs), within a tube-like region defined by the entanglements of an arbitrary chain (*i.e.*, the "probe" chain) with surrounding chains. To describe bidisperse or polydisperse linear polymers, "constraint-release Rouse" (CR-Rouse) dynamics must be added, in which repeated motions of short chains allow the tubes surrounding long chains to migrate. For monodisperse star polymers, constraint release is described by dynamic dilution, a.k.a. "dynamic tube dilation" (DTD), which allows the tube to enlarge its diameter in response to constraint release. Thorough discussions of these mechanisms can be found elsewhere.[8-16]

Using both CR-Rouse relaxation and DTD, Milner et al.[17] sought to use tube theory to predict the linear rheology of binary star-linear blends. The 1,4-polybutadiene blend set considered in their work was a linear chain of molecular weight 100,000 Da (hereby referred to as "105KL," where "K" represents molecular weight in kDa and "L" indicates linear polymeric

architecture) blended at different volume fractions with a three-arm star of arm molecular weight 42,300 Da (hereby referred to as "42.3KS," where "K" represents molecular weight in kDa and "S" indicates star polymeric architecture), which were synthesized and studied by Struglinski et al.[18] In these blends, the linear component relaxes much faster by reptation than the star arm does by contour length fluctuations. In the blend of the two, once the linear component relaxes, Milner et al.[17] proposed that the blend undergoes CR-Rouse relaxation, in which the unrelaxed star arm explores a "fat tube" whose diameter is defined by star-star entanglements. During this exploration, Milner et al. assumed that contour length fluctuations of the star arm are unimportant and can be taken to cease, but resume once exploration of the "fat tube" is complete; whereupon, the star arm resumes its contour length fluctuation until it relaxes completely. Thus, during the CR-Rouse regime, the star arm is considered to be "frozen." While this "arm frozen" assumption seemed to yield good agreement between the tube model and this particular set of experimental data, the freezing of the arm fluctuations during CR-Rouse relaxation is artificial. An alternative is to allow the slower species to undergo fluctuations within the original "thin tube" - that is the undilated tube defined by all entanglements of the chain with surrounding chains. The final, "fat tube," option allows the slower chain to fluctuate in a dilated tube whose diameter is at each instant defined by the constraint-release process itself. There has been controversy over which CR-Rouse criterion is most appropriate for star-linear blends. In addition to these options for arm fluctuations during CR-Rouse relaxation, there is in the Hierarchical model the possibility of allowing a "disentanglement relaxation" to occur when a species (typically a star polymer) has had its entanglement density diluted by constraint release to around 1-3 remaining diluted entanglements. Thus, there are multiple versions of the tube model, involving various assumptions and approximations.[19-23]

The seeming success of some versions of the tube model to describe linear and star polymers and their blends has inspired the development of generalized tube models to describe the linear rheology of arbitrary blends of linear and branched species. The Hierarchical 3.0 model, originally developed by Larson and further refined over the years by Park et al.[21] and Wang et al.,[20] and the "BoB" (or Branch-on-Branch) model[23] are two models that extend the work of Milner et al.,[16, 17] allowing the prediction of the rheology of mixtures of polymers of varying branched architectures. In addition, the "Time-Marching Algorithm" with similar physics, implemented somewhat differently, has been introduced recently by van Ruymbeke and coworkers.[24] Previous work has shown that these models can in many cases predict the rheology of asymmetric polyisoprene stars,[21, 24] H polymers,[21, 25] pom-pom polymers,[19, 25] comb polymers,[19, 21, 26] bidisperse linear 1,4-polybutadiene blends,[22] monodisperse star and linear polymers,[19, 24] and metallocene-catalyzed high density polyethylene.[27] However, these "successful" predictions have involved various choices of assumptions, such as the "arm frozen," "thin tube," and "fat tube" assumptions for fluctuations during CR-Rouse relaxation; "disentanglement" mechanisms; and choices of modeling parameters, including the choice of the so-called dilution exponent that determines the relationship between the degree of disentanglement and the diameter of the dilated tube. Various authors, using different software packages, applied to different polymer blends, have found that the assumptions and parameter values necessary to obtain "successful" predictions vary from one polymer mixture to another.[17-28] For star-linear blends, the Hierarchical and BoB models, both using the "thin tube" assumption and no "disentanglement," have very similar physics and give quite similar predictions for a given set of parameter values.[29]

To examine tube models and the assumptions within them more rigorously, with less freedom to obtain agreement with data through choice of model assumptions and parameters, Desai et al.[29] studied a new set of 1,4-polybutadiene star-linear blends consisting of a 4-arm star with arm molecular weight 24 kDa blended with a linear polymer of molecular weight 58 kDa, hereby referred to as "24KS" and "58KL" respectively. This 24KS-58KL blend set provides an alternative to the earlier 1,4-polybutadiene 42.3KS-105KL set of blends studied by Milner et al.[17] In addition, a third set of 1,4-polybutadiene blends was recently studied by Shivokhin et al.,[30] which consisted of a three-arm star with arm molecular weight of around 24.5 kDa, mixed with a low molecular linear chain of molecular weight 7.5 kDa, here referred to as 24.5KS-7.5KL. (We note that Desai et al. modeled the Shivokhin et al. data using star arm and linear molecular weights of 27.4 kDa and 6.9 kDa, respectively, for reasons discussed in their paper.) Since all three of these sets of blends are of nearly identical 1,4-polybutadiene chemistry, the same tube model with the same parameters ought to provide fits to the data for all three sets of data, at the same temperature. Although the Hierarchical version of the tube model was in fact able to predict the pure star and linear components, the model was not able to predict, even approximately, the rheology of the 24KS-58KL blend set, except by invoking the disentanglement mechanism discussed above. But invoking this mechanism led to massive failure to predict the rheology of the 24.5KS-7.5KL blends studied by Shivokhin et al. Thus, no single tube model was able to provide a good fit to all the (then) available data on star-linear blends of 1,4-polybutadienes. However, in the wake of the Hierarchical model's failure, a slip-link model from Schieber and coworkers[31, 32, 33] called the Clustered Fixed Slip-link Model (CFSM) was shown by Desai et al.[29] to be successful in modeling both the 24KS-58KL and the 24.5KS-7.5KL data sets, using a common set of model parameters and no ad hoc adjustments to

the model. The success of the CFSM suggests that it captures key physics that the Hierarchical model is missing and/or misrepresenting.

This slip-link model, developed by Schieber and coworkers,[31, 32, 33] unlike the tube model, does not require separate mathematical equations to account for various relaxation mechanisms. Instead of using a "tube" to represent a *mean-field* of constraints on a probe chain, the slip-link model confines the probe chain with "slip-links," which represent *discrete, local* constraints. An early version of the slip-link model, known as the Discrete Slip-link Model (DSM), discretizes the chain at the level of Kuhn steps, whose configuration at rest is a random walk. The DSM tracks the motion of these Kuhn steps as they "shuffle" diffusively between entanglement points (slip-links). Due to this more localized description of entanglements, the slip-link model does not need to consider explicitly multiple relaxation mechanisms such as "tube dilation" or dynamic dilution. However, it is computationally slow, limiting the polymer chain lengths that can be modeled. To help speed-up the computations, the "Clustered Fixed Slip-link Model,"[34, 35] or CFSM, was developed, which lumps multiple Kuhn steps into clusters. This reduces the computational time and increases the maximum arm length of a star-branched polymer that can be considered to roughly 20 entanglements, instead of 5 -10. While this simplification allows the slip-link model to be applied to the 24KS-58KL and the 24.5KS-7.5KL blends, which respectively have star polymers with arm lengths of 24 and 24.5 kDa, it cannot yet be applied to blends with longer star arms, such as the 42.3 kDa star-arms studied by Milner et al.[17]

To address the difficulties in the tube model, detailed studies[36-40] have been conducted to better understand constraint-release physics, in particular dynamic dilution, which is critical for describing the relaxation of branched polymers and polydisperse linear polymers. CR-Rouse

physics, mentioned above, is often implemented in conjunction with dynamic dilution to better describe the relaxation of binary blends of linear polymers[22] and star-linear blends.[17, 19, 20, 24, 29] For branched polymers, deep contour fluctuations (CLFs) of each branch are required for it to achieve terminal relaxation, since, unlike linear polymers, branched polymers are unable to undergo reptation due to the presence of branch points. Thus, the arms of a branched molecule must retract inward towards the branch point, starting from the chain end, to escape entanglements imposed by neighboring chains. Although this deep CLF process is entropically slow, experimental rheological data for pure star-shaped molecules suggest that the arm retraction process is much faster than expected based on CLF alone.[15] Ball and McLeish then proposed that, after initial rapid relaxation of the tips of the arms, the entanglements of these arm tips with the unrelaxed portion of a test-chain arm are also relaxed rapidly and thereby accelerate the deep CLF relaxation of the remaining entangled portion of the test-chain arm. This process is called "dynamic dilution" since the rapidly relaxing arm tips act as solvent. A key parameter that controls the rate of dynamic dilution is the dilution exponent, α, whose value, thought to be either α=1 or α=4/3, has been highly debated for over 20 years.[16-24, 28, 29, 41-44] Different versions of the tube model have used different values of α to fit experimental rheology data.

A recent study by our group[40] attempted to determine the correct value of the dilution exponent value (α) by measuring the linear rheology of blends of 1,4-polybutadiene 4-arm stars mixed with various volume fractions of unentangled linear 1,4-polybutadiene with a molecular weight 1 kDa ("1KL"). Unlike most previous studies, this work sought to determine α without relying on a particular tube model, by assuming that the material-dependent parameters controlling the rheology are limited to the plateau modulus (G_N^0), the tube-segment frictional Rouse time (τ_e), and the number of entanglements per star arm (Z), which are the parameters

present in all tube models. Plots of the terminal crossover frequency $\omega_{x,t}$ of the storage and loss moduli, multiplied by the frictional equilibration time τ_e, against the number of entanglements per chain Z for these star-1KL blends collapsed onto corresponding data for 1,4-polybutadiene star melts only for α=1, and not for α=4/3. Other recent studies of Shahid et al.,[38] Huang et al.[39] and van Ruymbeke and Watanabe[36,37] also support this finding that α =1.

Our goals for this present study are to further test the tube model and to find more precisely the conditions under which the Hierarchical 3.0 model fails. In light of recent work suggesting that the dilution exponent (α) is equal to unity, we specifically test the accuracy of Hierarchical model predictions implemented with the "Das" model parameters, which is a commonly used parameter set for 1,4-polybutadienes at 25° C in which α is taken to be unity, and we also implement the commonly used "thin tube" assumption. (A thorough comparison of the predictions of the Hierarchical model using "thin tube," "fat tube," and "arm frozen" CR-Rouse assumptions against experimental linear rheology data for star-linear 1,4-polybutadiene blends was previously presented in Desai et al.[29]) In addition, we also provide in this study multiple sets of "benchmark" data that should both inspire improvements in the tube model and allow tests of additional versions of the tube model that might be developed in the future.

For completeness, this paper will feature 1,4-polybutadiene star-linear data for both newly synthesized and characterized materials and data already in the literature, which includes the 24KS-58KL, 24.5KS-7.5KL, and 42.3KS-105KL data sets referred to above from Desai et al.,[29] Shivokhin et al.[30] and Struglinski et al.[18] The new 1,4-polybutadiene blends studied here include the same 4-armed 24 kDa star featured in Desai et al., but here mixed with both a 13.3 kDa linear and a 210 kDa linear 1,4-polybutadiene. These blends are labeled 24KS-13.3KL and 24KS-210KL, respectively. The other new 1,4-polybutadiene star-linear blends contain 4-arm

stars of 25.3 kDa per arm (referenced as “25.3KS”), 44 kDa per arm (referenced as “44KS”), and 47 kDa per arm (referenced as “47KS”). The synthesis and characterization of all new 1,4-polybutadiene stars (25.3KS, 44KS, and 47KS) are described here. The 25.3KS star is blended with a 73 kDa linear (“73KL”) and a 260 kDa linear (“260KL”), while the 44KS star is blended with a 13.3 kDa linear (“13.3KL”), the same linear that is also blended with the 24KS. The 47KS star is blended with two different linear 1,4-polybutadienes of molecular weights 73 kDa (“73KL”) and 260 kDa (“260KL”); these are the same linear polymers that are blended with the 25.3KS sample. In total, these seven new sets of blends, combined with the three previous sets mentioned above, provide us with ten separate sets of star-linear blends, each containing three or four blend compositions, providing us almost 60 sets of linear rheology data. This large collection will enable a thorough assessment of not only the Hierarchical 3.0 model, but also any other rheological model, tube or otherwise, that might be developed in the future. Note that all these data sets are for 1,4-polybutadiene star-linear blends at reference temperature 25° C. Thus, to be considered completely successful, a model must predict all these sets with the same material input parameters, which is an unlikely feat if the model does not accurately capture all of the important physics. This is especially so since data for star-linear blends have proven to be the most difficult to predict using tube models.

This manuscript is organized as follows. Section II describes the synthesis, preparation and characterization of the new 1,4-polybutadiene samples featured here, as well as the methods of blending and rheological testing of the samples. In Section III, the theoretical and computational methods based on the Hierarchical 3.0 tube model are summarized briefly. The results and discussion are presented in Section IV, including the horizontal shift factors obtained when generating master curves of the experimental data, along with an analysis of the associated

zero-shear viscosities of the data sets. The linear rheology master curves are then plotted along with predictions of the Hierarchical 3.0 model for comparison. Section V reports the conclusions.

II. Materials and Experimental Methods

II.1. Materials

Six star and five linear 1,4-polybutadienes are featured in this study. Four of the star polymers are composed of four arms, while the other two have three arms. The 4-armed star 1,4-polybutadiene molecules have arm molecular weights of 24 kDa, 25.3 kDa, 44 kDa and 47 kDa; we will refer to these stars as "24KS," "25.3KS," "44KS," and "47KS," respectively, where "K" represents "kDa" and "S" represents "star"; the number represents the molecular weight of the arm. The 24KS, 25.3KS, 44KS and 47KS samples were synthesized carefully and characterized by Gel Permeation Chromatography (GPC). In addition to GPC, the 24KS and 44KS samples were also subjected to characterization by Temperature Gradient Interaction Chromatography (TGIC). The synthesis and characterization of 24KS are detailed in Desai et. al.,[29] while details concerning the 25.3KS, 42KS and 47KS can be found in the next section. Data and characterization for the 3-armed stars are given in published literature. Specifically, rheological data for the 3-armed star with arm molecular weight of 25.4 kDa (referenced as "25.4KS" in this paper) were taken from Shivokhin et al.[30] while data for the other 3-armed star with arm molecular weight of 42.3 kDa (referenced as "42.3KS") were taken from Struglinski et al.[18]

Three of the five linear 1,4-polybutadiene samples were purchased from Polymer Source. Two of these have molecular weights (as reported by the manufacturer) of 58 kDa (PDI = 1.03, referenced as 58KL where "L" represents "linear") and 210 kDa (PDI= 1.052, referenced as 210KL). As reported by Polymer Source, the composition of the 58 kDa sample consists of

68%1,4-cis; 27% 1,4-trans; and 5% 1,2-vinyl, and we assume that the composition of the 210KL sample is similar. The third linear sample from Polymer Source was initially reported to have a molecular weight of 18.2 kDa (PDI = 1.15); however, we determined through additional GPC testing that the molecular weight of this linear sample is around 13.3 kDa (PDI= 1.016 and hereby referred to here as 13.3KL), and through H-NMR, we determined the 1,2-vinyl content to be 12.5%. The data for the 100 kDa linear sample (referenced to as 105KL for consistency with the literature) were taken from Struglinski et. al.,[18] while data for the 7.5kDa sample (referenced as 7.5KL) were taken from Shivokhin et. al.[30]

The above listed star and linear 1,4-polybutadienes were combined, either in this study or in previous studies, to make the following star-linear blends: *24.5KS-7.5KL*, 24KS-13.3KL, *24KS-58KL*, 25.3KS-73KL**, 24KS-210KL, 25.3KS-260KL, *42.3KS-105KL*, 44KS-13.3KL, 47KS-73KL, and 47KS-260KL. The italicized blends in the above list were studied in previous papers while the other blend series were prepared for the current studies. The 25.3KS-73KL blends were generated and their rheology measured after the conclusions of the paper were drawn based on the other nine blend series to provide a test of these conclusions, as discussed below. This final blend series includes star volume fractions (ϕ_s) of 1, 0.9, 0.6, 0.3, 0.1 and 0. The 24.5KL-7.5KL blend series were prepared with star volume fractions ϕ_s= 1, 0.5, 0.2, 0.1, 0.02, and 0. The 24KS-13.3KL blend series consists of ϕ_s= 1, 0.8, 0.4, 0.1, and 0. For the 24KS-58KL and the 44KS-13.3KL blends, ϕ_s=1, 0.9, 0.8, 0.6, 0.4, 0.2, 0. For the 25.3KS- 210KL blend series, ϕ_s=1, 0.8, 0.6, 0.4, 0.2, 0.1, and 0. The 24KS-260KL blend series consists of ϕ_s=1, 0.8, 0.6, 0.4, 0.2, 0.05, 0. For the 42.3KS-105KL blends, ϕ_s=1, 0.75, 0.5, 0.3, 0.2, 0.1, and 0. Lastly, the 44KS-73KL and the 47KS-260KL blends consist of star volume fractions ϕ_s=1, 0.8, 0.6, 0.4, 0.2, and 0.

The star-linear 1,4-polybutadiene blends listed above, except for those from the literature (24.5KS-7.5KL, 24KS-58KL, and 42.3KS-105KL blends), were freshly prepared by first weighing out the pure star and pure linear components in accordance with the desired blend composition. The star and linear samples were then mixed with dichloromethane solvent (Sigma Aldrich) and stirred at room temperature within a fume hood. The resulting blend was left in the fume hood for one week to evaporate the dichloromethane. The blended sample was then transferred to a vacuum chamber for two weeks to completely remove excess solvent. The success of solvent removal was checked through a sniff test and by comparing the weight of the blend with its initial mass before solvent was added. Once the solvent was completely removed, the blend was stored in a freezer to await rheological testing.

II.2. Synthesis

The newly prepared 1,4-polybutadiene star and linear samples (*i.e.*, 73KL, 260KL, 25.3KS, 44KS, and 47KS) were synthesized by anionic polymerization high vacuum techniques and appropriate chlorosilane chemistry as described in our previous paper.[40] The synthetic procedures are given in Scheme 3.1A (linear) and 3.1B (stars). Details of the synthesis and molecular characterization are given in the Appendix. The synthesis and characterization of 1,4-polybutadiene stars that were taken from the literature, namely the 24KS, 24.5KS, and 42.3KS, are respectively reported in the works of Desai et al.,[29] Shivokhin et al.,[30] Struglinski et al.[18]

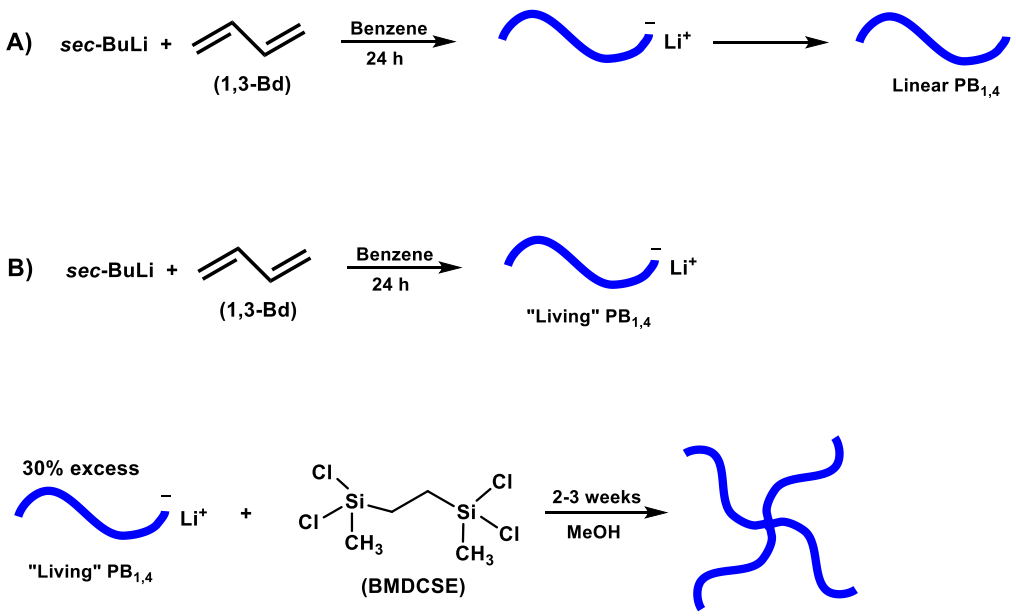

Scheme 3.1: General reactions for the synthesis of A) linear and B) 4-arm star 1,4-polybutadiene. **(Scheme provided by Nikos Hadjichristidis)**

II.3. Characterization

We report in Tables 3.1 and 3.2 the molecular weight, polydispersity and 1,2-vinyl content of the pure linear and pure star 1,4-polybutadienes presented in this study. Table 3.1 features the newly prepared linear and star samples, whereas Table 3.2 reports the star and linear 1,4-polybutadienes obtained from the literature. The data reported in both tables were obtained through gel permeation chromatography (GPC), temperature gradient interaction chromatography (TGIC), and proton nuclear magnetic resonance (^{1}H-NMR); details of these data can be found in the Appendix. As reported in the Results and Discussion Section IV.2, we checked the molecular weights of the new materials by comparing their zero-shear viscosities with those of other 1,4-polybutadienes in the literature.[42, 45-48] Also, in Section IV.1, we verify (or estimate in some cases) the 1,2-vinyl content, as reported by ^{1}H-NMR, of the pure star and pure linear samples by comparing the horizontal WLF shift factors of the linear rheology data with those of 1,4-polybutadienes from the literature.[30, 49-51]

In Table 3.1, we report the characterization of the newly synthesized (or purchased) pure star and pure linear 1,4-polybutadiene samples. We note that the GPC characterization by Polymer Source for the 13.3KL sample yielded a molecular weight of 18 kDa; however, we concluded that the molecular weight of the linear is instead 13.3 kDa from our own GPC testing. We verified this molecular weight by showing that its zero-shear viscosity (η_o) is in better agreement with the molecular weight dependence of the zero-shear viscosities of other 1,4-polybutadiene linear polymers collected from literature when we assign it a molecular weight of 13.3 kDa, rather than 18.2 kDa.

Also indicated in Table 3.1 are both the arm molecular weights of the freshly synthesized 4-arm 1,4-polybutadiene stars (*i.e.*, 25.3KS, 44KS, and 47KS), shown in parentheses, and the corresponding molecular weights of the linear arm precursors that were synthesized prior to the introduction of the branching reaction in Scheme 3.1A of the previous section. The molecular weight of the linear precursor is usually very close to that inferred by dividing the final star molecular weight by the number of arms (assumed to be four), although in one case (the 44KS sample) the difference is a factor of 1.2. For simplicity, we label these stars by the molecular weights of their linear precursors (*i.e.*, the 44KS has a linear precursor molecular weight of 44 kDa). We also note that only the 44KS sample was subjected to TGIC testing. TGIC is considerably more accurate than GPC in the characterization of branched polymers, since the technique is able to resolve peaks with different numbers of arms per polymer, which is generally not possible with GPC.[52-55] Although we do not have TGIC information for the 25.3KS and 47KS 1,4-polybutadiene star samples, we can check the length of the arms by comparing the zero-shear viscosities, which are obtainable through linear rheological testing, to those of other 1,4-polybutadiene stars in the literature. Note that the zero-shear viscosity is

highly sensitive to arm length but insensitive to the number of arms. Thus, nominally four-arm stars might have some three-arm impurities that will reduce the average molecular weight per arm, but not affect the viscosity. For this reason, using the molecular weight of the precursor arm is likely a better estimate of the arm molecular weight than is the total molecular weight of the star divided by four. Details regarding the zero-shear analysis will be presented in Results and Discussion Section IV.2, which confirm that the GPC characterizations of the arms of the 25.3KS and 47KS stars are reasonable.

Lastly, we note that the maximum polydispersity among all freshly synthesized star and linear 1,4-poybutadiene samples in Table 3.1 is 1.08, and that this highest polydispersity is for the relatively high-molecular-weight 260KL melt. The polydispersity of the final stars is somewhat higher than that of the individual arms, which suggests the presence of some dispersity in the number of arms per star in the final product. This supports our decision to use the precursor arm molecular weight rather than final molecular weight to estimate the arm molecular weight of the samples. In addition, the 1,2-vinyl contents of these samples are less than 10 wt%. We also note that the 210KL and 44KS samples were not subjected to ^{1}H-NMR testing; thus, the 1,2-vinyl contents for these samples are not explicitly known. However, as shown in Section IV.1, we are able to estimate the 1,2-vinyl contents of these samples by comparing their horizontal WLF shift factors, obtained from the time-temperature superposition, with those of 1,4-polybutadienes of known 1,2-vinyl content reported in literature.[30, 49-51]

Table 3.1: Arm molecular weight, polydispersity, and 1,2-vinyl content of the newly synthesized or acquired star and linear 1,4-polybutadienes, obtained through GPC, TGIC, and ^{1}H-NMR.

Sample Name	***Architecture***	***[(a)] Mw^{GPC} (kDa)***	***[(a)] Mw^{TGIC} (kDa)***	***[(b)] Mw/Mn^{GPC}***	***1,2-vinyl content (^{1}H-NMR) (% wt)***
[(c)]13.3KL	Linear	13.3	-----	1.02	7

73KL	Linear	73	-----	1.04	8
[c]210KL	Linear	210	-----	1.05	-----
260KL	Linear	260	-----	1.08	7
25.3KS	4-arm Star (from star)	25.3 (24.6)	-----	1.03 (1.05)	8
44KS	4-arm Star (from star)	44 (36.5)	44 (38.5)	1.07	-----
47KS	4-arm Star (from star)	47 (45.8)	-----	1.05 (1.07)	8

(a) In parentheses is the molecular weight per star arm obtained by dividing molecular weight (Mw) of the entire star by 4. Above this is the molecular weight of the linear precursor as determined by GPC using a light scattering detector.
(b) In parentheses is the polydispersity of the star. Above this is the polydispersity of the linear precursor.
(c) Polymer purchased from Polymer Source.

For completeness, we present in Table 3.2 the characterization results for 1,4-polybutadiene star and linear polymers from the literature[18, 29, 30] that are considered in this study. The samples in Table 3.2 are nearly monodisperse, and their 1,2-vinyl contents are no more than 10 wt%, which is comparable to those of Table 3.1. We note that the 1,2-vinyl content of the 24KS was not reported by Desai et al.,[29] but we are able to estimate it by analyzing the WLF horizontal shift factors of this sample, as described in Section IV.1. We also note that the 1,2-vinyl contents of the pure 105KL and 42.3KS samples were reported from infrared spectroscopy, not ^{1}H-NMR. Lastly, since TGIC testing was only conducted on the 24KS sample, we validate the GPC molecular weights of the 24.5KS and the 42.3KS by analyzing their zero shear viscosities, as shown in Results and Discussion Section IV.2.

Table 3.2: The same as Table 1, but for 1,4-polybutadienes in the literature, namely Shivokhin et al.,[30] Desai et al.,[29] and Struglinski et al.[18]

Sample Name	***Source***	***Architecture***	***[a] Mw^{GPC} (kDa)***	***[a] Mw^{TGIC} (kDa)***	***Mw/Mn^{GPC}***	***1,2-vinyl content (^{1}H-NMR) (% wt)***

7.5KL	Shivokhin et. al.	Linear	7.5	-----	1.02	10
24.5KS	Shivokhin et. al.	3-arm Star	24.5 (25.3)	-----	1.05	10
58KL	Desai et al.	Linear	58	-----	1.04	8
24KS	Desai et al.	4-arm Star	24 (24.3)	24 (22.3)	1.05	-----
105KL	Struglinski et al.	Linear	100	-----	< 1.1	[(b)] 7
42.3KS	Struglinski et al.	3-arm star	42.3	-----	< 1.1	[(b)] 10

(a) Same as Table 3.1
(b) 1,2-vinyl content obtained from infrared spectroscopy

II.4. Rheology

The linear rheological properties of the newly prepared star-linear blends were measured using 8 mm parallel plates with a sample gap of 1 mm. As mentioned in Desai et al.,[29] the blends were measured on both ARES-LS and RMS-800 rheometers. These tests were performed under strain-control and small-amplitude oscillatory shear flow settings with the same frequency ranges mentioned previously,[29] at temperatures ranging from 25°C to -100°C, with the aid of cooling using liquid nitrogen. The resulting linear viscoelastic G' and G" data were used to generate master curves via time-temperature superposition, at reference temperature 25°C. Through these master curves, WLF horizontal shift factors, $a_T(T)$, were obtained at each temperature, which are displayed in the Results and Discussion Section IV.1, for the 13.3KL, 73KL, 210KL, 260KL, 24KS, 25.3KS, 42KS, 44KS, and 47KS samples and compared to those of to 1,4-polybutadiene found in the literature.[50, 51] In addition to horizontal shifting, the linear viscoelastic data were vertically shifted, $b_T(T)$, in proportion to changes in temperature, as described in Hall et al.[40] The low-temperature data, after time-temperature superposition, reach frequencies high enough to extract the equilibration time, which matches for all samples the "universal" value for 1,4-polybutadiene at 25°C given in Park et al.,[49] namely 3.7×10^{-7}sec. As

an added measure, for select linear samples, we report rheological data at frequencies that are high enough to show the glassy crossover frequency (which will be shown later in Section IV.1).

III. Theoretical Modeling

A recent version of the tube model, the Hierarchical 3.0 model, as described in Wang et. al.,[20] was used for this study. As discussed in that paper,[20] for 1,4-polybutadienes at 25°C, the Hierarchical 3.0 model has been implemented with two possible parameter sets: the "Das parameters," which were originally developed for the BoB (branch-on-branch) model,[23] and the "Park parameters" from the work of Park et al.[21] A fundamental difference between the Park and the Das parameters is the value assigned to the dilution exponent (α), which is α=4/3 and α=1, respectively, for the "Park" and "Das" parameters. The value of α is critical, since it strongly influences the relaxation time of branched polymeric melts, binary blends of branched and linear melts,[17,29] binary blends of linear melts,[22] and polydisperse linear melts,[10-12] as discussed in the Introduction. However, due to recent work conducted by van Ruymbeke and Watanabe,[36,37] Shahid et al.,[38] Hall et al.,[40] and Huang et al.,[39] there is now strong reasons to believe that α=1. Therefore, we will only evaluate here the predictions of the Hierarchical model implemented with the Das parameters.

Besides the choice of parameter set, the Hierarchical 3.0 model has three options for handling primitive path fluctuations during constraint release Rouse (CR-Rouse) relaxation. These options, as discussed in the Introduction, are the "arm frozen," the "thin tube" and the "fat tube" options. In addition to these options for arm fluctuations during CR-Rouse relaxation, there is in the Hierarchical model the possibility of allowing a "disentanglement relaxation" to occur when a species (typically a star polymer) has had its entanglement density diluted by

constraint release to only 1-3 remaining diluted entanglements. Please see Wang et. al.[20] for further details regarding these options. In recent work conducted by Desai et al.,[29] both the use of various CR-Rouse assumptions and "disentanglement relaxation" in predictions yielded mixed results in the modeling of the 24KS-58KL blends; some model predictions had improved agreement with the experimental data, whereas other predictions were worsened. In this paper, we will only utilize the Hierarchical model with the Das parameters and with the most commonly used "thin tube" option, with the acknowledgement that the resulting predictions of experimental data will not yield an all-encompassing assessment of tube model accuracy. Disentanglement relaxation will not be considered. We note that these restrictions render the Hierarchical model very similar to the BoB model, at least for star-linear blends, and the conclusions drawn here using the Hierarchical model also apply when using BoB, as shown in the Appendix. We give the Das parameters G_N^0, M_e, τ_e and α for 1,4-polybutadiene chemistry in Table 3.3 below.

Table 3.3: Das parameters used in Hierarchical model predictions of 1,4-polybutadiene.

Das Model Parameters	
G_N^0	9.7 x 10^5 Pa
M_e	1836 Da
τ_e	2.75 x 10^{-7} sec
α	1

IV. Results and Discussion

IV.1. Time-Temperature Superposition

We assess and verify the 1,2-vinyl content of the freshly synthesized pure linear (Figure 3.1) and pure star (Figure 3.2) 1,4-polybutadiene samples by comparing their WLF horizontal shift factors, plotted against temperature, with those of other 1,4-polybutadienes found in

literature, whose 1,2-vinyl content has been reported. The literature polymers featured in Figures 1 and 2 include a 70.6 kDa linear ("70.6KL"), a 24.5 kDa per arm star ("24.5KS") and a 95.5 kDa linear, which were respectively taken from Palade et al.,[51] Shivokhin et al.[30] and Li et al.[50] These literature WLF horizontal shift factors were reconstructed through use of the time-temperature superposition C_1 and C_2 reported in those papers. We report the C_1 and C_2 factors of the freshly prepared pure star and pure linear samples from our study in the Appendix. In Figure 3.1, the 1,2-vinyl contents of nearly all freshly synthesized linear 1,4-polybutadine samples featured in this study (shown as symbols), obtained from ^{1}H-NMR, are given in the parentheses of the legend. We verify these and estimate 1,2 contents for samples not so characterized by using benchmarks from the literature (shown as lines in Figure 1). The WLF shift factor curves for the freshly synthesized linear samples (*i.e.* 13.3KL, 73KL, and 260KL) are clearly bounded between the 5% 1,2-vinyl content for the linear polymer reported by Li et al.[50] and the 10% 1,2-vinyl content for the star reported by Shivokhin et al.,[30] which supports the ^{1}H-NMR assessment. Since we do not explicitly know the 1,2-vinyl content of the 210KL from ^{1}H-NMR, we estimate it from its shift factor curve in Figure 1 to be between 5% and 10%, consistent with the other freshly synthesized linear 1,4-polybutadienes examined in this study.

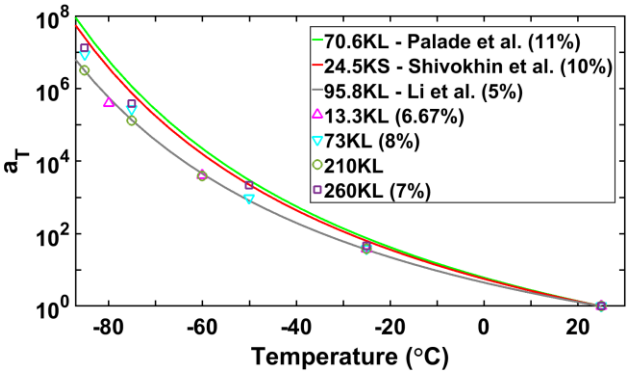

Figure 3.1: WLF horizontal shift factors for both linear polymers studied here (symbols) and the

literature (lines), which were reconstructed from the reported C_1 and C_2 time-temperature superposition constants. In parentheses are the 1,2-vinyl contents reported for each sample, where available. For this plot, and in all subsequent plots, the reference temperature is 25°C.

Similar to Figure 3.1, we observe in Figure 3.2 that the freshly synthesized 1,4-polybutadiene stars in this study (symbols) have 1,2-vinyl contents ranging between 5% and 10%, again based on bounds determined by the reference samples from the literature (lines). This observation both helps verify the 1,2-vinyl content determined by ^{1}H-NMR for the 25.3KS and 47KS samples and provides an estimate of the 1,2-vinyl content of the 44KS sample. In addition, we estimate that the pure 24KS, which was taken from Desai et al.,[29] has a vinyl content between 5% and 10%. Within this range of 1,2-vinyl contents, our earlier work[49] shows that the tube model parameters are nearly constant, or within experimental error, which is around 25% for the equilibration time, and much less than this for the plateau modulus.

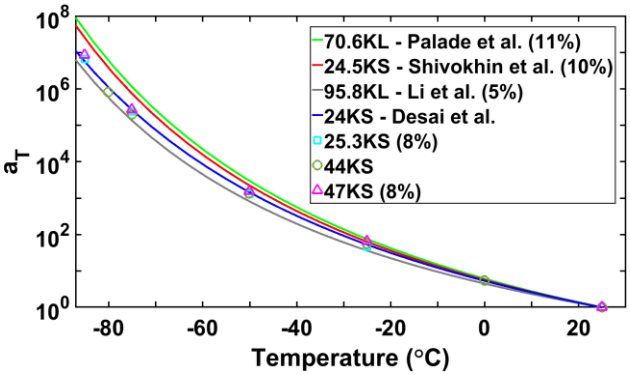

Figure 3.2: The same as Figure 1, but for freshly prepared 4-armed star 1,4-polybutadiene samples. Also included are the WLF shift factors for the pure 24KS obtained from Desai et al.[29] plotted here to help estimate its 1,2-vinyl content.

Corresponding with the horizontal WLF shift factors reported in Figure 3.1, we present in Figure 3.3 the resulting G' and G" linear rheology master curves of the new linear 1,4-polybutadiene samples featured in this study. These data show both the low-frequency crossover

and intermediate-frequency crossover of G' and G'', but omit the high frequency crossover, which is shown for some samples in Figure 3.4. We note in Figure 3.3 that the relaxation curves for all four linear polymers superpose closely at the intermediate G' /G" crossover region to the right of the rubbery plateau, indicating that they possess similar 1,2-vinyl content and have equilibration time τ_e consistent with the universal value, τ_e= 3.7 x 10^{-7} sec, reported in Park et al.[49] We also note that, except for the sample with lowest molecular weight, G' data for these linear samples converge to a similar plateau modulus (G_N^0) at frequencies higher than 10^4 rad/s. The 13.3KL sample presumably fails to reach a similar value of G_N^0 because of the small number of entanglements in this sample. As noted previously, in addition to horizontal shifting, a vertical shift factor (b_T), proportional to absolute temperature, is used in the generation of rheological master curves. This method used here is not the only vertical shifting approach possible; other methods include A) omitting vertical shifting (b_T = 1)[30] or B) utilizing a statistical shifting approach.[29]

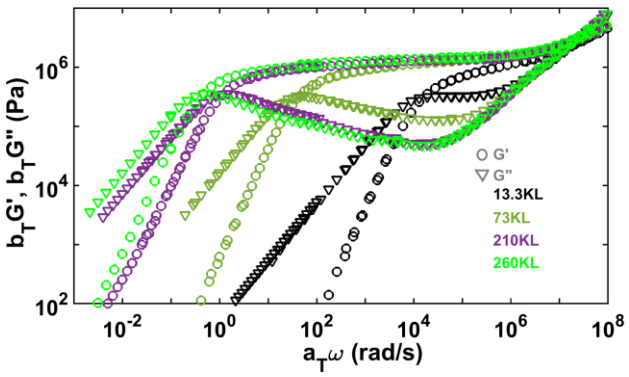

Figure 3.3: G' and G" linear rheology master curves of the new linear 1,4-polybutadienes studied here.

Figure 3.4 focuses on moderate and high frequencies regimes of the 13.3KL and 210KL linear samples and of the pure StarB star reported in Hall et al.[40] The very close superposition

of the datasets throughout the transition and glassy regions (above a frequency of around 10^7 rad/s), suggests that the molecular weight of the 13.3KL sample is high enough to avoid a significant change in segmental friction. Thus, no adjustment for changes in friction, either due to small molecular weights, or to 1,2-vinyl content, are needed for any of the data reported here.

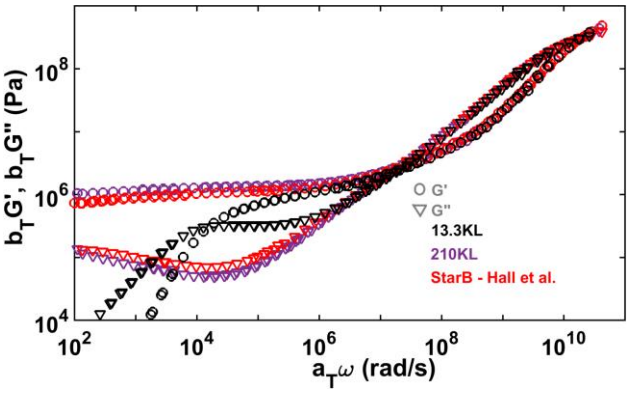

Figure 3.4: Time-temperature superimposed G' and G" linear rheology against reduced frequency, plotted up to frequencies in the glassy region, for 13.3KL and 210KL linear samples and a 4-arm star reported in Hall et al.[40]

Similar to Figure 3.3, we report in Figure 3.5 the linear rheology of the newly synthesized 4-arm 1,4-polybutadiene stars featured in this study. Once again, we observe close superposition of the rheology datasets at the intermediate crossover frequency to the right of what would be the plateau region in a linear sample, signifying a similarity in the 1,2-vinyl content among the samples. We note that the plateau modulus (G_N^0) we infer for the 44KS sample is slightly higher than those of the 25.3KS and 47KS samples, which is observable in the higher G' values for this sample between frequencies of 10^3 and 10^7 rad/s. This difference in G_N^0 may arise from imperfections in rheological testing at reduced temperatures and/or imperfections of the temperature-dependent vertical shifting, b_T used to generate the rheological master curves. At any rate, this modest difference should have little effect on the main results of this paper.

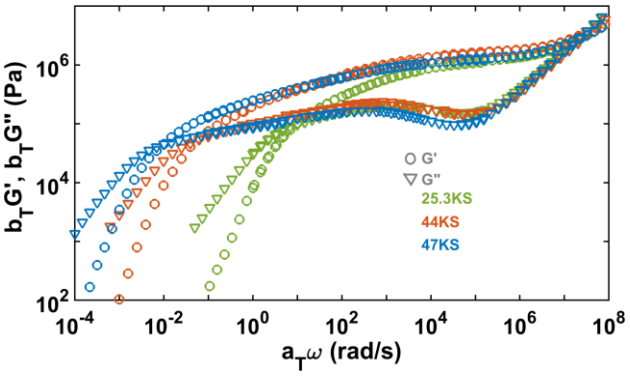

Figure 3.5: The same as Figure 3.3, but for the freshly synthesized symmetric 4-arm star 1,4-polybutadiene 25.3KS, 44KS, and 47KS melts.

IV.2. Analysis of Zero-Shear Viscosity

We now assess the accuracy of the GPC and TGIC molecular weight measurements of the 1,4-polybutadienes reported in Tables 3.1 and 3.2 by comparing the zero-shear viscosities (η_o) of these polymers, obtained from the linear rheology data, with those of other 1,4-polybutadienes found throughout the literature. In addition, we obtain from these viscosity data estimates of the molecular weights that we will use, along with the molecular weights from GPC, in the Hierarchical model, as discussed below. Throughout this paper, the Hierarchical model is implemented with the Das parameters and thin-tube CR-Rouse relaxation, as alluded to earlier.

Figure 3.6 depicts the zero-shear viscosities, scaled by molecular weight to the 3.4 power, of the linear 1,4-polybutadienes explored in this study (closed circles) compared with literature sources, which includes Colby et al.[45] (open squares) and Struglinski et al.[46] (open triangles). We scaled the zero-shear viscosity to observe more clearly deviation from the $\eta_o \propto M_w^{3.4}$ power law. We note that there are two sets of zero-shear viscosity data from Colby et al. for linear polymers with molecular weights below 10,000 Da. The "Colby et al." data are the unadjusted zero-shear viscosities extracted from linear rheology, whereas the "Colby et al. (free volume)" data were adjusted to correct for the reduction in segmental friction coefficient that occurs in

low-molecular weight melts. Also included in Figure 6 is a trend line (black line) that fits the reference data of Colby et al. and of Struglinski et al., and a (green) line showing predictions of the Hierarchical model, which of course fails drastically at low molecular weights where melts are unentangled.

We observe that in Figure 3.6 the zero-shear viscosities of the linear 1,4-polybutadiene polymers featured in this study, given by solid symbols, agree reasonably with the black trend line summarizing the literature data, which are given by open symbols. An exception is the 7.5KL melt reported by Shivokhin et al,[30] whose η_o value is roughly a factor of 3 below the black trend line along the y-axis, indicating that the molecular weight of this linear is possibly lower than the reported value, 7.5 kDa. To achieve reasonable superposition with the black trend line, the 7.5KL melt would instead need to be assigned a molecular weight ranging between 5kDa and 6kDa. (We noted in the Introduction that Desai et al.[29] assigned this melt a molecular weight of 6.9 kDa.) The zero-shear viscosities of both the 210KL and the 260KL melts are somewhat above the black trend line, by a factor of 1.5 for the 210KL and a factor of 1.6 for the 260KL melt. To achieve agreement with the trend line, the molecular weight of the 210KL would have to be increased to roughly 235 kDa, while that of the 260KL melt would need to be roughly 295 KDa, which are likely within the error of the GPC measurements of these melts. Also in Figure 3.6, with the exception of the 7.5KL melt taken from Shivokhin et al., the zero-shear viscosities predicted by the Hierarchical model (green line) are notably lower than both the linear melts featured in the star-linear blends of this study (closed circles) and the other linear polymers found in the literature.[45,46]

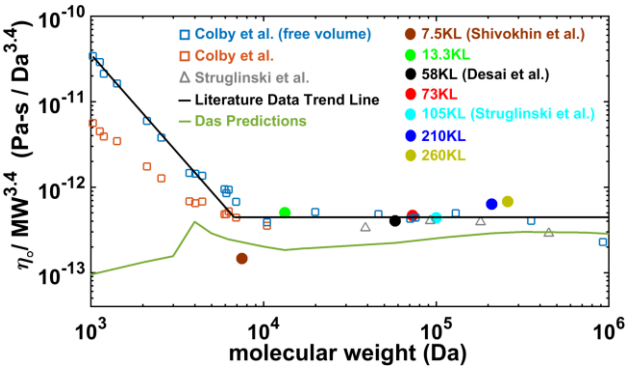

Figure 3.6: Scaled zero-shear viscosities of individual linear 1,4-polybutadienes, from this work, and from Struglinski et al.,[18] Desai et al.[29] and Shivokhin et al.,[30] (solid circles) and from reference sets of multiple samples from the literature[45,46] (open symbols) versus molecular weight. The zero-shear viscosities are scaled by the molecular weight (MW) to the 3.4 power. For molecular weights below 10,000 Da, the "Colby et. al." data are unadjusted zero-shear viscosities collected from the linear rheology, whereas the "Colby et. al. (free volume)" data are adjusted to account for changes in free volume (or segmental friction). Also plotted are zero-shear viscosities predicted by the Hierarchical model (green line, labelled "Das predictions") and a power law fit to the literature benchmark data (black line).

Figure 3.7 plots the zero-shear viscosities against the star-arm molecular weight of both the freshly synthesized and literature[18, 29, 30] star 1,4-polybutadiene samples analyzed in this paper (closed circles) as well as those for other benchmark star 1,4-polybutadiene polymers from the literature.[30, 42, 47] Also presented is the plot of the zero-shear viscosities from Hierarchical model predictions (green line). The zero-shear viscosities for both the freshly prepared and the featured literature stars superpose within scatter with the benchmark data represented by open symbols. Therefore, it is reasonable to assume that the arm molecular weights of the freshly prepared 25.3KS, 44KS, and 47KS samples, which were only subjected to GPC analysis, are relatively accurate and that the samples are largely comprised of 4-arm star molecules. In addition, the zero-shear viscosities predicted by the Hierarchical model are roughly equal to the measured values except for the higher-molecular weight values, which are over-predicted by a factor of two on average.

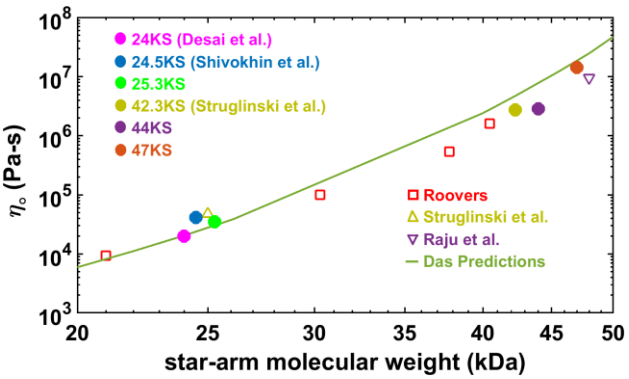

Figure 3.7: The same as Figure 3.6, except for star polymers and the viscosities are not re-scaled.

The zero-shear viscosities presented in Figures 3.6 and 3.7 indicate that the pure star and pure linear 1,4-polybutadienes used in the star-linear blends of this study are reasonably well characterized, although we note that the two high molecular weight linear polymers used in our study, 210KL and 260KL, may have a higher molecular weight than indicated by GPC, since their viscosities in Figure 3.6 lie above the trend line from the literature, and the 7.5 KL linear may have lower molecular weight than the value obtained by GPC characterization. In addition, the Hierarchical model with α = 1 seems to systematically underpredict the viscosity of the pure linear melts, and somewhat overpredict the viscosity of the stars with arm molecular weight above around 30 kDa. Thus, to correct for modest random errors in characterization and counteract systematic errors in the tube model for the pure materials, we will use in our predictions for the blends both the GPC molecular weights, and molecular weights that are modestly adjusted to obtain better agreement with the zero-shear viscosity. These viscosity-adjusted molecular weights are reported in Table 3.4. The maximum difference between the zero-shear viscosities from model predictions with revised molecular weights and the experimental values is a factor of 1.2. For the star polymer samples, the molecular weight reported is the arm molecular weight. We observe in Table 3.4 that, as expected, the molecular

weight used in the Hierarchical model prediction for each linear sample is consistently higher than the associated GPC molecular weight, with the exception of the 7.5KL sample reported by Shivokhin et al.[30] The molecular weights of the star polymers used in the model predictions of viscosity in Table 3.4 are very similar to the molecular weights measured by GPC, for molecular weights below 30 kDa, but somewhat lower than the GPC molecular weights for higher arm lengths, as reported in Tables 1 and 2. These results are consistent with earlier observations; when Das parameters, with α = 1, are used, the Hierarchical model is typically not able to fit both star and linear molecules of the same species as well as when α = 4/3 is used,[20] and so the Das parameters (other than α) provide a compromise that under-predicts the viscosities of the linear polymers, but over-predicts those of stars. A better simultaneous prediction of both the pure star and pure linear viscosities is obtained for α = 4/3.[20] As remarked earlier, however, the choice α = 4/3 is no longer tenable, based on recent studies. Thus, the systematic increase in molecular weight needed to match viscosities of the linear polymers is likely offsetting some systematic error in the Hierarchical model, which exists in the Bob model as well. To make sure that our conclusions are robust against errors in molecular weight characterization, we will use in our Hierarchical model predictions the pure star and the pure linear molecular weights from both GPC measurements and from zero-shear viscosity assessments. We note that in the case of the pure stars, the GPC molecular weights used in model predictions corresponds with the linear precursor that was characterized prior to branching reaction. In the main text we will show summary plots of our results for both choices of molecular weight characterization. To reduce the number of plots in the main text, comparisons of experimental and predicted G' and G'' curves for the individual blends will be presented only for the viscosity-based molecular weights for the pure star and linear melts, while results based on GPC characterizations are given in the

SI. These plots show that the conclusions drawn from our work are the same whether we use molecular weights based on viscosity or based on the GPC characterizations of the molecular weights.

Table 3.4: Experimental zero-shear viscosities (column 4) of the pure star and pure linear 1,4-polybutadienes in this study, and viscosities (column 3) computed from the Hierarchical model with the Das parameters, using molecular weights (column 2) chosen to fit the experimental zero-shear viscosities. The footnotes identify the data obtained from the literature measured in this work. Any polymer samples listed without notation are newly introduced in this study.

Sample	**[a]Hierarchical Das MW Approximations (kDa)**	**Hierarchical Das Zero-Shear Viscosity (Pa-s)**	**Experimental Zero-Shear Viscosity (Pa-s)**
[b]7.5KL	6.25	1.98	2.19
13.3KL	17	46.4	52.7
[c]58KL	69	6.56×10^3	6.35×10^3
73KL	88	1.59×10^4	1.6×10^4
[d]105KL	115	4.18×10^4	4.37×10^4
210KL	260	7.61×10^5	7.91×10^5
260KL	320	1.56×10^6	1.75×10^6
[c]24KS	24	2.04×10^4	2.01×10^4
[b]24.5KS	26.2	3.92×10^4	4.12×10^4
25.3KS	25.6	3.32×10^4	3.5×10^4
[d]42.3KS	40	2.4×10^6	2.75×10^6
44KS	40.5	2.78×10^6	2.86×10^6
47KS	45.5	1.2×10^7	1.43×10^7

(a) Molecular weight per star arm is reported for the star samples
(b) Source: Shivokhin et al.[30]
(c) Source: Desai et al.[29]
(d) Source: Struglinski et al.[18]

IV.3. Evaluation of Hierarchical Model Using Star-Linear Blend Rheology Data

As stated in a previous section, we will implement the Hierarchical model with the Das parameters set only, which takes the dilution exponent value (α) to be unity, and uses the "thin tube" assumption. In addition, we will not employ the "disentanglement relaxation" option. The star-linear blends analyzed in this study are divided into two categories. One category features

star-linear blends in which the star component has an arm molecular weight ranging between 20 kDa to 30 kDa; this includes the 24.5KS-7.5KL blends taken from Shivokhin et al.,[30] the 24KS-13.3KL blends, 24KS-58KL blends taken from Desai et al.,[29] 25.3KS-73KL blends**, 24KS-210KL blends, and the 25.3KS-260KL blends. (The labeling of one of the blends with asterisks is explained below.) The other category features star components with arm molecular weights ranging between roughly 40 kDa and 50 kDa; this includes the 42.3KS-105KL blends taken from Struglinski et al.,[18] 44KS-13.3KL blends, 47KS-73KL blends, and the 47KS-260KL blends. To save space, we only report in Figures 3.10- 3.14 the linear rheology data of star-linear blends with star-arm molecular weights ranging between 20kDa and 30kDa. The Appendix presents the corresponding results for the star-linear blends with star-arm molecular weights between 40kDa and 50kDa, as well as the 25.3KS-73KL blend series. We note that the 25.3KS-73KL blends were prepared and tested after the other results had been gathered and conclusions of the paper had been made and written up, and this last data set was gathered to confirm these conclusions.

We begin our assessment of the Hierarchical model by plotting in Figure 3.8 what we will here call the "terminal frequency" of the blends $\omega_{t,blend}$, normalized by the terminal frequency of the pure star $\omega_{t,star}$, as a function of the star volume fraction (ϕ_s) from both model predictions (lines) and experimental data (symbols). Both "terminal frequencies," $\omega_{t,blend}$ and $\omega_{x,star}$, are defined as the frequency at which G'= 10^3 Pa. We choose this definition of "terminal frequency" because we found that the more obvious choice, namely the frequency at the terminal crossover of G' and G'', is too high a frequency to capture adequately the predictive failure of the tube model in the terminal region for some of the blends. The frequency at which G'= 10^3 Pa is low enough to capture this failure, and the modulus G'= 10^3 Pa is high enough to be largely free from measurement error. We normalize $\omega_{t,blend}$ by $\omega_{t,star}$ to more easily judge the success

or failure of model predictions by the magnitude of the difference in terminal relaxation time between the blend and the pure star. Figure 3.8A features model predictions that utilize the viscosity-based molecular weights reported in Table 3.4, whereas the molecular weights from GPC measurements are used in model predictions in Figure 3.8B.

We observe in Figure 3.8A that model predictions superpose rather well with experimental data for most star-linear blend sets. The 24KS-13.3KL blend series, for example, is captured reasonably well by the model, with the exception of the ϕ_s= 0.1 blend. However, as observed earlier in the work of Desai et al.,[29] Hierarchical model predictions fail when the relaxation time of the pure linear increases to within 3-4 orders of magnitude of the star polymer, which is the case for the 24KS-58KL and the 25.3KS-73KL blend series. Specifically, the model predicts a non-monotonic dependence of the terminal frequency on star volume fraction, which is not observed in the experimental data. The 24KS-210KL and the 25.3KS-260KL blend series also present predictions of non-monotonic behavior, and, surprisingly, this non-monotonic behavior is actually observed in these blends. In Figure 3.8B, we use the GPC molecular weights instead of those determined by fits with the zero-shear viscosities of the pure star and the pure linear; thus, the predictions of the pure linear do not superpose as closely with the data in Figure 3.8B as they due in Figure 3.8A. However, we observe in Figure 3.8B the same trend in model prediction successes and failures as we do in Figure 3.8A. Specifically, in Figure 3.8B, the model predicts reasonably well the 24KS-13.3KL blends. Model predictions of the 24KS-58KL blend series show a non-monotonic dependence of $\omega_{t,blend}$ on blend composition that is not seen experimentally. Lastly, in Figure 3.8B, non-monotonic model predictions of the 24KS-210KL and the 25.3KS-260KL blend are consistent with those of Figure 3.8A. This is the first report of experimentally validated non-monotonic dependence of terminal relaxation on blend

composition in the literature, which we will discuss in more detail in what follows.

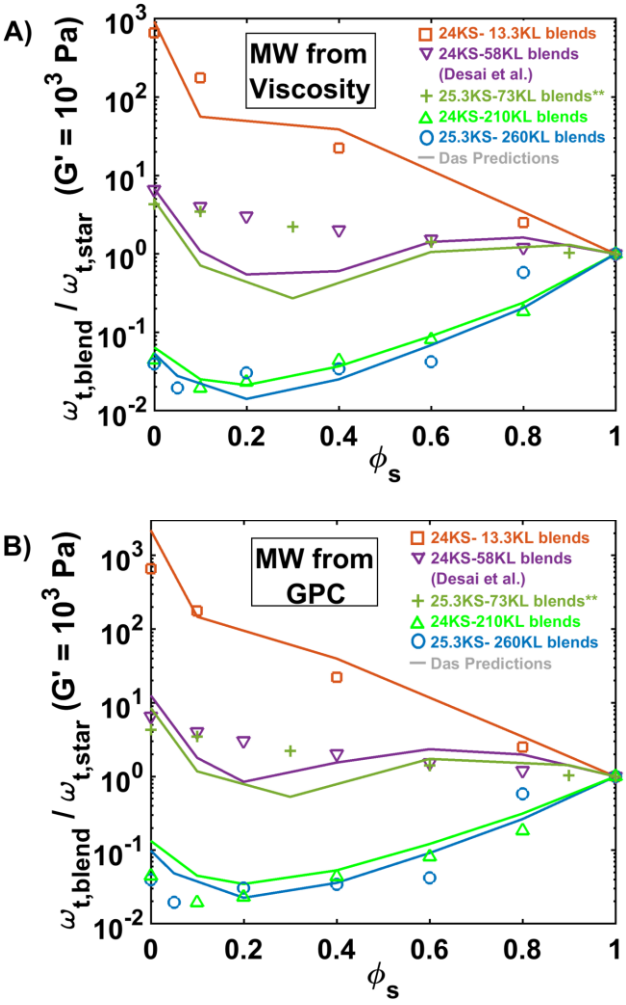

Figure 3.8: "Terminal relaxation frequency" of star-linear blends, defined as the frequency at which G' = 10^3 Pa and normalized by terminal frequency of the pure star (also the frequency at which G'=10^3 Pa), versus star volume fraction, ϕ_s. Symbols are experimental data, and lines are Hierarchical model predictions generated with Das parameters and "thin tube" option as in all subsequent figures. A) Molecular weights used in model predictions obtained from zero shear viscosities are taken from Table 4, and B) molecular weights were measured by GPC. The 24KS-58KL experimental blend data was taken from Desai et al.[29] We note that the 25.3KS-73KL blend series is marked with "**" in the legend because it was prepared and tested after the rest of the samples, to confirm the conclusions presented in this work.

Similarly to Figure 3.8, we define in Figure 3.9 a characteristic "terminal frequency" for each blend ($\omega_{t,blend}$) as the frequency at which G' reaches the value of 1000 Pa; however, in

Figure 3.9 we plot data for the star-linear blends (symbols) for stars with arm molecular weight above 40kDa, namely 44KS-13.3KL, 47KS-73KL, 47KS-260KL and the 42.3KS-105KL blends taken from Struglinski et al.**[18]** Each $\omega_{t,blend}$ value was again normalized by the terminal frequency of the respective pure star ($\omega_{t,star}$) of the blend series, also at G'=1000 Pa. Figure 3.9A features model predictions that utilize the molecular weights reported in Table 3.4, whereas the molecular weights from GPC measurements are used in model predictions in Figure 3.9B. Shown in Figure 3.9A, the Hierarchical model predictions (lines) are mostly in reasonable agreement with the 44KS-13.3KL and 47KS-73KL star-linear blend data. The largest deviation from the 44KS-13.3KL data are at star volume fractions (ϕ_s) of 0.2 and 0.4, where the model underpredicts the experimental data by factors of 2.6 and 2.3, respectively. For the 47KS-73KL blend series, predictions differ from data by no more than a factor of 1.8 for any blend.

In contrast to the model agreements for the cases of 44KS-13.3KL and 47KS-73KL blends, the model fails more seriously to predict the relaxation of the 42.3KS-105KL blends, from Struglinski et al.[18] in Figure 3.9A. Not only is there a deviation of up to a factor 6.4 for the 42.3KS-105KL (ϕ_s=0.1) blend, the model also inaccurately predicts a non-monotonic dependence on ϕ_s, while the experimental data show roughly a linear dependence. In addition, the Hierarchical model incorrectly predicts a non-monotonic dependence of the terminal frequency on star volume fraction for the 47KS-260KL blends; however, in this case, the predicted terminal frequency for the ϕ_s=0.2 blend is only a factor 1.4 lower than that for the ϕ_s=0.4 blend. This modest predicted non-monotonicity is absent from the experimental rheology, for which the terminal frequency for the ϕ_s=0.2 blend is a factor of 1.4 *higher* than that for the ϕ_s=0.4 blend.

The model predictions that utilize the pure star and pure linear molecular weights from GPC, as featured in Figure 3.9B, obtain similar success in superposing the experimental data as in Figure 3.9A. Although the terminal frequencies of the pure linear polymers are captured rather poorly in comparison to Figure 3.9A, the predictions in Figure 3.9B lead to the same conclusions as those of Figure 3.9A. We note that model predictions of the 44KS-13.3KL blends in Figure 3.9B may appear considerably poorer those of Figure 3.9A; however, this discrepancy is due to the model's inability to capture accurately the relaxation of the both the pure 44KS and the pure 13.3KL when using the molecular weights given by GPC, as shown in Figure 3.A20 of the Appendix. Despite this shortcoming, Figure 3.A20 shows that model predictions of the resulting 44KS-13.3KL blends superpose reasonably well with the experimental data.

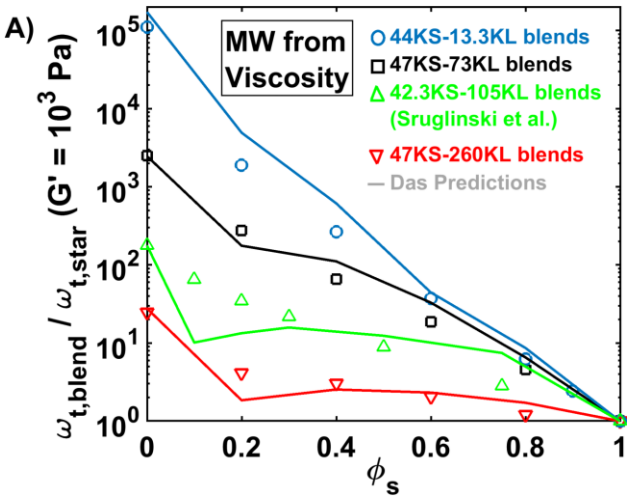

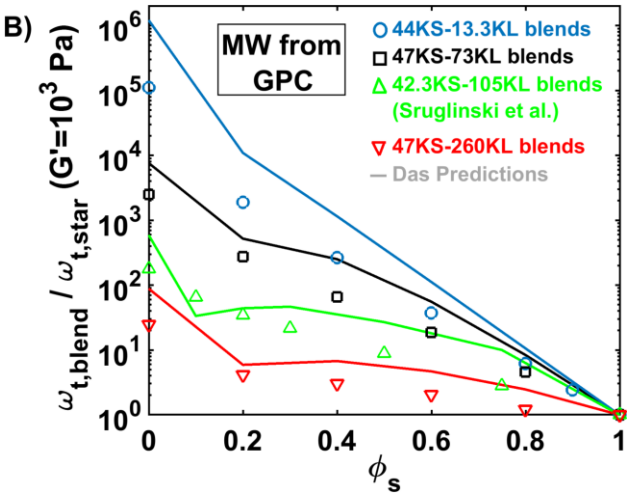

Figure 3.9: The same as Figure 3.8, but for the star-linear blends of 44KS-13.3KL, 47KS-73KL, 42.3KS-105KL taken from Struglinski et al.[18] and 47KS-260KL.

We next compare in Figures 3.10- 3.14 model predictions of G' and G'' with the corresponding experimental data for multiple blend series. Figure 3.10 compares the rheology of the 24.5KS-7.5KL blend series (symbols) taken from Shivokhin et al.[30] against the Hierarchical model predictions (lines) with molecular weights adjusted to fit the pure materials as listed in Table 3.4, as is done for all results from this point forward (while including the corresponding results based on molecular weights from GPC or TGIC in the SI). Model predictions superpose reasonably well with the experimental data but with deviations in Figure 3.10A at star volume fractions of ϕ_s= 0.5, 0.2, and 0.1, especially at frequencies just above the terminal range.

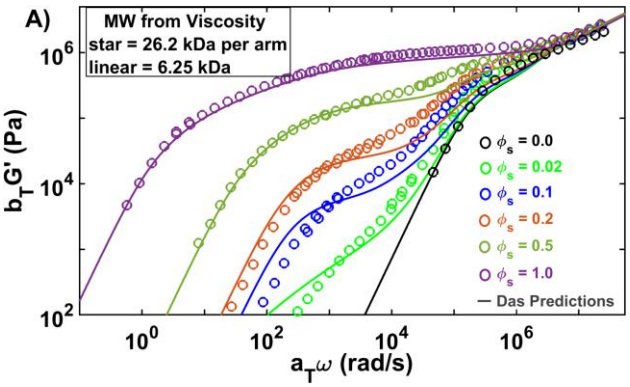

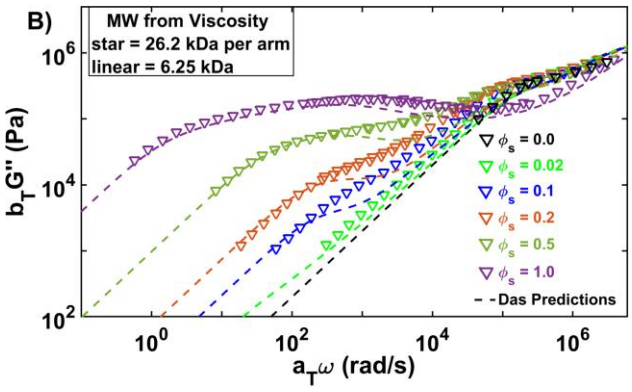

Figure 3.10: Experimental (symbols) A) G' and B) G" linear rheology data of the 25.4KS-7.5KL blends series, obtained from Shivokhin et al.,[30] for star volume fractions (ϕ_s) 0, 0.02, 0.1, 0.2, 0.5 and 1, compared with predictions of the Hierarchical model. As elsewhere in this section, the molecular weights used in the predictions are given in the legend and taken from Table 3.4.

Figure 3.11 is similar to Figure 3.10, except for the 24KS-13.3KL blend series. Despite adjusting molecular weights to match the pure star and the pure linear relaxation, as well as successful modeling of low-frequency crossover frequency $\omega_{x,t}$ in Figure 3.11, the terminal relaxation is incorrectly predicted for low star volume fractions, especially for ϕ_s=0.1. In the experiments, the lifetimes of the relatively dilute, long-lived star-star entanglements seem to be reduced by the linear chains, resulting in faster CR-Rouse relaxation than predicted by the tube model. This accelerated relaxation might be due to additional relaxation mechanisms, such as the thin tube contour length fluctuations discussed in Read et al.[56] or the "tension re-equilibration" mechanism discussed in van Ruymbeke.[36,37] Alternatively, and possibly in conjunction with the failure of CR-Rouse physics, the tube model may not be capturing correctly the dynamic dilution physics in the limit of sparse star-star entanglement interactions present in star-linear blends of high linear content. Note that the difference in terminal relaxation between the pure star and the pure linear for this 24KS-13.3KL blend series is roughly 3 orders of magnitude, as opposed to the 4-plus orders of magnitude difference between the pure 24.5KS and the pure 7.5KL melts in

Figure 3.10. As remarked earlier, the tube model seems to fail increasingly as the ratio of the relaxation time of the linear to that of the star increases towards unity.

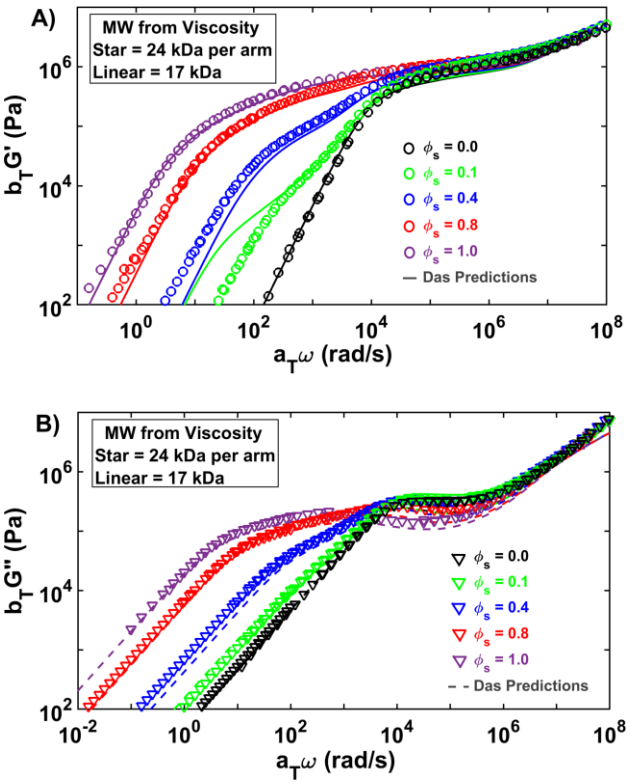

Figure 3.11: The same as Figure 3.10, but for the 24KS-13.3KL blend series.

Next, we revisit in Figure 3.12 the comparison of Hierarchical model predictions (lines), again with the Das parameters and "thin tube" assumption, for the 25KS-58KL blends (symbols), initially featured in Desai et al.[29] As in Figures 3.10 and 3.11, and unlike the modeling in Desai et al., the molecular weights were adjusted to fit the rheology of the pure 24KS and the pure 58KL. Despite this adjustment, and consistent with the original findings reported in Desai et al., model predictions fail to match the blend data, with the exception of the 24KS-58KL (ϕ_s=0.6) blend. Furthermore, the model predictions falsely predict non-monotonicity, with terminal relaxation times for star volume fractions ϕ_s=0.1, 0.2, and 0.4 exceeding those for both the pure star and the pure linear polymers. Note that the relaxation time of the pure star is less than an

order of magnitude different from that of the linear, consistent with increasing disagreement between tube model and data with increasing ratio of linear to star relaxation times.

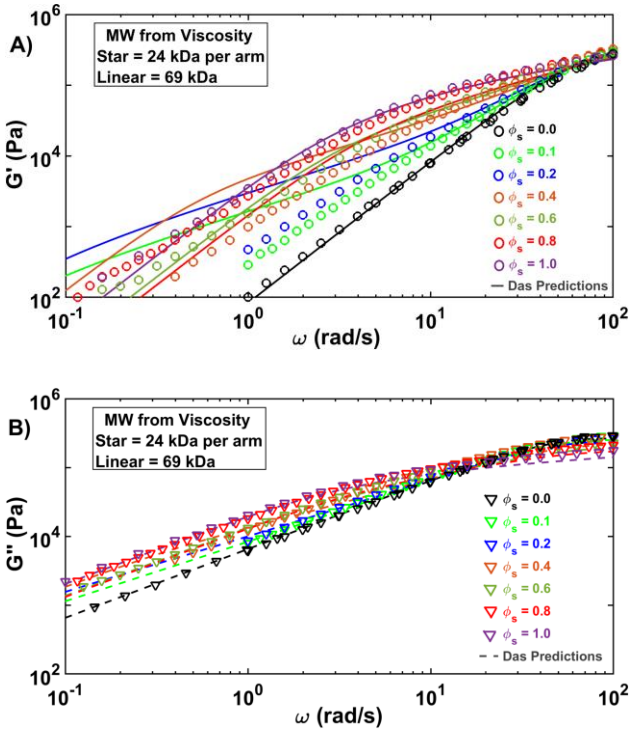

Figure 3.12: The same as Figure 3.10, but for the 24KS-58KL blend series. Experimental data was taken from Desai et al.[29]

In Figures 3.13 and 3.14, we report results for star-linear blends in which the pure linear component has a longer relaxation time than the pure star component. The 24KS-210KL blends in Figure 3.13, with star volume fractions ϕ_s= 0.4, 0.2 and 0.1, have longer relaxation times than both the pure linear and pure star components. This shows up especially strongly in the G' linear rheology in Figure 3.13A but also, to a lesser extent, in the G" linear rheology in Figure 3.13B. We note in Figure 3.13A that the Hierarchical model predicts this non-monotonic relaxation of the star-linear blends, superposing rather closely with the measured rheology.

We note in Figure 3.13 that the terminal rheology of the pure 210KL shows a slight tail at low frequency, indicating the presence of some higher molecular weight species within the melt.

While this tail is small, we investigated the possibility that it might be responsible for the observed non-monotonicity in the Appendix by using the Hierarchical model to determine the molecular weight and volume fraction of long linear chains needed in the pure linear material to fit the pure linear data, and then seeing the effect of this on the 24KS-210KL blend predictions. Despite having fit the polydispersity-induced long tail of the pure 210KL, model predictions for the blend are only slightly changed, and continue to show non-monotonicity in the dependence of terminal relaxation time on star concentration. While it is always possible that this non-monotonicity might conceivably be absent in rigorously monodisperse materials, it remains the case that, whatever causes it, we find a non-monotonic dependence of terminal relaxation time on the blending ratio of a linear, slightly polydisperse, sample, with a star polymer.

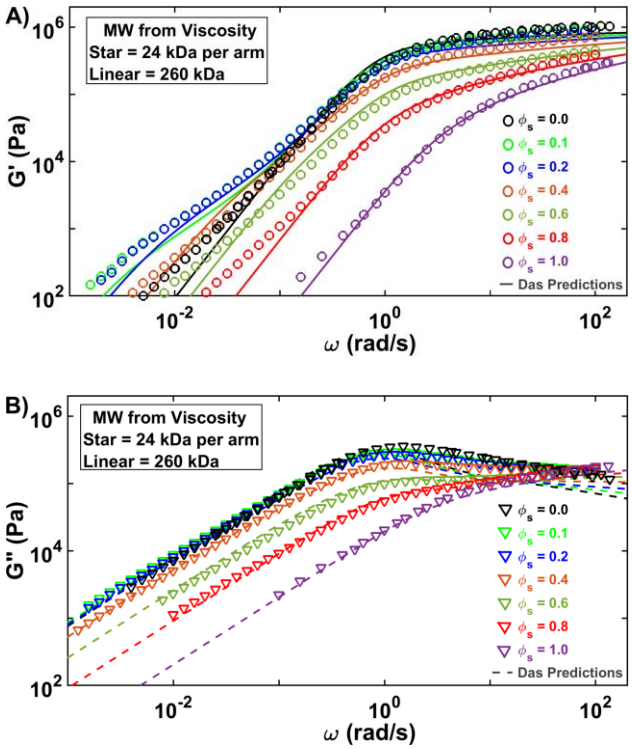

Figure 3.13: The same as Figure 3.10, but for the 24KS-210KL blend series.

To further confirm this non-monotonic behavior, we acquired new star and linear 1,4-polybutadiene samples, similar in molecular weights to those of Figure 3.13. The new linear component, 260KL was synthesized and characterized by our team (Hadjichristidis lab), while the linear polymer in Figure 3.13, 210KL, was purchased from Polymer Source, thus giving us similar material from two different labs. In Figure 3.14, the linear rheology of the 25.3KS-260KL blends again displays non-monotonic behavior, again in agreement with predictions of the Hierarchical model. Slight polydispersity is also evident in the terminal rheology of the pure 260KL which we again explore in the Appendix and show that it does not change the non-monotonic behavior significantly.

We note that the hierarchical model *correctly* predicts non-monotonic behavior in these two blend series, but also *incorrectly* predicts it for the 24KS-58KL blend series depicted in Figure 3.12. In Figure 3.12, however, the pure star melt relaxes more slowly than the linear melt, while the reverse is the case in Figures 3.13 and 3.14. It is noteworthy that the CFSM slip-link model of Schieber and coworkers *correctly* predicts monotonic behavior of the terminal relaxation time with blend composition for the 24KS-58KL blend data.[29] It would be of great interest to see whether slip-link models predict non-monotonic behavior of blends in which the linear melts relaxes slower than the star. If not, this would represent a case in which the tube model captures constraint release behavior that is not captured by slip-link models. This would indicate a subtlety in constraint release dynamics that is not yet consistently implemented in either class of models. A careful study of the source of the non-monotonicity in the tube model and its lack in slip-link models might then open the door to deeper understanding of constraint release in general, and to improvements in the modeling of constraint release in tube and slip-link models. We believe that since constraint release is so difficult to model consistently in star-

linear blends, a future model that successfully predicts the rheology of these blends is likely to be successful also for polydisperse mixtures of well entangled star and linear blends. This, in turn, would provide a strong basis for consistently accurate modeling of commercial branched polymer melts.

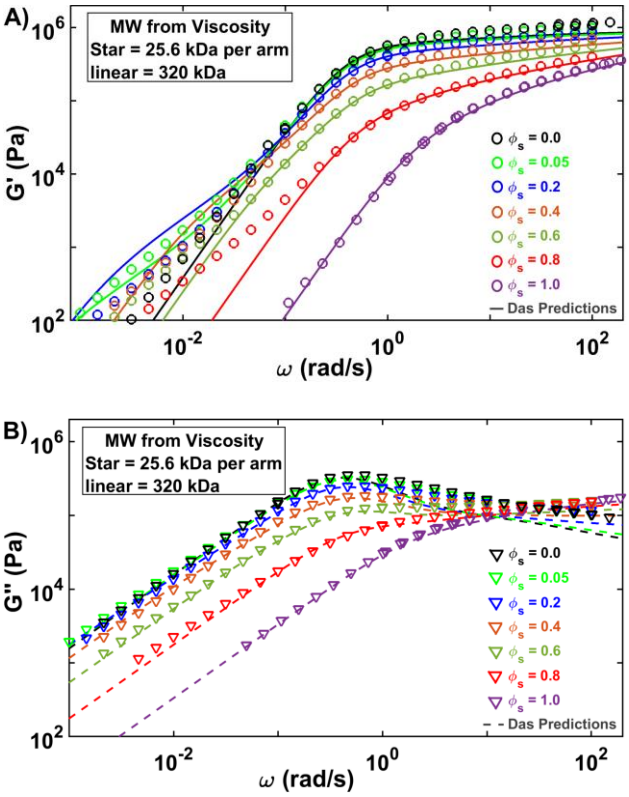

Figure 3.14: The same as Figure 3.10, but for the 25.3KS-260KL blend series.

Finally, to summarize our results, in Figure 3.15 we organize our data onto a "phase map" of the zero-shear viscosity (η_o), obtained from experiment, of the pure star paired with that of its pure linear counterpart, labeling each of the ten blend series with a symbol of its own distinct color. Along the red dashed line, the zero-shear viscosities of the pure star and linear polymers are equal. To the right of the blue line in Figure 3.15, the Hierarchical model predicts non-monotonic dependence of terminal relaxation time on star volume fraction, while to the left,

it does not. The model falsely predicts non-monotonicity in all the blends featured to the right of the blue solid line, but to the left of the red dashed line, namely the 24KS-13.3KL, 24KS-58KL, 25.3KS-73KL**, 47KS-73KL, 42.3KS-105KL and 47KS-260KL blends. The 25.3KS-73KL was prepared and tested, after completion and plotting of the others, to further verify the absence of non-monotonicity in the experimental data, although predicted to be present by the Hierarchical model, when the zero-viscosities of the pure star and pure linear are near, but to the left of, the red dashed line. To the right of the red dashed line, the non-monotonic predictions prove accurate for the 24KS-210KL and the 25.3KS-260KL blends.

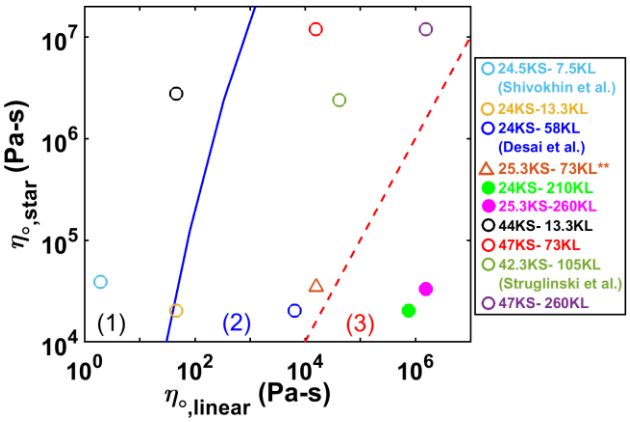

Figure 3.15: Experimental zero-shear viscosities of each pure star plotted against that of the linear polymer for each of the ten blend series (symbols). The blue line indicates the transition from monotonic (left of the line) to non-monotonic (right of the line) dependence of terminal relaxation on composition in Hierarchical model predictions. The dashed red line marks equality in the zero-shear viscosities of the pure linear and the pure star melts. The filled symbols represent the two blend series for which both theory and experiment show non-monotonic dependence of the terminal relaxation time on blend composition. We note that the 25.3KS-73KL was prepared and tested at the end of our study to confirm the absence of monotonicity in the experimental blend data when the zero-shear viscosities of pure 25.3KS and pure 73KL are close to, but to the left of, the red dashed line.

We note that Figure 3.15 places the 24KS-13.3KL and the 47KS-73KL series in the region for which non-monotonicity is predicted by the theory. While this might seem to conflict

with the apparently monotonic dependence of terminal relaxation time on ϕ_s seen, respectively, in Figures 3.11 and 3.A6 (the latter in the Appendix Section VI.2.ii), the presence of non-monotonicity is revealed in Figures 3.16 and 3.17 when we include model predictions (pink lines) of additional 24KS-13.3KL and 47KS-73KL blend compositions that were not explored experimentally within the existing datasets (pink symbols). With the addition of the 24KS-13.3KL ϕ_s=0.2 and the 47KS-73KL ϕ_s=0.1 blends respectively to Figures 3.16 and 3.17, we observe clearly the emergence of non-monotonicity in the predictions for both of these blend series; yet the experimental data retain a monotonic dependence of terminal relaxation on ϕ_s. Non-monotonicity is falsely predicted whether the molecular weights used in the predictions are obtained from zero-shear viscosity fitting or from GPC. This confirms the accuracy of the boundary given by the blue line in Figure 3.15 separating the *predictions* of non-monotonicity (to the right of the solid blue line) from the predictions of monotonic composition dependence (to the left of the solid blue line).

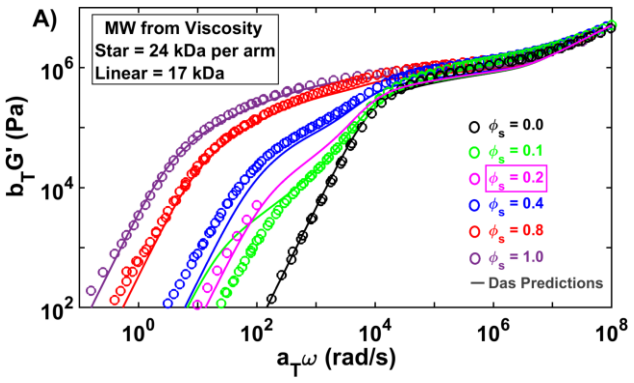

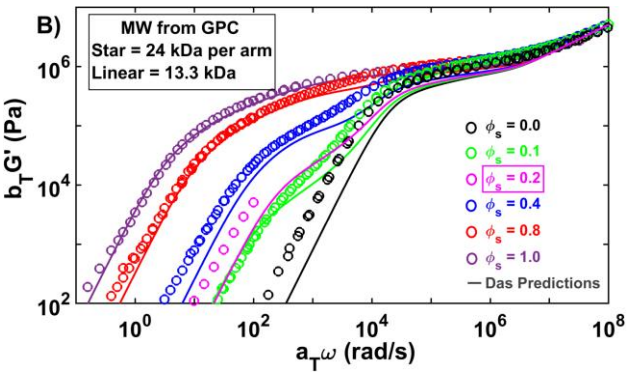

Figure 3.16: Experimental (symbols) linear rheology data of the 24KS-13.3KL blends series for star volume fractions (ϕ_s) 0, 0.1, *0.2*, 0.4, 0.8 and 1, compared with predictions of the Hierarchical model that use star and linear molecular weights obtained from A) zero-shear viscosity and B) GPC. The 24KS-13.3KL(ϕ_s = 0.2) blend (pink symbols) was prepared after the others to confirm the inaccuracy of the prediction of non-monotonic dependence of terminal relaxation in G' on composition at low star volume fraction.

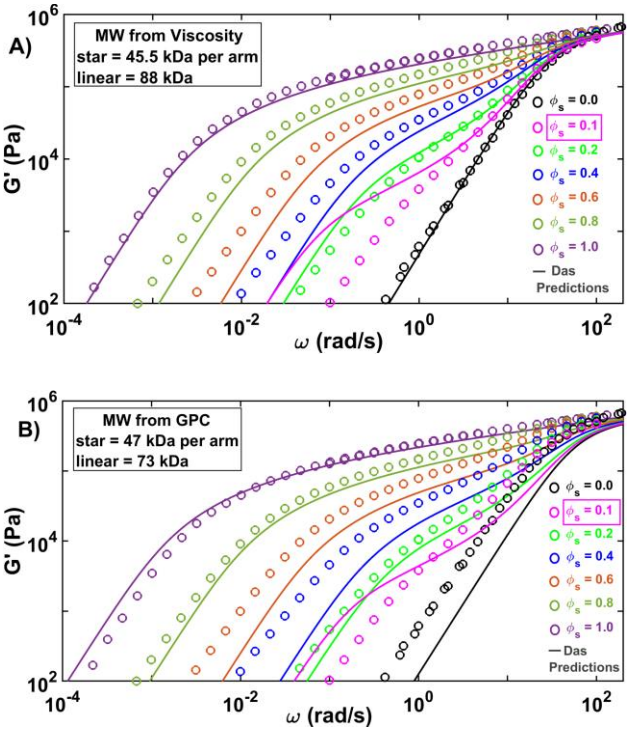

Figure 3.17: As in Figure 3.16, the 47KS-73KL(ϕ_s=0.1) was prepared after the others to confirm the absence of non-monotonicity in the experiments.

Although the Hierarchical model has its shortcomings, its success in predicting the non-monotonicity of 24KS-210KL and 25.3KS-260KL star-linear blends should not be overlooked.

There may be physics captured by the tube model that are not yet fully understood. Thus far, we only observe non-monotonicity experimentally in star-linear blend cases where the pure linear has a higher viscosity than the pure star. With the use of the phase diagram featured in Figure 3.14, additional star-linear blends could be created to determine more precisely the transition from monotonic to non-monotonic behavior in the experimental rheology. In addition, by examining in more detail the constraint release dynamics in both the tube and the slip-link models, in the regimes where the tube model correctly, and incorrectly, predicts non-monotonic behavior, it should be possible to develop a deeper understanding of constraint release dynamics. The results will also be important to confirm or refute the robustness of slip-link models in predicting star-linear rheology, and help to improve the accuracy and robustness of both tube and slip-link models.

V. Conclusions

The limits of an advanced tube model, the Hierarchical model with the "standard" Das parameter set and the assumption of primitive path fluctuations in the "thin tube" during constraint release Rouse (CR-Rouse) relaxation, were thoroughly tested against the linear rheology of ten series of 1,4-polybutadiene star-linear blends at several volume fractions of stars. Seven of these series were produced using three newly synthesized stars which were mixed with linear polymers either synthesized or purchased. The 1,2-vinyl contents of the new pure star and pure linear melts were found to be within the range 5-10% by ^{1}H-NMR and by comparing the WLF horizontal shift factors with literature references. The accuracy of GPC and TGIC characterization of the molecular weights of our new materials was assessed by comparing their zero shear viscosities with the molecular-weight dependencies of viscosity drawn from data in

the literature for 1,4-polybutadiene star and linear polymers, and molecular weights were found generally to be within around 20% of each other. We then compared predictions of the Hierarchical model against the linear rheology of ten series of star-linear blends, seven of which were newly prepared samples and the other three drawn from existing literature, for a total over 50 samples, providing the most comprehensive data base of star-linear blends ever assembled for any polymer chemistry.

To be sure that our results are robust to possible modest errors in sample characterization and in the tube model as applied to the pure materials, we assessed the Hierarchical model using both the GPC-characterized molecular weights of the pure star and linear melts, and the molecular weights needed to gain agreement of the model with the measured zero-shear viscosities of all pure components. Using either method, reasonably good agreement of measured and predicted linear viscoelasticity of the star-linear blends is obtained when the terminal relaxation time of the linear polymer is more than three orders of magnitude shorter than that of the star polymer. Agreement worsens markedly as the terminal relaxation time of the linear polymer approaches more closely that of the star, with the Hierarchical model incorrectly predicting a "non-monotonic" behavior in which the terminal relaxation time of some the blends is longer than that of either the pure star or pure linear polymer in the blend. Remarkable, once the terminal relaxation time of the linear polymer becomes longer than that of the star, the experimental results actually confirm this predicted non-monotonic behavior, and the frequency dependent moduli are in good agreement with Hierarchical model. Thus, our thorough study of these many samples reveals surprising successes, and surprising failures, of the tube model. The most surprising success is the prediction of the non-monotonic dependence of terminal relaxation time on blend composition when the pure linear chain relaxes more slowly

than does the pure star chain. The most surprising failure, remarkably enough, is that the model continues to predict this non-monotonic behavior even when the pure linear melt relaxes more rapidly, but not too much more rapidly, than the pure star melt, while the experimental data revert to a monotonic dependence on star volume fraction in these cases. These successes and failures are robust, as both were revealed in more than one blend series. Our previous very detailed study on three of the same star-linear blend series showed that variations of the tube model, obtained by using the BoB formulation, by deviating from the "thin tube" assumption, by allowing "disentanglement" relaxation, or by changing tube model parameters, fail to bring the tube model into even approximate agreement with more than a fraction of the relaxation data. Thus, the new work reported here, combined with our previous study, demonstrates that, despite remarkably accurate predictions in some cases, no widely used version of the tube model is able to predict rheology consistently for all entangled star-linear blends with the same chemical structure.

The study thus demonstrates the remarkably subtle effects of constraint release in star-linear blends, and the ability of an advanced version of the tube model to capture such phenomena for some blends, although not accurately enough to predict the range of molecular weights and compositions over which they occur. The work presented here, while not overcoming the limitations of the tube model, does help define the conditions under which it succeeds or fails, and thus suggests directions for future research. Our work also provides extensive data sets that can be used for testing other tube models, slip-link models, or other theories and simulations that might be forthcoming.

VI. Appendix

To supplement the analysis of star-linear blends featuring 1,4-polybutadiene stars of arm molecular weights near 24 kDa, shown in Figures 3.10- 3.14 in the main text, we here present and analyze additional star-linear blend data sets. Specifically, we assess the ability of the Hierarchical model predictions, implemented with Das parameters and "thin tube" relaxation, consistent with the main text, to match rheological data for our new 1,4-polybutadiene star-linear blend series 44KS-13.3KL, 47KS-73KL, and 47KS-260KL, as well as previously published data for 42.3KS-105KL blends from Struglinski et al.[18] We will refer to this group of blends containing star polymers with arm molecular weights of 42.3kDa, 44kDa, and 47kDa, as the "~40KS-linear blend sets." Similarly, we will refer to the star-linear blends presented in Figures 10-14 of the main text, with star arm molecular weights of approximately 24kDa, 25.3kDa, and 25.4kDa, as "~20KS-linear blend sets." For the ~40KS-linear blend sets, we conclude, in agreement with the findings presented in the main paper, that the accuracy of the Hierarchical model is poor for star-linear blends in which the pure linear component has terminal relaxation time less than, but within 3-4 orders of magnitude of that of the star component. In addition to exploring the ~40KS-linear blends sets, we also here provide a deeper analysis of the 24KS-210KL and 25.3KS-260KL blends, respectively featured in Figures 3.12 and 3.13 in the main text, to determine whether or not polydispersity in the linear component significantly influences the non-monotonic dependence of terminal relaxation time on star volume fraction. Lastly, we repeat the comparisons of the Hierarchical model predictions with both the ~20KS-linear and ~40KS-linear blend sets, except that instead of using molecular weights obtained from the zero-

shear viscosities of the pure linear and star polymers (presented in Table 4 of the main text), we use the molecular weights obtained from gel permeation chromatography (GPC).

This appendix is organized as follows. In Section VI.1, we disclose details concerning the synthesis and characterization of the new 1,4-polybutadiene star and linear polymers in this study. In Section VI.2.i, we report the WLF C_1 and C_2 coefficients of the pure stars and the pure linear polymers, as well as of the star-linear blends featured here in the SI and in the main text. In Section VI.2.ii, we analyze the accuracy of Hierarchical model predictions against the ~40KS-linear blend sets. In Section VI.2.iii, we assess the dependence of the non-monotonicity referred to above on the presence of polydispersity in pure linear components of the 24KS-210KL and 25.3KS-260KL blends presented in the main text. In Section VI.2.iv, we compare predictions of the Branch-on-Branch (BoB) model originating from Das et al.[23] with those of the Hierarchical model. In all predictions in the main text and in the SI, Sections VI.2.ii through VI.2.iv, the molecular weights used for the model predictions are those estimated from their zero-shear viscosities. In Section VI.2.v of this appendix, however, we re-analyze the accuracy of Hierarchical model predictions for the ~20KS-linear and ~40KS-linear blend sets using the molecular weights of pure star and pure linear 1,4-polybutadienes from GPC analysis instead of from estimates based on the zero-shear viscosity. Lastly, in Section VI.2.vi, we investigate further the accuracy of non-monotonic model predictions by assessing select star-linear blends.

VI.1. Synthesis and Characterization of Star and Linear 1,4-Polybutadiene Polymers

VI.1.i. 73KL, 260KL, 25.3KS, 44KS and 47KS Synthesis and Characterization (Hadjichristidis Lab)

Chemicals. All chemicals were purified according to the standards required for anionic polymerization, using well-established high-vacuum procedures.[57] 1,3-Butadiene (Sigma-Aldrich, 99%) was purified *via* consecutive distillations over *n*-BuLi, at -10^{o}C using ice/salt bath, prior to addition to the polymerization reactor. Benzene (Sigma-Aldrich, 99.8%) was purified *via* distillation from CaH_2 and stored in a round bottom flask, under high vacuum. *sec*-Butyllithium (*s*-BuLi, 1.4 M in cyclohexane, Sigma-Aldrich) was used without purification and diluted with dry n-hexane. 1,2-bis(dichloromethylsilyl)ethane (Gelest, 95%) was purified by crystallization from *n*-hexane, followed by three crystallizations from the bulk and subsequently diluted in *n*-hexane and stored under high vacuum at -30 ^{o}C. Methanol (Sigma-Aldrich, 99.8%) (terminating agent) was stored under high vacuum and used as received.

Synthesis of linear 1,4-polybutadiene ($PBd_{1,4}$). A typical procedure for the synthesis of the linear $PBd_{1,4}$ 73KL and 260KL melts is as follows.[57-59] 7g of 1,3-butadiene was polymerized at room temperature, using 0.03 mmol of *sec*-butyllithium as initiator and benzene as solvent. The mixture was left to react for 1 day and finally, the polymerization quenched with methanol and the polymer precipitated in a large amount of methanol. The final product was dried in a vacuum oven until constant weight.

Synthesis of 1,4-polybutadiene ($PBd_{1,4}$) 4-arm stars. A typical procedure for the synthesis of the 4-arm star $PBd_{1,4}$ 25.3KS, 44KS and 47KS melts is as follows.[57-59] 10g of 1,3-butadiene was polymerized at room temperature, using 0.22 mmol of *sec*-butyllithium as initiator and benzene as solvent. The mixture was left to react for 1 day and then an aliquot was taken by heat-sealing the corresponding constriction tube for molecular characterization. The rest of the "living" polymer solution was reacted with 0.044 mmol of 1,2-bis(dichloromethylsilyl)ethane (BMDCSE). The linking reaction was monitored by GPC and lasted, depending on the sample,

2-3 weeks. After the completion of the reaction, the excess of the living chains were terminated by the addition of degassed methanol and the solution precipitated in a large amount of methanol. The 4-arm star $PBd_{1,4}$ melts were purified from the unreacted linear chains by repeated solvent/non-solvent (toluene/methanol) fractionations.

Characterization. The weight average molecular weights (M_w) of all samples were determined using the light scattering detector on a triple detection GPC. THF was the eluent, at a flow rate of 1 mL/min at 30^0C. Refractive index increments, dn/dc, were measured with a Brookhaven BI-DNDCW refractometer, at 30^0C, calibrated with KCl solutions. Figures 3.A1-A, A1-B, A1-C and A1-D feature the GPC curves of the 73KL, 26KL, 25.3KS and 47KS. ^{1}H-NMR spectroscopy measurements were carried out using $CDCl_3$ (Sigma-Aldrich, 99.6%) on a Brücker AV-500 spectrometer. Figures 3.A2-A, A2-B, A2-C, and A2-D respectively feature the ^{1}H-NMR results of the pure 73KL, 260KL, 25.3KS and 47KS.

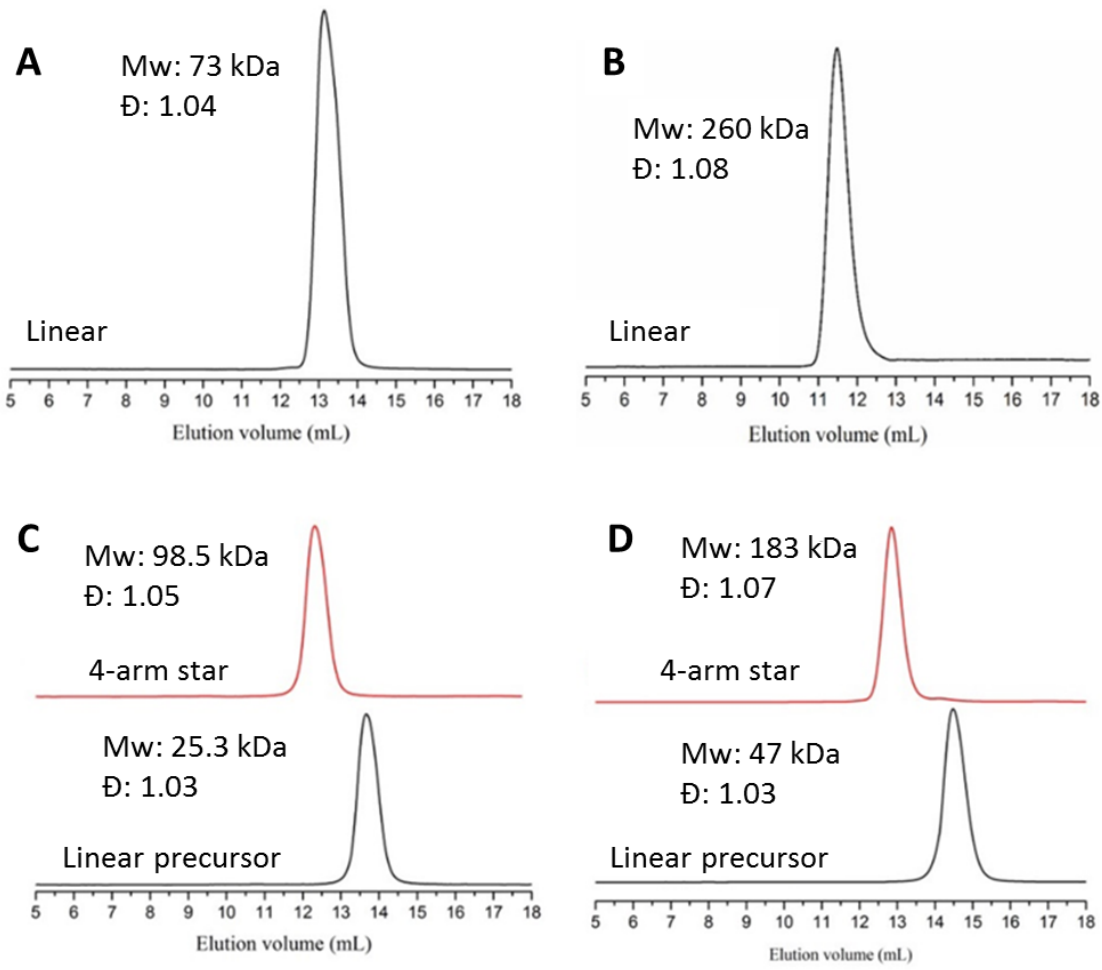

Figure 3.A1: Gel permeation chromatography (GPC) of two linear and two four-arm star 1,4-polybutadienes A) 73KL, B) 260KL, C) 25.3KS, and D) 47KS. Also Included in C) and D) are the GPC curves of the linear precursors prior to branching synthesis of the 25.3KS and 47KS, respectively. The linear molecular weights (Mw) listed in Table 3.1 of the main text were determined by GPC, using a light scattering detector. The arm molecular weights of the stars, shown in parentheses in Table 3.1, were obtained by dividing the peak molecular weights by 4, which is the nominal number of arms per star molecule. Also reported here are the polydispersity (Đ) for each sample. **(Figure provided by Nikos Hadjichristidis)**

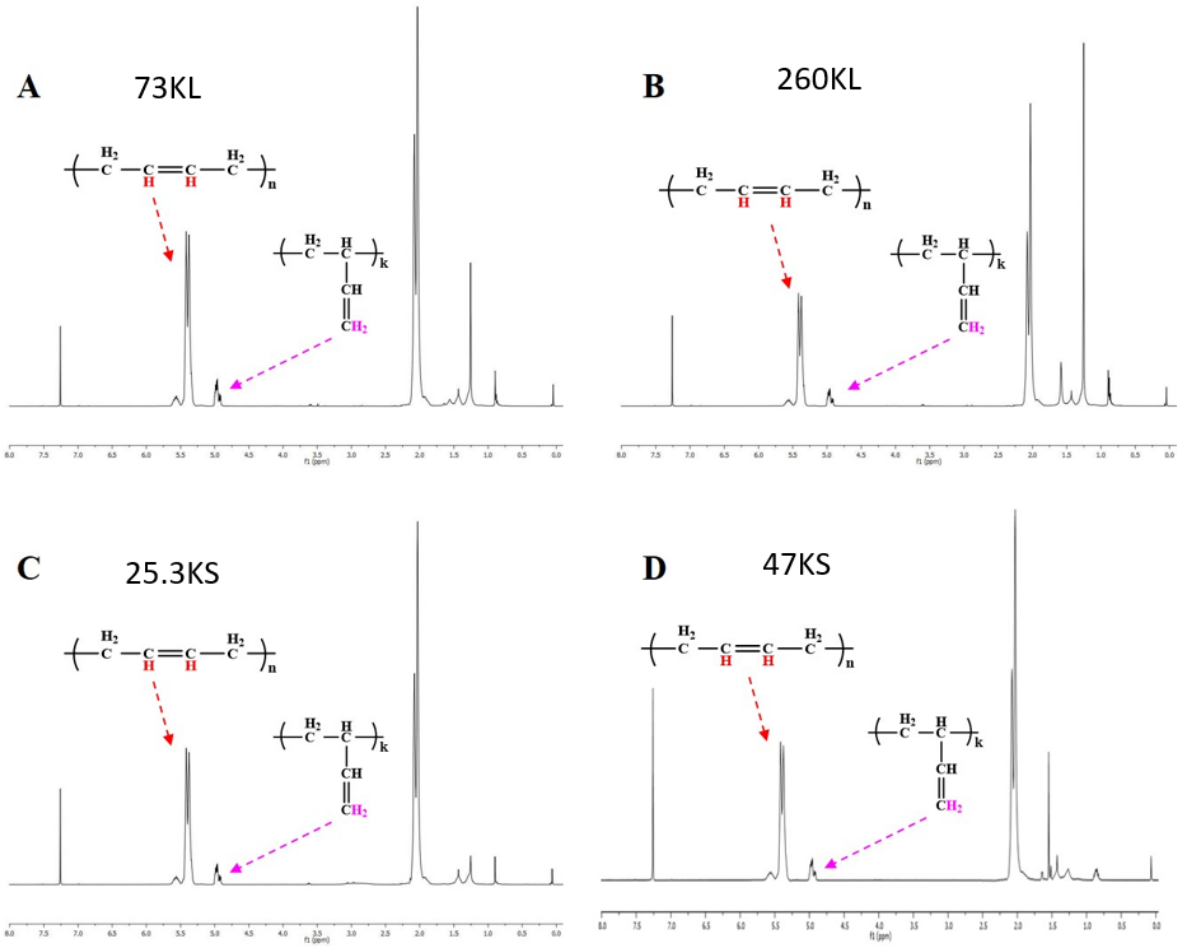

Figure 3.A2: ^{1}H-NMR of 1,4-polybutadienes A) 73KL, B) 260KL, C) 25.3KS, and D) 47KS **(Figure provided by Nikos Hadjichristidis)**

VI.1.ii. GPC and TGIC Measurements of the 4-Arm Star 44KS (Chang Lab)

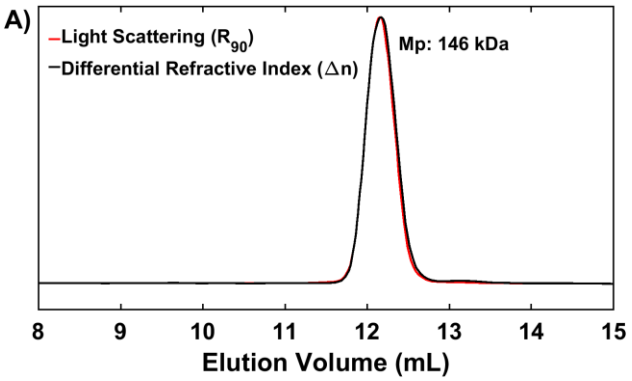

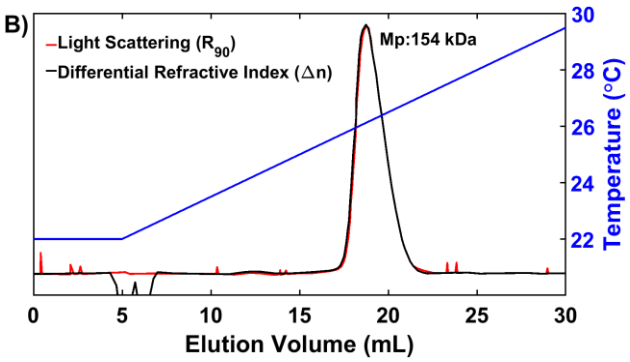

Figure 3.A3: A) GPC and B) TGIC characterization of the 1,4-polybutadiene 4-arm star 44KS. The GPC and TGIC arm molecular weights observed in Table 3.1 of the main text were obtained by dividing the peak molecular weight, "Mp", value depicted in the above figures by 4, which is the nominal number of arms per star molecule. The polydispersity index of this melt is 1.07, as reported in Table 3.1 of the main text. **(Figure provided by Sanghoon Lee)**

VI.1.iii. GPC and H-NMR Measurements of the Linear 13.3KL (Mays Lab)

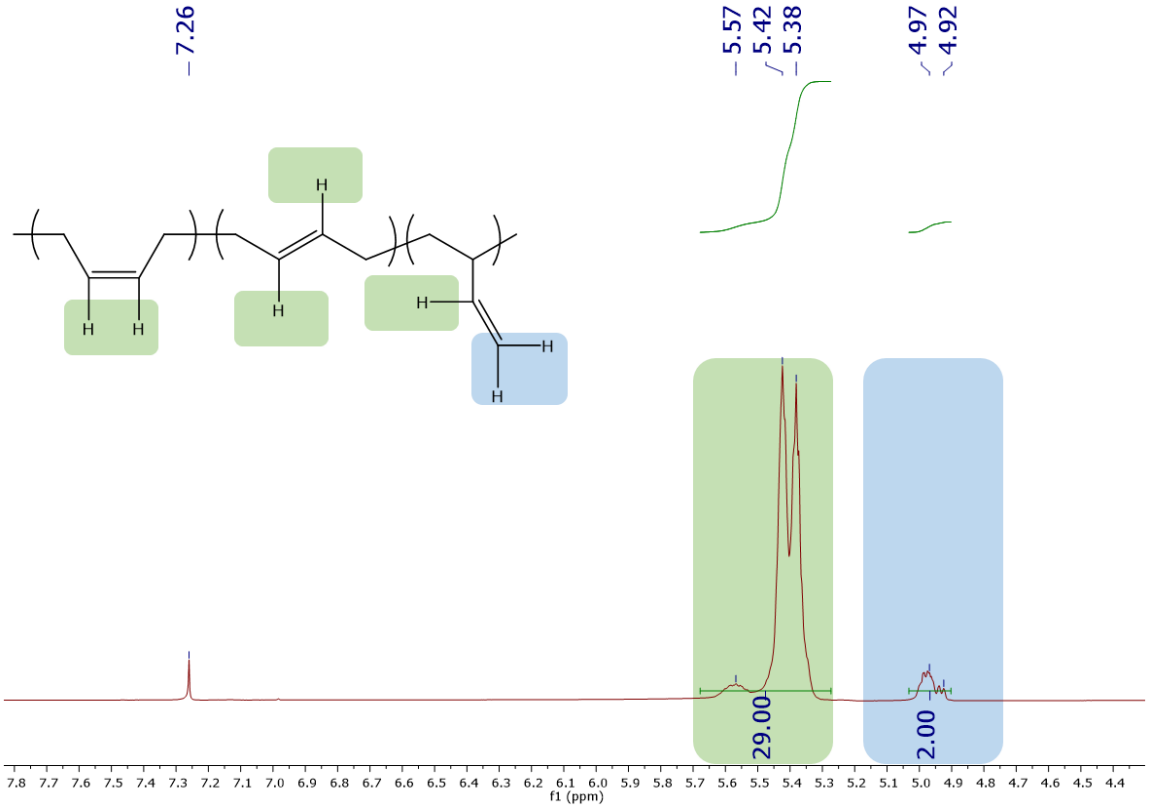

Figure 3.A4: ^{1}H-NMR of the 1,4-polybutadine 13.3KL **(Figure provided by Jimmy Mays)**

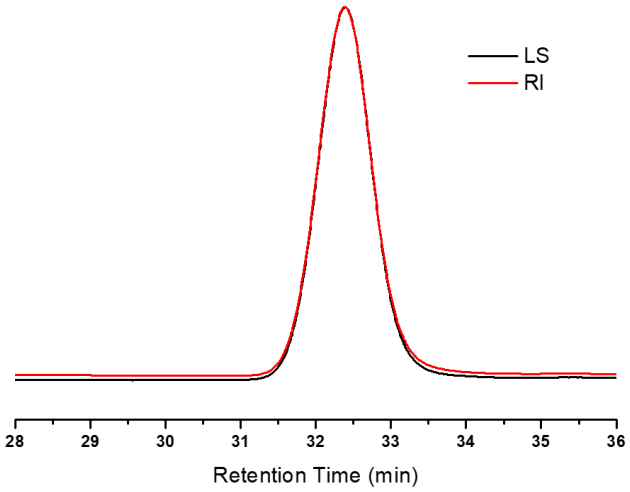

Figure 3.A5: GPC measurements of the 13.3KL. The black line represents measurements conducted by light scattering; the red line is the refractive index (RI). The polydispersity index of this sample is 1.02, as reported in Table 3.1 of the main text. **(Figure provided by Jimmy Mays)**

VI.2. Rheology of 1,4-Polybutadiene Star-Linear Blends

VI.2.i. Time-Temperature Superposition

In supplement to the plots of horizontal temperature shift factors depicted in Figures 3.1 and 3.2 of the main text, we report here the WLF C_1 and C_2 coefficients obtained from the shift factor curves of the pure star and pure linear 1,4-polybutadienes used in this study. We note that the C_1 and C_2 coefficients of the pure 105KL and 42.3KS samples taken from Struglinski et al.[18] were not reported in the original work, and so are absent from Table 3.A1. In Tables 3.A2 and A3, we report the WLF C_1 and C_2 coefficients of the new 24KS-13.3KL and 44KS-13.3KL star-linear blends, respectively. For both of these star-linear blend series, the WLF C_1 and C_2 coefficients are organized by star volume fraction (ϕ_s).

Table 3.A1: WLF time-temperature superposition constants C_1 and C_2 of the pure star and pure linear 1,4-polybutadienes. The reference temperature for all figures and tables featured in the main text and in this Appendix, is 25°C.

Sample	Source	Architecture	C_1	C_2

7.5KL	Shivokhin et al.[30]	Linear	4.7	154.3
24.5KS		3-arm Star	4.7	154.3
58KL	Desai et al.[29]	Linear	3.9	178.9
24KS		4-arm Star	4.7	187.1
105KL	Struglinski et al.[18]	Linear	------	------
42.3KS		3-arm Star	------	------
13.3KL	Polymer Source	Linear	3.9	175.6
210KL		Linear	4.0	176.3
73KL	Fresh synthesis	Linear	3.9	169.9
260KL		Linear	4.2	174.3
25.3KS		4-arm Star	4.4	180.3
44KS		4-arm Star	5.0	194.4
47KS		4-arm Star	5.2	194.1

Table 3.A2: The WLF C_1 and C_2 constants of the 24KS-13.3KL blend series.

Star volume fraction (ϕ_s)	**C_1**	**C_2**
1	4.7	187.1
0.8	4.8	188.3
0.4	4.4	183.1
0.1	4.2	181.5
0	3.9	175.6

Table 3.A3: The same as Table 3.A2, but for 44KS-13.3KL blend series.

Star volume fraction (ϕ_s)	**C_1**	**C_2**
1	5.0	194.4
0.9	5.0	194.2
0.8	4.8	197.0
0.6	4.8	195.0
0.4	4.6	189.2
0.2	4.3	185.3
0	3.9	175.6

VI.2.ii. Hierarchical Model Predictions of the 40KS-Linear Blend Data

Similar to Figures 3.10- 3.14 in the main text that feature the ~20KS-linear blend sets, we analyze in Figures 3.A6- 3.A9 how well the Hierarchical model, with Das parameters and thin tube CR-Rouse dynamics, predicts the rheology of the ~40KS-linear blend sets, including blends

newly prepared here and data borrowed from the literature. In addition, the molecular weights of the pure star and the pure linear polymers used in model predictions in Figures 3.A6- 3.A14 are taken from Table 3.4 of the main text, which are estimated from their zero-shear viscosities. To assess the effect of this choice of molecular weights, in Section VI.2.v, Figures 3.A15- 3.A23 contain predictions of blend rheology using the GPC molecular weights of the pure components.

Figure 3.A6 shows that Hierarchical model predictions (lines) are in relatively good agreement with measurements (symbols) for the 44KS-13.3KL blends. However, in Figure 3.A6-A, the model predicts faster terminal relaxation of the ϕ_s=0.6 blend by a factor of roughly 1.6, which increases to a factor of 2.4 for ϕ_s=0.2. Similar modeling success is observed in Figure 3.A7-A for the 47KS-73KL blends, for which faster relaxation by factors of roughly 1.5, 2.3, and 2.3 are predicted for ϕ_s=0.8, 0.6, and 0.4, respectively. The success of model predictions in Figures 3.A6 and 3.A7 are consistent with the observations in the main text and in Desai et al.,[29] which find that Hierarchical model predictions tend to agree with star-linear blend data when the terminal relaxation times of the pure star are at least 3-4 orders of magnitude longer than that of the pure linear. The terminal relaxation times of the pure star and pure linear 1,4-polybutadines in Figure 3.A6-A are in fact separated by roughly 5 orders of magnitude, while this separation is over 3 orders of magnitude in Figure 3.A7-A.

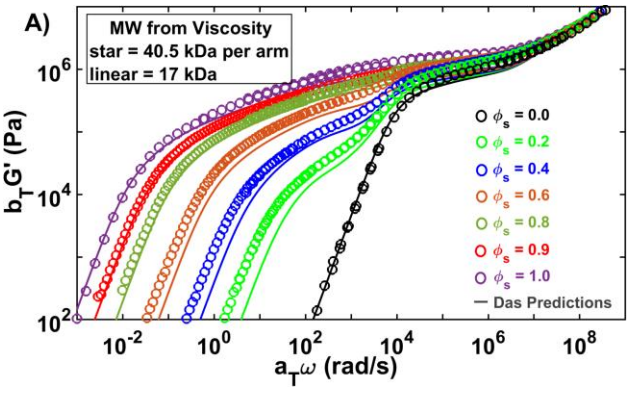

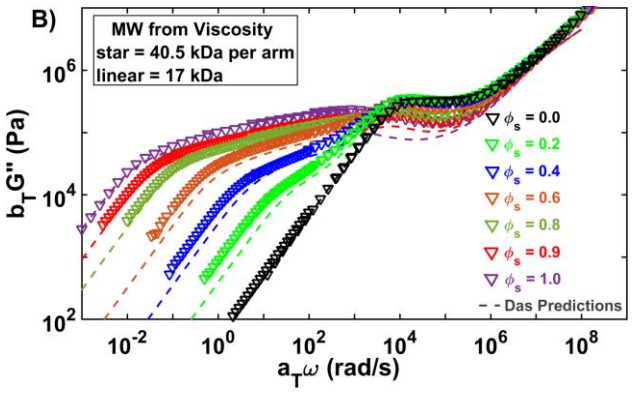

Figure 3.A6: Experimental (symbols) A) G' and B) G" linear rheology of the 44KS-13.3KL blend series at various star volume fractions ϕ_s, compared with predictions of the Hierarchical model (lines). The star and linear molecular weights used in the model predictions, listed in the legend, are from Table 3.4 of the main text.

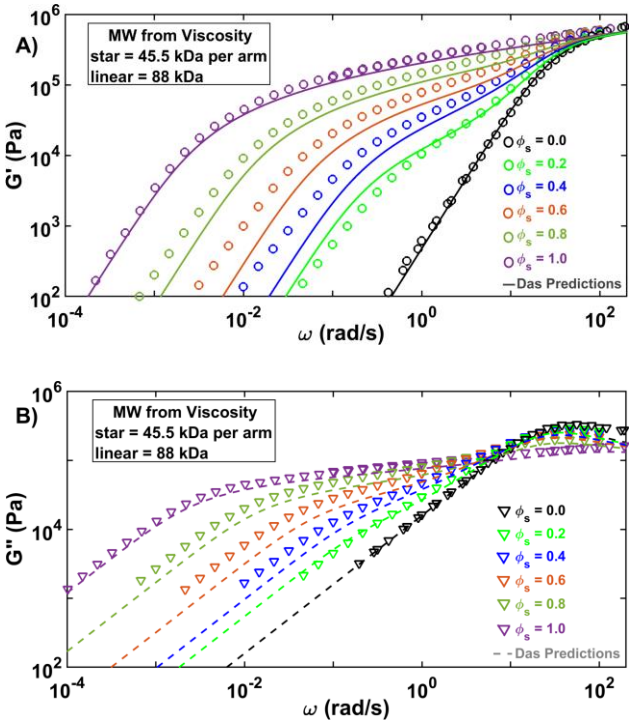

Figure 3.A7: The same as Figure 3.A6, but for the 47KS-73KL blend series.

Figure 3.A8 shows, in contrast, a notable failure of the Hierarchical predictions (lines) for the 42.3KS-105KL rheological data (symbols) of Struglinski et al.[18] The experimental data clearly show a monotonic dependence of terminal time on ϕ_s; however, model predictions of the

relaxation time of the ϕ_s=0.1 blend is clearly longer than for the ϕ_s=0.75, 0.5, 0.3 and 0.2 blend compositions. In addition, the relaxation time for the ϕ_s=0.2 blend is longer than that for the ϕ_s=0.3 blend. Besides the erroneously predicted non-monotonicity, the Hierarchical model also underpredicts the relaxation time for the ϕ_s=0.75 blend by a factor of roughly 2.5. Unlike the 44KS-13.3KL and 47KS-73KL blends depicted in Figures 3.A6-A and 3.A7-A, the terminal relaxation of the pure 42.3KS star and the pure 105KL linear in Figure 3.A8-A are separated by less than 3 orders of magnitude, which seems to correlate with the failure of the model.

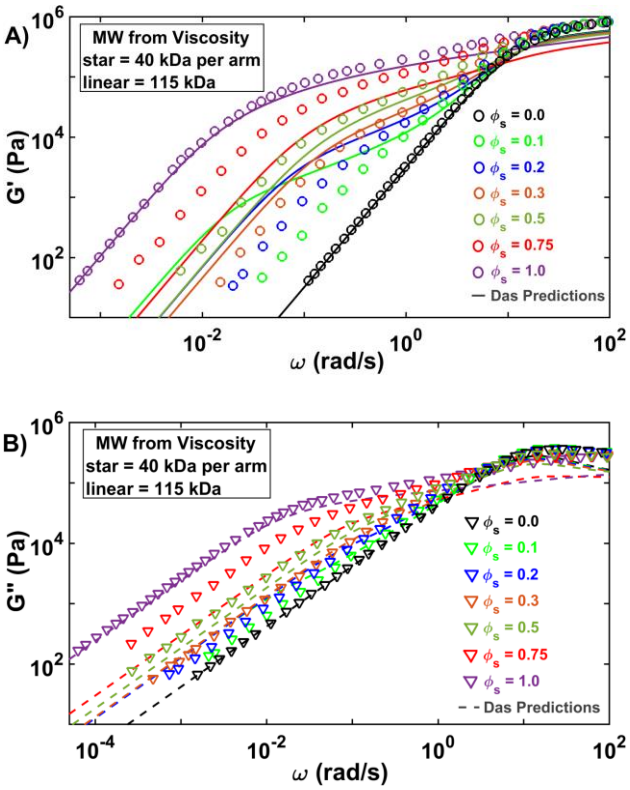

Figure 3.A8: The same as Figure 3.A6, but for the 42.3KS-105KL blend series, from Struglinski et al.[18]

Figure 3.A9 shows that the model predictions for the 47KS-260KL blends incorrectly predict a slight non-monotonic dependence of terminal relaxation time on ϕ_s in Figure S9-A.

Given that the 24KS-210KL and 25.3KS-260KL blends, presented respectively in Figures 3.13 and 3.14 of the main text, show non-monotonic experimental behavior, we suggest that had the pure 47KS star been blended with a somewhat higher molecular weight linear polymer, non-monotonic behavior might well have been observed in the resulting star-linear blends. Since the data for the ϕ_s=0.2, 0.4, and 0.6 are already close to each other in Figure 3.A9-A, it seems reasonable that only a modest increase (less than a factor of two) in linear molecular weight might be sufficient to provoke non-monotonic behavior in the data. If so, since the terminal relaxation of the pure 47KS star is at least one magnitude larger than that of the pure 260KL linear, non-monotonicity in a 47KS-linear blend might occur even before the relaxation time of the linear chain exceeds that of the star.

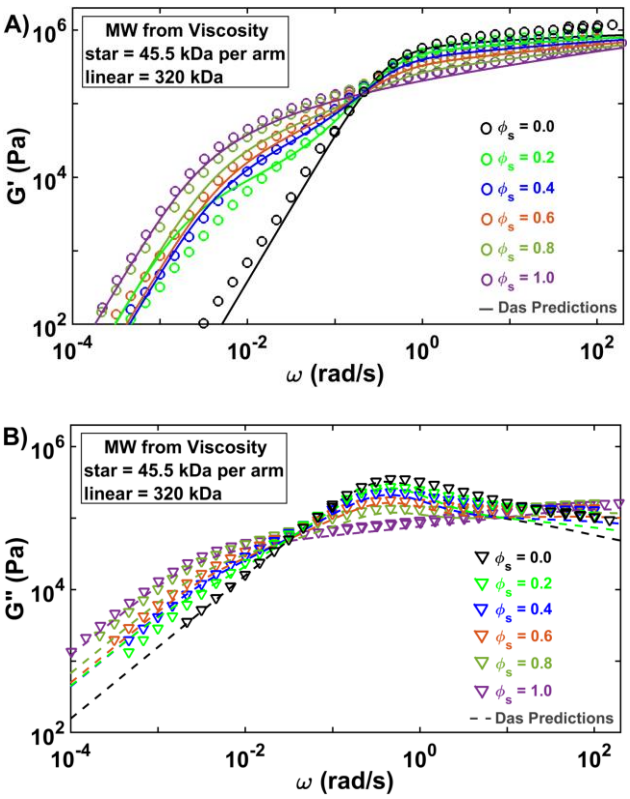

Figure 3.A9: The same as Figure 3.A6, but for the 47KS-260KL blend series.

VI.2.iii. Influence of Polydispersity on Non-Monotonicity

In Figures 3.13 and 3.14 of the main text, the 24KS-210KL and 25.3KS-260KL star-linear blends present surprising non-monotonicity, in which the blends have a longer relaxation time than either the pure star or the pure linear polymer. These blends are the first to be studied at multiple star volume fractions in which the pure linear polymer has a somewhat longer relaxation time than the pure star. (There are, however, some polyisoprene blends with 10% star in which the star relaxation time is much shorter than the linear polyisoprene.[60] These were studied to assess the case in which the linear polymer is considered to be a "fixed matrix" in which the dilute star polymer relaxes. Since these studies did not encompass multiple star volume fractions, non-monotonicity of the kind considered here could not be observed.) However, the pure 210KL and pure 260KL linear polymers in these blends show in their terminal relaxation evidence of some polydispersity. It is worth considering if this polydispersity could potentially contribute to, or be entirely responsible for, the observed non-monotonicity in the rheology of the 24KS-210KL and 25.3KS-260KL blends.

We therefore here investigate the impact of this polydispersity on the non-monotonic behavior of the blends by first fitting the pure 210KL (symbols) and 260KL (symbols) with Hierarchical model predictions (pink lines) which accommodate polydispersity, shown respectively in Figures 3.A10 and 3.A11. As a reference, we include the initial Hierarchical model predictions (green lines) that utilize the molecular weights from Table 3.4 in the main text. The pink lines, which are model predictions with polydispersity identified through model fitting, superpose better with the 210KL and 260KL melts. The polydispersity in the pure 210KL is captured with a binary linear blend of 260 kDa (95% volume) and 500 kDa (5% volume),

whereas the 260KL is also modeled by a binary linear blend of a 320 kDa (95% volume) and a 560 kDa linear chain (5% volume).

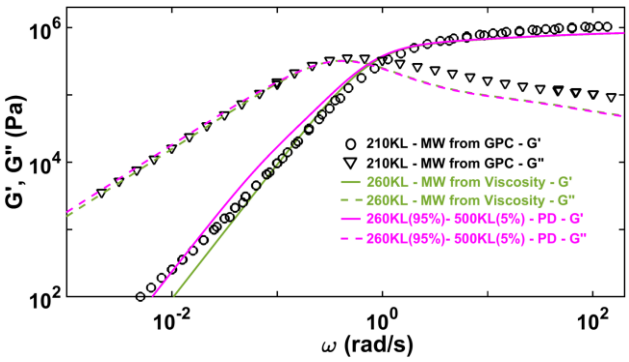

Figure 3.A10: Linear rheology of the pure 210KL melt (symbols) compared with Hierarchical model predictions (lines). The pink lines are model fits using 2-component polydispersity "PD" in the pure 210KL melt, as discussed in the text of this appendix, while the green lines are for a single-component linear with molecular weight taken from Table 3.4 of the main text.

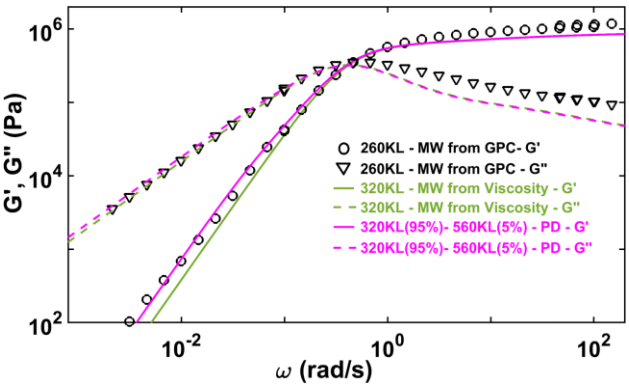

Figure 3.A11: The same as Figure 3.A10, but for the pure 260KL 1,4-polybutadiene melt.

After modeling the polydispersities of the pure 210KL and 260KL polymers with the Hierarchical model, we generated model predictions (lines) to compare with the data (symbols) for the 24KS-210KL and 25.3KS-260KL star-linear blends, shown respectively in Figures 3.A12 and 3.A13. Although accounting for polydispersity, the model continues to predict non-monotonicity in the 24KS-210KL and 25.3KS-260KL blends, and gives reasonable agreement

with each blend composition. Thus, it is unlikely that the non-monotonicity in the dependence of relaxation time on blend composition is a result of the slight polydispersity in the pure 210KL and pure 260KL melts.

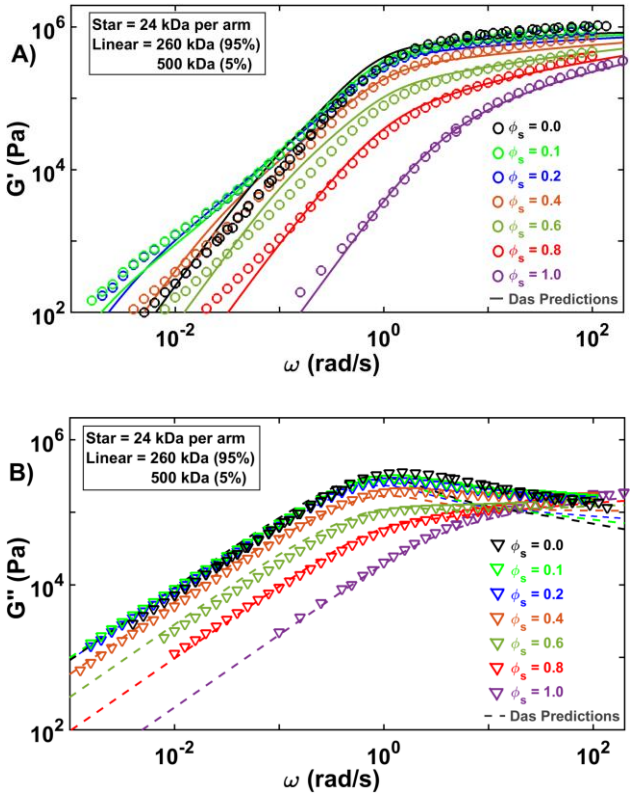

Figure 3.A12: A) G' and B) G" of the 24KS-210KL blends (symbols), compared with Hierarchical model predictions (lines) using the polydispersity obtained by the fits in Figure 3.A10, and listed in the legend.

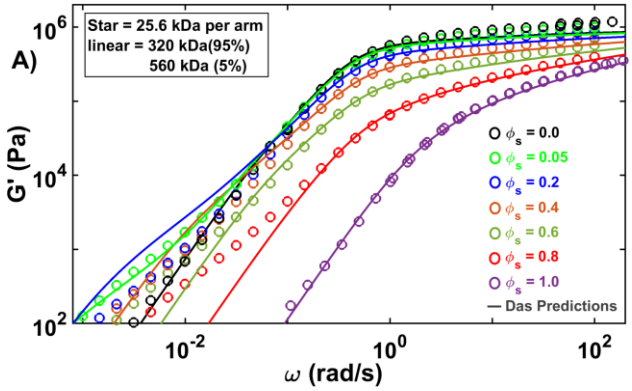

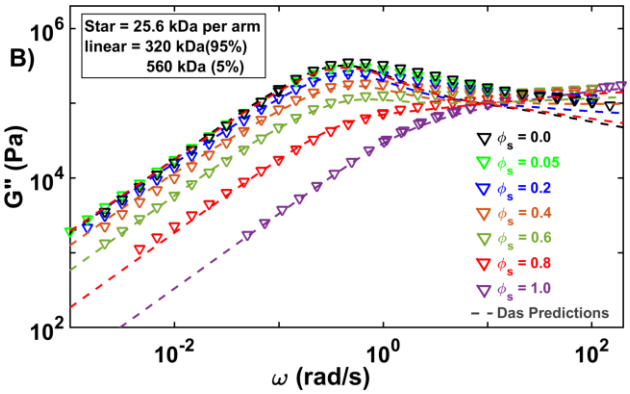

Figure 3.A13: The same as Figure 3.A12, but for the 25.3KS-260KL blends with polydispersity determined by the fits in Figure 3.A11.

VI.2.iv Comparison of Star-Linear Predictions of the BoB and the Hierarchical Models

In the Theoretical Modeling section of the main text (Section III), we stated that predictions of the Hierarchical model, using the Das parameters and thin tube CR-Rouse, are similar to predictions of the Branch-on-Branch (BoB) model, which originates from the work of Das et al.[23] Here in Figure 3.A14, we demonstrate this by comparing Hierarchical model and BoB model predictions (lines) for the 25.3KS-260KL star-linear blend series (symbols), which is one of the blend series that show non-monotonic dependence of terminal relaxation time on star volume fraction. The molecular weights of the pure star and pure linear utilized in both Hierarchical and BoB model predictions are based on fits to the experimental viscosities, an are given in Table 3.4 in the main text. Figure 3.A14 shows no significant difference between predictions of the BoB and Hierarchical models.

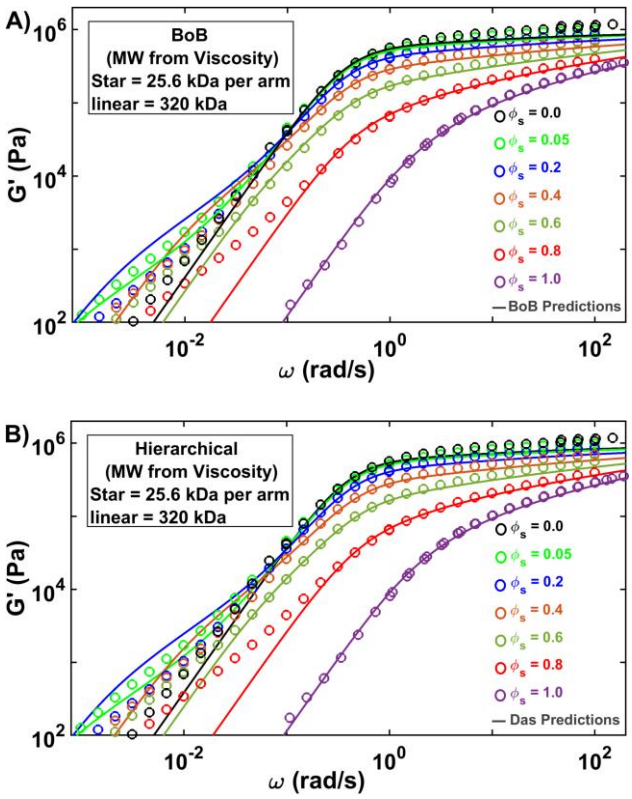

Figure 3.A14: Predictions of A) Branch-on-Branch (BoB) model[23] and B) Hierarchical model, for 25.3KS-260KL blend series, where symbols are experimental data and the molecular weights of the pure components are based on their viscosities.

VI.2.v. Hierarchical Model Predictions of Star-Linear Blend Data Using MW Given by GPC

VI.2.v.a. Model Predictions of the ~20KS-Linear Blend Sets

The accuracy of the Hierarchical model predictions of ~20KL-linear blends featured in Figures 3.10- 3.14 of the main text were assessed after generating a baseline of model predictions that fit the zero-shear viscosities of the pure star and pure linear components of each blend, as given in Table 3.4. We now assess the success of Hierarchical model predictions in capturing the star-linear blend rheology when using the molecular weights measured by gel permeation chromatography (GPC). The model assessment here will focus on the ~20KL-linear blend sets shown in Figures 3.A15- 3.A19. Hierarchical model predictions (lines) for the

24.5KS-7.5KL and the 24KS-13.3KL blends (symbols) depicted in Figures 3.A15 and 3.A16 are minimally impacted by use of the molecular weights measured by GPC rather than using those determined from the viscosities. The relaxation behavior of the pure 24.5KS and the pure 24KS are captured reasonably well by the model predictions. However, using the molecular weight measured by GPC causes an overprediction of the pure 7.5KL data by a factor of roughly 1.8 along the x-axis in Figure 3.A15-A, but leads to an underprediction of the relaxation time of the pure 13.3KL data by roughly a factor of 2.4 in Figure 3.A16-A. Despite these deviations, the model's predictions for the 24.5KS-7.5KL and 24KS-13.3KL blends in Figures 3.A15 and 3.A16 are similar to those in Figures 3.10 and 3.11 in the main text, respectively.

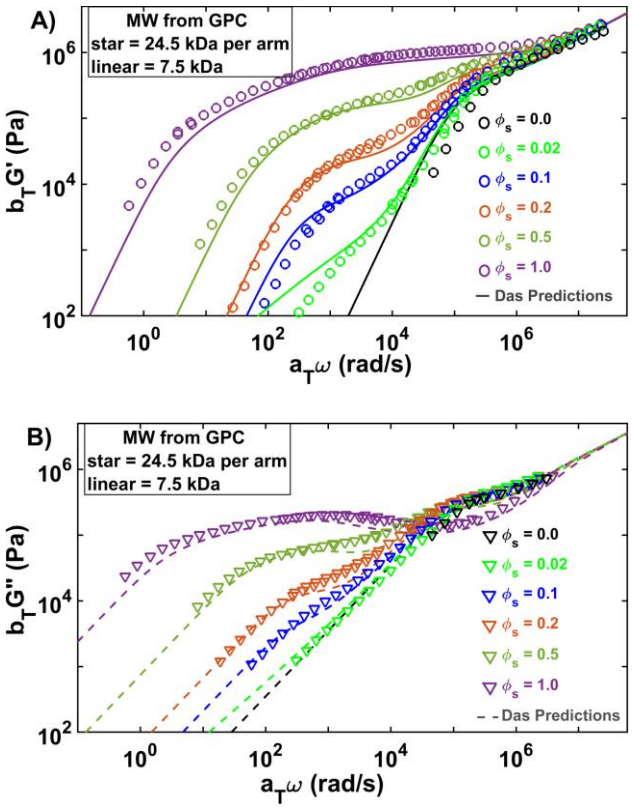

Figure 3.A15: A) G' and B) G" linear rheology of the 24.5KS-7.5KL 1,4-polybutadiene star-linear blends with star volume fractions (ϕ_s) 1, 0.5, 0.2, 0.1, 0.02, and 0, taken from Shivokhin et al.[30] compared to Hierarchical model predictions (lines) that use the pure star and pure linear molecular weights measured by GPC, given in the legend.

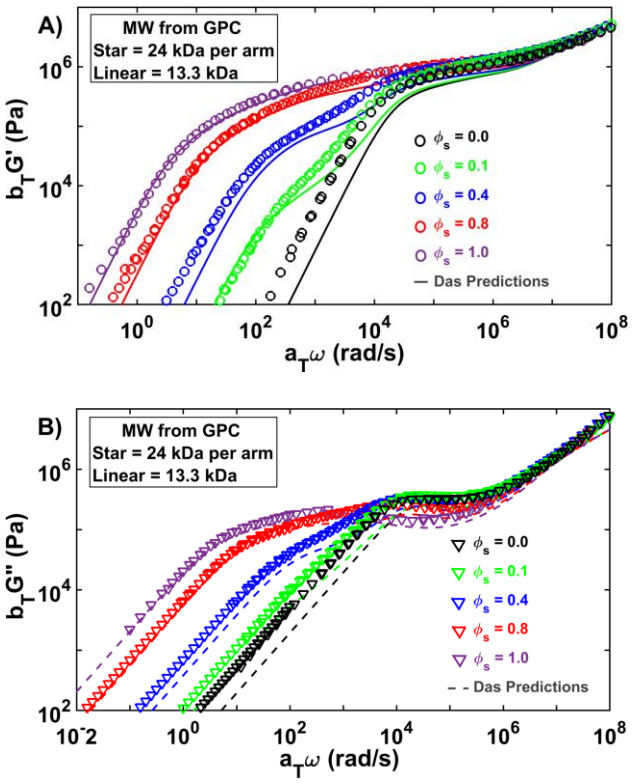

Figure 3.A16: The same as Figure 3.A15, but for the 24KS-13.3KL star-linear blends.

As shown in Figure 3.A17, the Hierarchical model predictions (lines), using GPC molecular weights for the pure 24KS and the pure 58KL, do not improve the predictions of the 24KS-58KL star-linear data (symbols) from Desai et al.,[29] relative to the results in Figure 3.12 of the main text. Using molecular weights from GPC or from zero-shear viscosities, model predictions falsely predict non-monotonic dependence of terminal relaxation time on star volume fraction for these 24KS-58KL blends.

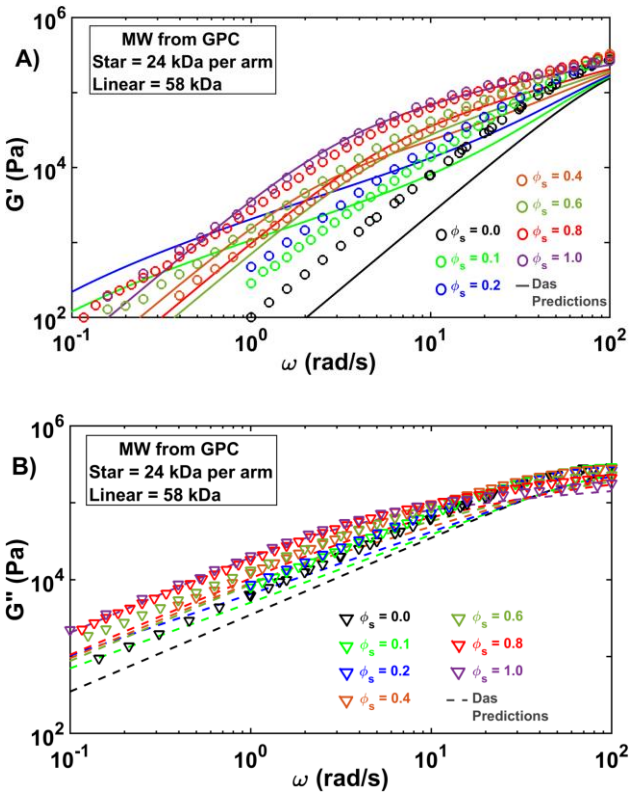

Figure 3.A17: The same as Figure 3.A15, but for the 24KS-58KL star-linear blends taken from Desai et al.[29]

In the main text, Figures 3.13 and 3.14 show non-monotonic dependence of terminal relaxation time on star volume fraction in the experimental rheology for the 24KS-210KL and 25.3KS-260KL blends; the Hierarchical model, with molecular weights obtained from fitting of zero-shear viscosities, predicts this non-monotonicity. We now show in Figures 3.A18 and 3.A19 that the Hierarchical model predictions (lines), with the molecular weights given by GPC, also predict non-monotonicity in the 24KS-210KL and 25.3KS-260KL blends (symbols), consistent with the findings in the main text. However, since the GPC molecular weights of the pure linear melts, 210 kDa and 260 kDa, are notably lower than the molecular weights obtained from fitting the zero-shear viscosities of the same linears, namely 260 kDa and 320 kDa, the Hierarchical model drastically underpredicts the relaxation times of these linear polymers when the GPC

molecular weights are used, which is shown very clearly in Figures 3.A18-A and 3.A19-A. As detailed in the discussion of Figure 3.6 in the main text, the GPC molecular weights of the 210KL and the 260KL melts are arguably a little lower than expected based on the zero-shear viscosities of similar samples in the literature. Since the Hierarchical model underpredicts the pure linear melts with the GPC molecular weight measurements, predictions of the associated 24KS-210KL and 25.3KS-260KL blends, shown in Figures 3.A18 and 3.A19, fit poorer the data for with each blend composition than is achieved in Figures 3.12 and 3.13 of the main text. Nevertheless, the non-monotonicity seen in the experiments is predicted by the model, regardless of whether the GPC molecular weight of that inferred from the zero-shear viscosity is used.

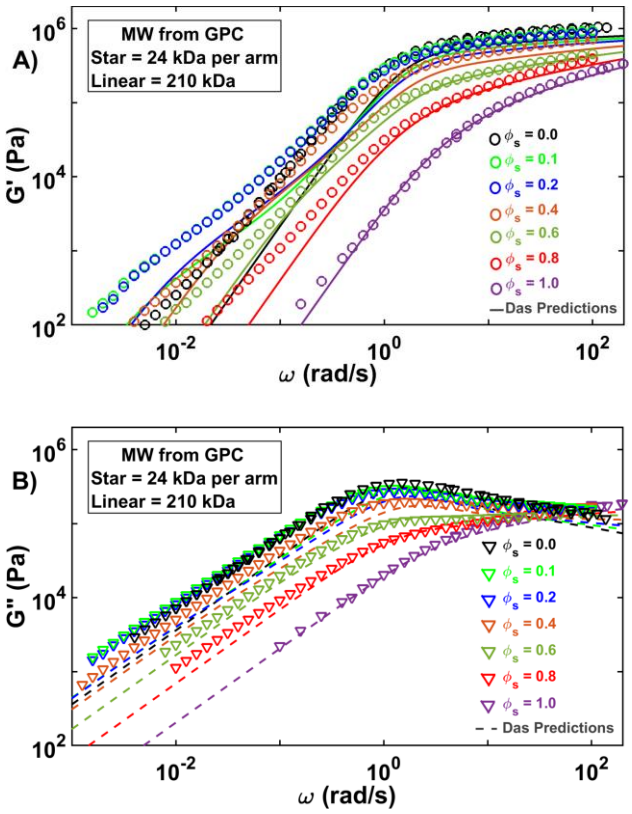

Figure 3.A18: The same as Figure 3.A15, but for the 24KS-210KL blends.

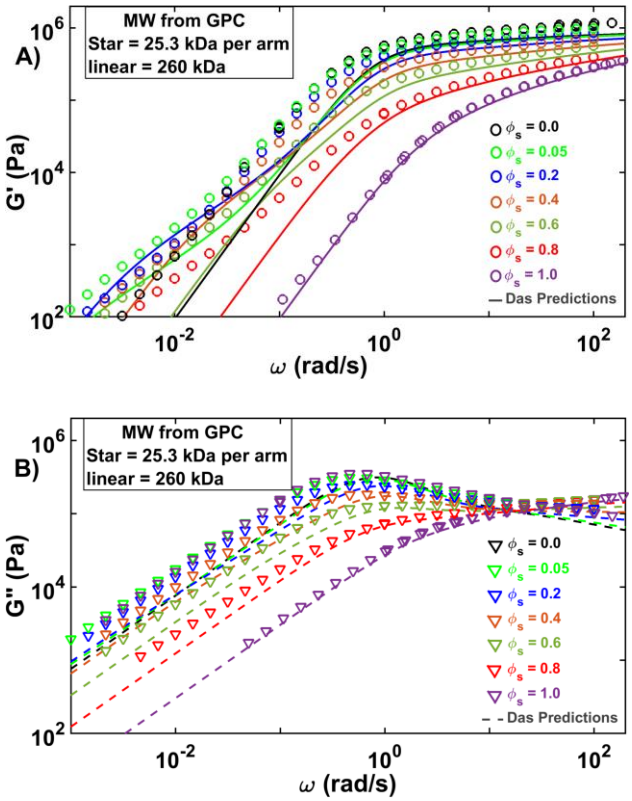

Figure 3.A19: The same as Figure 3.A15, but for the 25.3KS-260KL blends.

VI.2.v.b Model Predictions of the ~40KS-Linear Blend Sets

Similar to Figures 3.A15- 3.A19, which shows Hierarchical model predictions using GPC molecular weights for the ~20KS-linear blend sets, we perform the same analysis with the ~40KS-linear blend sets. Figures 3.A20- 3.A23 depict model predictions for 44KS-13KL, 47KS-73KL, 42.3KS-105KL blends, with the latter obtained from Struglinski et al.,[18] and 47KS-260KL blends. As shown by comparing Figure 3.A20 with Figure 3.A6, model predictions for the 44KS-13.3KL rheology are less accurate with the GPC molecular weights than with molecular weights based on zero-shear viscosity data, given in Table 3.4 of the main text. In Figure 3.A20-A, the model overpredicts the relaxation time of the pure 44KS by a factor of roughly 3 along the x-axis, while that for the pure 13.3KL is underpredicted by a factor of 2.2. In addition, the relaxation times for ϕ_S=0.9 and 0.8 blends are overpredicted by roughly factors of

2.3 and 2, respectively. In contrast, model predictions for ϕ_s= 0.6, 0.4 and 0.2 blends are improved in Figure 3.A20 relative to Figure 3.A6. Overall, the use of GPC molecular weights in the Hierarchical model predictions of the 44KS-13.3KL does not contradict the conclusion drawn from Figure 3.A7, that model predictions are in general agreement with the star-linear blend experimental rheology, as long as the terminal relaxation time of the pure star is at least 3-4 orders of magnitude larger than that of the pure linear component.

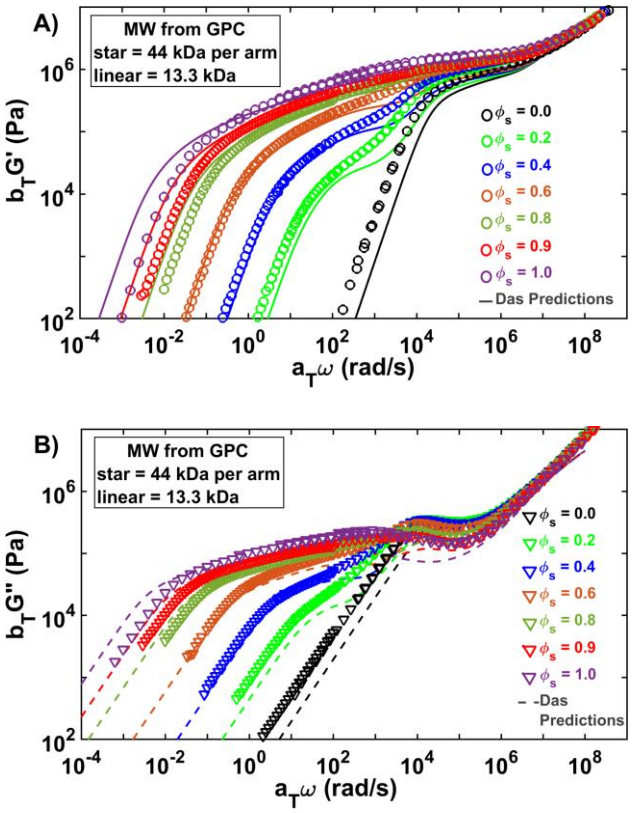

Figure 3.A20: The same as Figure 3.A15, but for 44KS-13.3KL blends.

Hierarchical model predictions (lines), using GPC molecular weights, are reasonably successful in predicting the 47KS-73KL rheology data (symbols) shown in Figure 3.A21. Model predictions in Figure 3.A21-A of the 73KL linear polymer do not match as closely the data as do predictions for the same linear molecules in Figure 3.A7, which use the molecular weights from

fits to zero-shear viscosity. However, predictions of the 44KS-73KL blends in Figure 3.A21 are overall quite comparable to those in Figure 3.A7. Therefore, as already stated in the discussion concerning Figure 3.A21, the use of GPC molecular weights in the Hierarchical model yields results consistent with the conclusions from predictions based on star and linear molecular weights determined by the zero-shear viscosity.

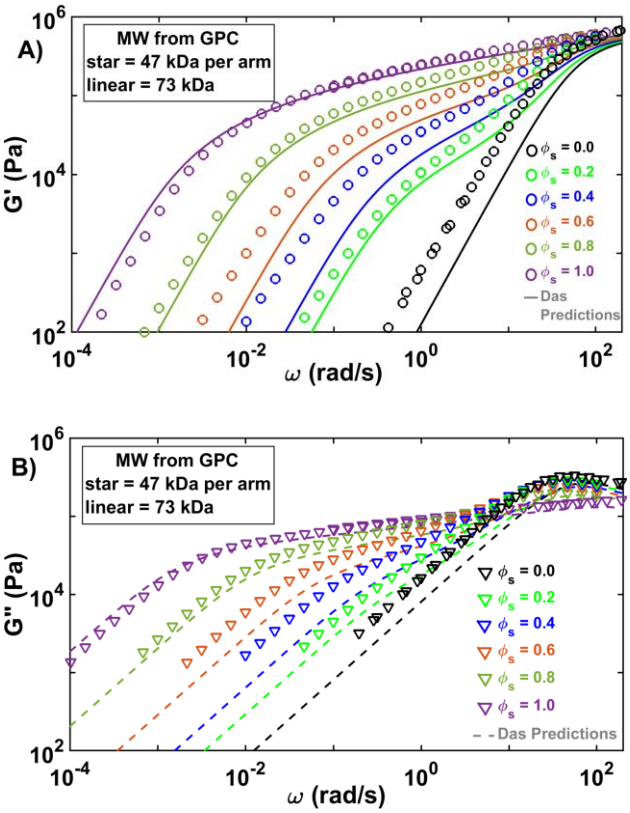

Figure 3.A21: The same as Figure 3.A15, but for 47KS-73KL blends.

Figure 3.A22 shows that using molecular weights given by GPC in the Hierarchical model does not improve the predictions (lines) of the 42.3KS-105KL data (symbols) of Struglinski et al.[18] As in Figure 3.A8, which compares 42.3KS-105KL data with predictions using molecular weights from zero-shear viscosity (in Table 3.4 of the main text), predictions in Figure 3.A22 also incorrectly show non-monotonicity of the dependence of terminal relaxation

time on ϕ_s. Likewise, in Figure 3.A23, the Hierarchical model with GPC molecular weights predicts 47KS-260KL rheology consistent with that of Figure 3.A9, whose molecular weights are based on zero-shear viscosities.

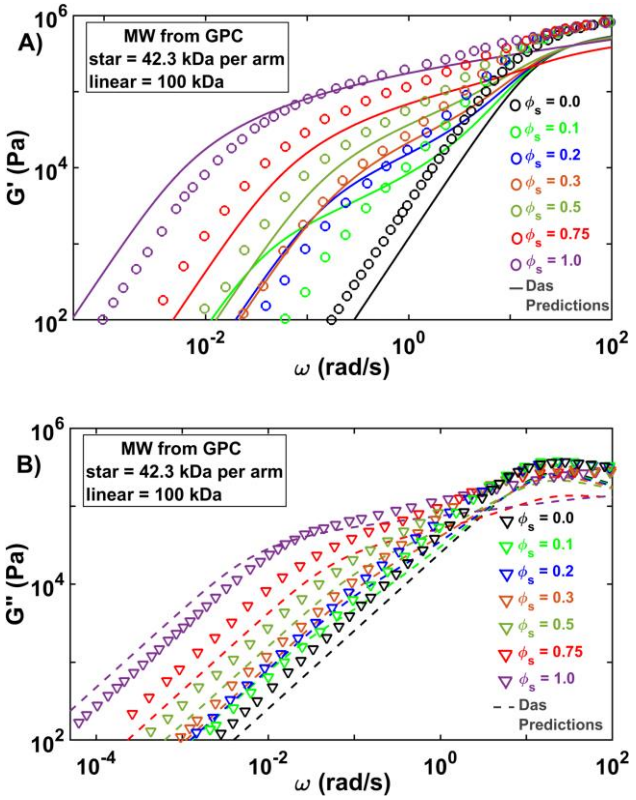

Figure 3.A22: The same as Figure 3.A15, but for 42.3KS-105KL blends taken from Struglinski et al.[18]

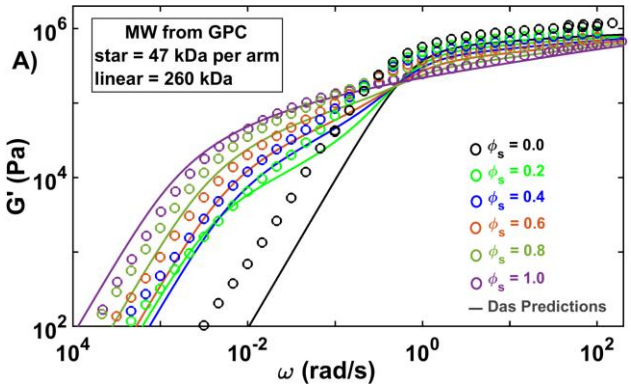

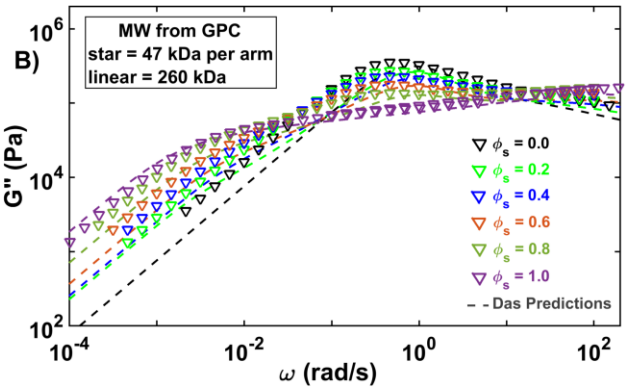

Figure 3.A23: The same as Figure 3.A15, but for 47KS-260KL blends.

VI.2.vi Clarifying Model Predictions of Non-Monotonicity of Star-Linear Blends

In Figures 3.A8 and 3.A15 of the main text, we introduced the 25.3KS-73KL blend series to assess further the onset of non-monotonic relaxation time dependence on star volume fraction (ϕ_s) in the experimental data. This blend series corresponds to a case in which the terminal relaxation frequency of the pure linear polymer is shorter than, but separated by less than one order of magnitude, from the pure star. As shown in Figure 3.8 of the main text, the 25.3KS-73KL blends did not yield non-monotonic behavior experimentally, although non-monotonic behavior was predicted by the by the Hierarchical model. Here we supplement Figure 3.8 by providing the linear rheology data of the 25.3KS-73KL blends, as shown in Figures 3.A24 and 3.A25. Figure 3.A24 compares experimental data (symbols) with Hierarchical model predictions (lines) that utilize star and linear molecular weights obtained from fitting the zero-shear viscosity, while in Figure 3.A25 the star and linear molecular weights were measured by GPC.

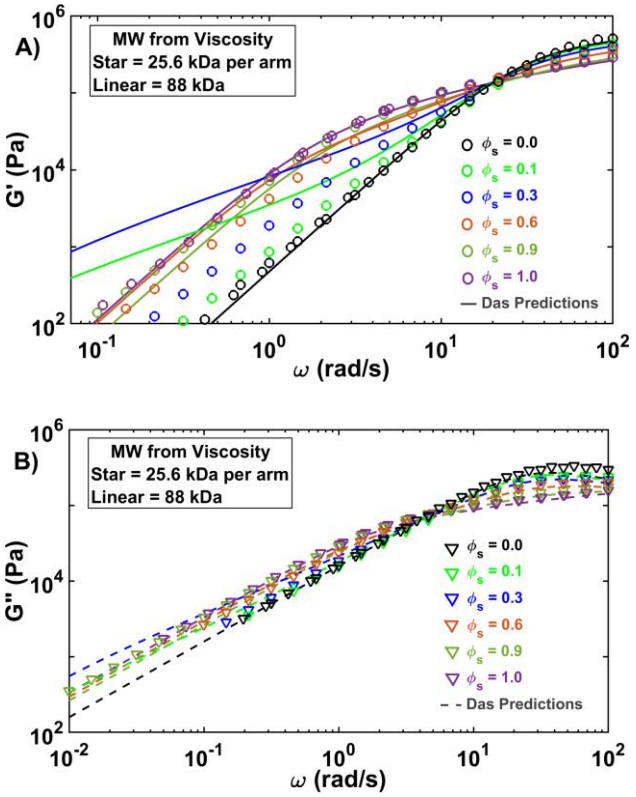

Figure 3.A24: Experimental (symbols) A) G' and B) G" linear rheology data of the 25.3KS-73KL blends series, for star volume fractions (ϕ_s) 0, 0.1, 0.3, 0.6, 0.9 and 1, compared with predictions of the Hierarchical model using molecular weights obtained from zero-shear viscosity fitting.

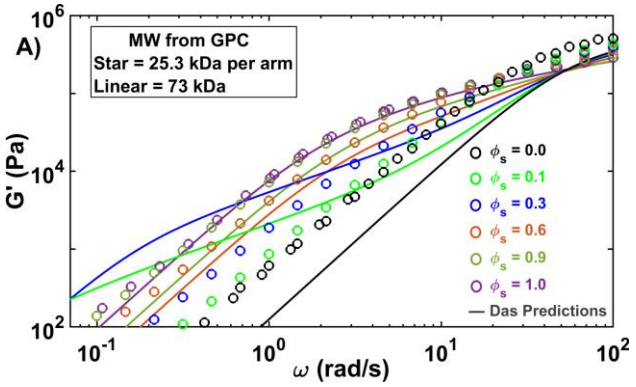

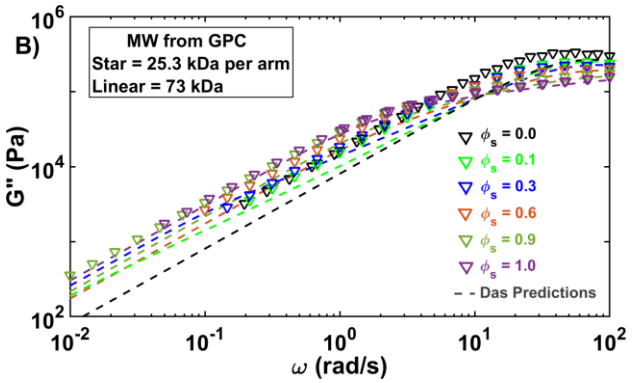

Figure 3.A25: The same as Figure 3.A24, but using molecular weights from GPC.

VII. References

[1] Doi, M.; Edwards, S. F. Dynamics of Concentrated Polymer Systems Part 1: Brownian Motion in the Equilibrium State. *J. Chem. Soc., Faraday Trans. 2* **1978**, 74, 1789−1801.

[2] Doi, M.; Edwards, S. F. Dynamics of Concentrated Polymer Systems Part 2: Molecular Motion Under Flow. *J. Chem. Soc., Faraday Trans. 2* **1978**, 74, 1802−1817.

[3] Doi, M.; Edwards, S. F. Dynamics of Concentrated Polymer Systems Part 3: The Constitutive Equation. *J. Chem. Soc., Faraday Trans. 2* **1978**, 74, 1818−1832.

[4] Doi, M.; Edwards, S. F. Dynamics of Concentrated Polymer Systems Part 4: Rheological Properties. *J. Chem. Soc., Faraday Trans. 2* **1979**, 75, 38−54.

[5] de Gennes, P. G. Reptation of a Polymer Chain in the Presence of Fixed Obstacles. *J. Chem. Phys.* **1971**, 55, 572.

[6] Rubinstein, M. Discretized Model of Entangled-Polymer Dynamics. *Phys. Rev. Lett.* **1987**, 59 (17), 1946−1949.

[7] O'Connor, N.P.T. and Ball, R.C. Confirmation of the Doi Edwards Model. *Macromolecules* **1992**, 25, 5677-5682

[8] de Gennes, P.G. Dynamics of Entangled Polymer Solutions. II. Inclusion of Hydrodynamic Interactions. *Macromolecules* **1976**, 9 (4), 594-598

[9] de Gennes, P.G. Theory of Polymer Absorption. *J. Phys. (Paris)* **1976**, 37 (12), 1445-1452

[10] Doi, M.; Graessley, W. W.; Helfand, E.; Pearson, D. S. Dynamics of Polymers in Polydisperse Melts. *Macromolecules* **1987**, 20 , 1900−1906.

[11] Viovy, J.; Rubinstein, M.; Colby, R. Constraint Release in Polymer Melts: Tube Reorganization versus Tube Dilation. *Macromolecules* **1991**, 24, 3587−3596.

[12] Marrucci, G. Relaxation by Reptation and Tube Enlargement: A Model for Polydisperse Polymers. *J. Polym. Sci., Polym. Phys. Ed.* **1985**, 23, 159−177.

[13] Klein, J. The Onset of Entangled Behavior in Semidilute and Concentrated Polymer Solutions. *Macromolecules* **1978**, 11 (5), 852− 858.

[14] Daoud, M.; de Gennes, P. G. Some Remarks on the Dynamics of Polymer Melts. *J. Polym.*

Sci., Polym. Phys. Ed. **1979**, 17, 1971− 1981.

[15] Ball, R. C.; McLeish, T. C. B. Dynamic Dilution and the Viscosity of Star-Polymer Melts. *Macromolecules* **1989**, 22, 1911− 1913.

[16] Milner, S.T.; McLeish, T.C.B. Parameter-Free Theory for Stress Relaxation in Star Polymer Melts. *Macromolecules* **1997**, 30, 2159-2166.

[17] Milner, S. T.; McLeish, T. C. B.; Young, R. N.; Hakiki, A.; Johnson, J. M. Dynamic Dilution, Constraint-Release, and Star-Linear Blends. *Macromolecules* **1998**, 31, 9345−9353.

[18] Struglinski, M. J.; Graessley, W. W.; Fetters, L. J. Effects of Polydispersity on the Linear Viscoelastic Properties of Entangled Polymers. 3. Experimental Observations on Binary Mixtures of Linear and Star Polybutadienes. *Macromolecules* **1988**, 21, 783−789.

[19] Larson, R. G. Combinatorial Rheology of Branched Polymer Melts. *Macromolecules* **2001**, 34, 4556−4571.

[20] Wang, Z.; Chen, X.; Larson, R. G. Comparing Tube Models for Predicting the Linear Rheology of Branched Polymer Melts. *J. Rheol.* **2010**, 54, 223−260.

[21] Park, S. J.; Shanbhag, S.; Larson, R. G. A Hierarchical Algorithm for Predicting the Linear Viscoelastic Properties of Polymer Melts with Long-Chain Branching. *Rheol. Acta* **2005**, 44, 319−330.

[22] Park, S. J.; Larson, R. G. Tube Dilation and Reptation in Binary Blends of Monodisperse Linear Polymers. *Macromolecules* **2004**, 37, 597 −604.

[23] Das, C.; Inkson, N. J.; Read, D. J.; Kelmanson, M. A.; McLeish, T. C. B. Computational Linear Rheology of General Branch-on-Branch Polymers. *J. Rheol.* **2006**, 50 (2), 207−234.

[24] van Ruymbeke, E.; Keunings, R.; Bailly, C. Prediction of Linear Viscoelastic Properties for Polydisperse Mixtures of Entangled Star and Linear Polymers: Modified Tube-Based Model and Comparison with Experimental Results. *J. Non-Newtonian Fluid Mech.* **2005**, 128, 7-22

[25] van Ruymbeke, E.; Bailly, C.; Keunings, R.; Vlassopoulos, D. A General Methodology to Predict the Linear Rheology of Branched Polymers. *Macromolecules* **2006**, 39, 6248-6259

[26] Ahmadi, M.; Bailly, C.; Keunings, R.; Nekoomanesh, M.; Arabi, H.; van Ruymbeke, E. Time Marching Algorithm for predicting the Linear Rheology of Monodisperse Comb Polymer Melts. *Macromolecules* **2011**, 44, 647-659.

[27] Park, S.J. and Larson, R.G. Modeling the Linear Viscoelastic Properties of Metallocene-Catalyzed High Density Polyethylenes with Long-Chain Branching. *J. Rheol.* **2005,** 49, 523-536.

[28] Park, S. J.; Larson, R. G. Dilution Exponent in the Dynamic Dilution Theory for Polymer

Melts. *J. Rheol.* **2003**, 47, 199−211.

[29] Desai, P.S.; Kang, B.G.; Katzarova, M.; Hall, R.; Huang, Q.; Lee, S.; Shivokhin, M.; Chang, T.; Venerus, D.C.; Mays, J.; Schieber, J.D.; and Larson, R.G. Challenging Tube and Slip-Link Models: Predicting the Linear Rheology of Blends of Well-Characterized Sar and Linear 1,4-Polybutadienes. *Macromolecules* **2016**, 49(13), 4964-4977

[30] Shivokhin, M. E.; van Ruymbeke, E.; Bailly, C.; Kouloumasis, D.; Hadjichristidis, N.; Likhtman, A. E. Understanding Constraint Release in Star/Linear Polymer Blends. *Macromolecules* **2014**, 47 (7), 2451−2463.

[31] Schieber, J.D. and Andreev, M. Entangled Polymer Dynamics in Equilibrium and Flow Modeled Through Slip Links. *Annu. Rev. Chem. Biomol. Eng.* **2014**, 5, 367-381

[32] Khaliulin, R.N. and Schieber, J.D. Self-Consistent Modeling of Constraint Release in a Single-Chain Mean-Field Slip-Link Model. *Macromolecules* **2009**, 42 (19), 7504-7517

[33] Pilyugina, E.; Andreev, M.; and Schieber, J.D. Dielectric Relaxation as an Independent Examination of Relaxation Mechanisms in Entangled Polymers Using the Discrete Slip-Link Model. *Macromolecules* **2012**, 45 (14), 5728-5743

[34] Andreev, M. and Schieber, J.D. Accessible and Quantitative entangled Polymer Rheology Predictions, Suitable for Complex Flow Calculations. *Macromolecules* **2015**, 48(5), 1606-1613

[35] Andreev, M.; Feng, H.; and Schieber, J.D. Universality and Speedup in Equilibrium and Nonlinear Rheology Predictions of the Fixed Slip-Link Model. *J. Rheol.* **2014**, 58, 723

[36] van Ruymbeke, E.; Masubuchi, Y.; Watanabe, H. Effective Value of the Dynamic Dilution Exponent in Bidisperse Linear Polymers: From 1 to 4/3. *Macromolecules* **2012**, 45, 2085−2098

[37] van Ruymbeke, E.; Shchetnikava, V.; Matsumiya, Y.; Watanabe, H. Dynamic Dilution Effect in Binary Blends of Linear Polymers with Well-Separated Molecular Weights. *Macromolecules* **2014**, 47, 7653− 7665

[38] Shahid, T.; Huang, Q.; Oosterlinck, F.; Clasen, C.; van Ruymbeke, E. Dynamic Dilution Exponent in Monodisperse Entangled Polymer Solutions. *Soft Matter* **2017**, 13, 269−282.

[39] Huang, Q.; Hengeller, L.; Alvarez, N. J.; Hassager, O. Bridging the Gap between Polymer Melts and Solutions in Extensional Rheology. *Macromolecules* **2015**, 48, 4158−4163.

[40] Hall, R; Kang, B.; Lee, S.; Chang, T.; Venerus, D.C.; Hadjichristidis, N.; Mays, J.; Larson, R.G. Determining the Dilution Exponent for Entangled 1,4-Polybutadienes Using Blends of Near-Monodisperse Star with Unentangled, Low Molecular Weight Linear Polymers. *Macromolecules* **2019**, 52 (4),1757–1771

[41] Daniels, D. R.; McLeish, T. C. B.; Kant, R.; Crosby, B. J.; Young, R. N.; Pryke, A.;

Allgaier, J.; Groves, D. J.; Hawkins, R. J. Linear Rheology of Diluted Linear, Star and Model Long Chain Branched Polymer Melts. *Rheol. Acta* **2001**, 40, 403−415

[42] Raju, V. R.; Menezes, E. V.; Marin, G.; Graessley, W. W.; Fetters, L. J. Concentration and Molecular Weight Dependence of Viscoelastic Properties in Linear and Star Polymers. *Macromolecules* **1981**, 14, 1668−1676.

[43] Tao, H.; Huang, C.; Lodge, T. P. Correlation Length and Entanglement Spacing in Concentrated Hydrogenated Polybutadiene Solutions. *Macromolecules* **1999**, 32, 1212−1217

[44] Brochard, F.; de Gennes, P. G. Dynamical Scaling for Polymers in Theta Solvents. *Macromolecules* **1977**, 10 (5), 1157−1161.

[45] Colby, R. H.; Fetters, L. J.; Graessley, W. W. The Melt Viscosity-Molecular Weight Relationship for Linear Polymers. *Macromolecules* **1987**, 20 (9), 2226−2237.

[46] Struglinski, M.J.; Graessley, W.W. Effects of Polydispersity on the Linear Viscoelastic Properties of Entangled Polymers. 1. Experimental Observations for Binary Mixtures of Linear Polybutadiene. *Macromolecules* **1985**, 18, 2630-2643

[47] Roovers, J. Properties of the Plateau Zone of Star-Branched Polybutadienes and Polystyrenes. *Polymer* **1985**, 26, 1091–1095.

[48] Roovers, J. Tube Renewal in the Relaxation of 4-Arm Star Polybutadienes in Linear Polybutadienes. *Macromolecules* **1987**, 20, 148–152

[49] Park, S. J.; Desai, P. S.; Chen, X.; Larson, R. G. Universal Relaxation Behavior of Entangled 1,4-Polybutadiene Melts in the Transition Frequency Region. *Macromolecules* **2015**, 48, 4122−4131

[50] Li, S.W.; Park, H.E.; and Dealy, J.M. Evaluation of Molecular Linear Viscoelastic Models for Polydisperse H Polybutadienes. *J. Rheol.* **2011,** 55, 1341-1373

[51] Palade, L. I.; Verney, V.; Attane, P. Time-Temperature Superposition and Linear Viscoelasticity of Polybutadienes. *Macromolecules* **1995**, 28, 7051.

[52] Chang, T. Polymer Characterization by Interaction Chromatography. *J. Polym. Sci. Part B: Polym Phys.* **2005**, 43, 1591.

[53] Perny, S.; Allgaier, J.; Cho, D.; Lee, W.; Chang, T. Synthesis and Structural Analysis of an H-Shaped Polybutadiene. *Macromolecules* **2001**, 34, 5408

[54] Li, S.W.; Park, H.E.; Dealy, J.M.; Maric, M.; Lee, H.; Im, K.; Choi, H.; Chang, T.; Rahman, M.S.; Mays, J. Detecting Structural Polydispersity in Branched Polybutadienes. *Macromolecules* **2001**, 44, 208

[55] Chen, X.; Rahman, M.S.; Lee, H; Mays, J.; Chang, T.; Larson, R.G. Combined Synthesis, TGIC Characterization, and Rheological Measurement and Prediction of Symmetric H Polybutadienes and Their Blends with Linear and Star-Shaped Polybutadienes. *Macromolecules* **2011**, 44, 7799-7809.

[56] Read, D.J.; Jagannathan, K.; Sukumaran, S.K. A Full-Chain Constitutive Model for Bidisperse Blends of Linear Polymers. *J. Rheo.* **2012**, 56, 823-873.

[57] Hadjichristidis, N.; Iatrou, H.; Pispas, S.; Pitsikalis, M. Anionic polymerization: High vacuum techniques. *J. Polym Sci A: Polym. Chem.* **2000**, 38, 3211.

[58] Hadjichristidis, N.; Roovers, J. Linear viscoelastic properties of mixtures of 3- and 4-arm polybutadiene stars. *Polymer,* **1985**, 26, 1087.

[59] Polymeropoulos, G.; Zapsas, G.; Ntetsikas, K.; Bilalis, P.; Gnanou, Y.; Hadjichristidis, N. 50th Anniversary Pespective: Polymers with complex architectures. *Macromolecules* **2017**, 50, 1253.

[60] Matsumiya, Y.; Masubuchi, Y.; Inoue, T.; Urakawa, O.; Liu, C.; van Ruymbeke, E.; Watanabe, H. Dielectric and Viscoelastic Behavior of Star-Branched Polyisoprene: Two Coarse-Grained Length Scales in Dynamic Tube Dilation. *Macromolecules* **2014**, 47(21), 7637–7652.

Chapter 4: Conclusions and Future Work

I. Conclusions

We have addressed three different shortcomings concerning tube theory: the confusion in the value of the dilution exponent (α), the failure of Dynamic Tube Dilation (DTD), and the uncertainty of Constraint Release-Rouse (CR-Rouse) physics.

In Chapter 2, we described the preparation of three 1,4-polybutadiene 4-arm stars with arm molecular weights of roughly 48 kDa, 61.5 kDa and 70.1 kDa. Each of these stars were diluted with a sub-entangled linear polymer of the same chemistry, which served as a theta-like solution. When the reduction in segmental friction contributed from the sub-entangled linear polymer and the star volume concentration of each diluted star blend are accounted for, we have shown that a plot of terminal crossover modulus ($\omega_{x,t}$) vs. entanglement density (M_e) of the diluted stars superposes with that of pure stars from literature, also of 1,4-polybutadiene chemistry, when the dilution exponent is taken as unity; the utilization of α = 4/3 does not create such superposition. However, a similar plot of the terminal crossover modulus ($G_{x,t}$) vs. M_e does not demonstrate such defined superposition of experimental and literature datasets, indicating that $G_{x,t}$ is not sensitive to the value of α. Furthermore, Hierarchical 3.0 model[1] predictions with use of the "Das" parameter set, which assumes α=1, is in much closer agreement with the linear rheology of the diluted stars in comparison to when α=4/3 is observed in the "Park" parameter set. Overall, this study is in agreement with the findings of Shahid et al.,[2] Huang et al.,[3] and van Ryumbeke and Watanabe,[4,5] which observes α in the context of linear polymers.

In Chapter 3, leveraging the conclusion of Chapter 2 that α=1, we observed that predictions from the Hierarchical 3.0 model,[1] using the Das set of parameters, and the BoB model[6] accurately captured the non-monotonic dependence of terminal relaxation time on star volume fraction of select star-linear blends, where the pure linear component possessed a longer relaxation time than the pure star, that appeared in the experimental linear rheology data. This modeling success is of great surprise, considering that neither the Hierarchical nor BoB models predicted accurately the star-linear blend data, where the pure star has a longer relaxation time, but is less than 3-4 orders of magnitude, of the pure linear component.[7] Such a revelation suggests that the Hiearchical and BoB models are capturing unknown physics based on the current understanding of DTD and CR-Rouse. In addition to revealing additional details to constraint release physics, the vast datasets of over 50 star-linear blends reported in this study will serve as a rigorous benchmark for testing other predictive models, such as slip-link models, and for developing future models.

II. Future Work

The work presented here has established the value of the dilution exponent for well-entangled stars and illuminated additional details of the DTD and CR-Rouse constraint release mechanisms; however, there is still much work to be done to completely address the failures of tube theory and begin the model rebuilding process.

First, a comprehensive study of star polymers in transition from well-entangled to semi-dilute conditions is needed to develop a refined understanding of the dilution exponent (α). Presented in the work of Shahid et al.,[2] the scaling of the terminal relaxation time and plateau modulus with respect to polymer concentration transitioned from *an apparent* value of α=1 to roughly α=4/3 (the exact value is slightly higher than 4/3) as well-entangled polystyrene linear

melts were gradually diluted to semi-dilute conditions with the use of an oligomer of the same chemistry and analyzed using predictions from the Time-Marching Algorithm (TMA). Specifically, the transition from α=1 to α=4/3 occurred in the scaling of the terminal relaxation time when the number of effective entanglements per linear chain dropped below 20. Similarly, this transition occurred for the plateau modulus when the number of entanglements dropped below 12. However, when the linear polystyrene melts were diluted with a small molecule solvent, the scaling of both the terminal relaxation time and plateau modulus was larger than α=1, even for cases when the linear is considered well-entangled. Ultimately, the Shahid et al. study concluded that α=1 for well-entangled linear melts, in consensus with the findings of Chapter 2 of this dissertation that features well-entangled star melts. However, given that an α value greater than unity is found for weakly entangled linear melts and for linear melts suspended in small molecule solvent, a future study could focus on determining the unique conditions of which α=1 fails for star polymers (and branched systems in general) by using the model-independent approach explained in Chapter 2 of this dissertation.

Second, there is a possibility that additional chemistry-dependent model parameters may need to be included into tube theory, beyond the established ones, which are the plateau modulus (G_N^0), entanglement density (M_e), and the tube-segment frictional Rouse time (τ_e). Shown in the Supplemental Information of the study conducted by Matsumiya et al.,[8] the ratio of constraint release time to terminal time differs between linear polystyrene and linear polyisoprene when the number of entanglements is constant. Such an observation suggests that constraint release physics is more complex than initially realized and may require an additional model parameter to maintain a universal α=1 scaling of terminal relaxation time with respect to polymer volume fraction and entanglement density for statically diluted, well-entangled melts. However, there is

also the possibility that no such model parameter exists, which would suggest that the dilution exponent could be chemistry dependent and hence would need to be retained as an additional tube model parameter.

Third, comprehensive physics for star polymers (and branched polymers in general) that are both more realistic and self-consistent with the physics of linear polymers needs to be developed. The current DTD relaxation picture was initially shown to fail in predicting star polymer melts, as reported by Watanabe et al.[9] Particularly, Watanabe et al. showed the that DTD physics captured measured viscoelastic data of polyisoprene polymers, but overpredicted the associated dielectric relaxation data. Watanabe et al. proposed that this failure of DTD physics is due to its inability to capture the constraint release of entanglements located near the branch point of star molecules, which ultimately contributes to an overall faster relaxation time of the star melt than predicted by the model. This suggestion of entanglement constraint release occurring near the branch point of star molecules is corroborated through slip-link model studies conducted by Shanbhag et al.[10] and Cao et. al.[11] These slip-link simulations show that these near-branch-point-entanglements are able to shuffle towards the free end of each star arm, which ultimately reduces both the time and distance needed for each arm to retract out of these last remaining entanglements.

Fourth, the physics of CR-Rouse remains ambiguous, both in the establishment of a self-consistent method for implementing the existing physics and the identification of physics that may be missing and/or misrepresented. Currently, there are no set guidelines for implementing the three CR-Rouse relaxation approaches: “thin tube,” “fat tube” and “arm frozen.” Depending on the version of tube model implemented and/or the polymer system to be predicted, the CR-Rouse model assumption used may vary.[12-14] In addition, there are additional CR-Rouse physics

that need to be observed in greater detail such as the “thin tube contour length fluctuations” identified by Read et al.[15] and the “tube re-equilibration” process suggested by van Ruymbeke et al.[4,5] Ideally, CR-Rouse physics should be implemented self-consistently without the need to electing specific model assumptions, which has been demonstrated by the Clustered Fixed Slip-link Model (CFSM) developed by Scheiber et al.[16-18] However, the CFSM is not only computationally slow, but is also limited in polymer molecular weight, particularly the number of entanglements, due to the model’s detailed handling of constraints along an arbitrary polymer chain (*i.e.*, probe chain).[7] Therefore, until the limitations of computation are removed, improvements to CR-Rouse understanding, as well other constraint release physics, of tube theory will remain as a topic of interest.

III. References

[1] Wang, Z.; Xue, C.; and Larson, R.G. Comparing Tube Models for Predicting the Linear Rheology of Branched Polymer Melts. *J. Rheol* **2010**, 54, 223-260.

[2] Shahid, T.; Huang, Q.; Oosterlinck, F.; Clasen, C.; van Ruymbeke, E. Dynamic Dilution Exponent in Monodisperse Entangled Polymer Solutions. *Soft Matter* **2017**, 13, 269-282.

[**3]** Huang, Q.; Hengeller, L.; Alvarez, N.J.; Hassager, O. Bridging the Gap between Polymer Melts and Solutions in Extensional Rheology. *Macromolecules* **2015**, 48, 4158-4163.

[4] van Ruymbeke, E.; Masubuchi, Y.; Watanabe, H. Effective Value of the Dynamic Dilution Exponent in Bidisperse Linear Polymers: From 1 to 4/3. *Macromolecules* **2012**, 45, 2085-2098.

[5] van Ruymbeke, E.; Shchetnikava, V.; Matsumiya, Y.; Watanabe, H. Dynamic Dilution Effect in Binary Blends of Linear Polymers with Well-Separated Molecular Weights. *Macromolecules* **2014**, 47, 7653-7665.

[6] Das, C.; Inkson, N.J.; Read, D.J.; Kelmanson, M.A.; McLeish, T.C.B. Computational Linear Rheology of General Branch-on-Branch Polymers. *J. Rheol* **2006**, 50 (2), 207-234.

[7] Desai, P.S.; Kang, B.G.; Katzarova, M.; Hall, R.; Huang, Q.; Lee, S.; Shivokhin, M.; Chang, T.; Venerus, D.C.; Mays, J.; Schieber, J.D.; and Larson, R.G. Challenging Tube and Slip-Link Models: Predicting the Linear Rheology of Blends of Well-Characterized Sar and Linear 1,4-Polybutadienes. *Macromolecules* **2016**, 49(13), 4964-4977

[8] Matsumiya, Y.; Kumazawa, K.; Nagao, M.; Urakawa, O.; Watanabe, H. Dielectric relaxation of Monodisperse Linear Polyisoprene: Contribution of Constraint Release. *Macromolecules* **2013**, 46, 6067-6080.

[9] Watanabe, H.; Matsumiya, Y.; and Inoue, T. Dielectric and Viscoelastic Relaxation of Highly Entangled Star Polyisoprene: Quantitative Test of Tube Dilation Model. *Macromolecules* **2002**, 35, 2339-2357.

[10] Shanbhag, S.; Larson, R.G.; Takimoto, J.; Doi, M. Deviations from Dynamic Dilution in the Terminal Relaxation of Star Polymers. *Phy. Rev. Lett.* **2001**, 87 (19), 195502(1) -195502(4).

[11] Cao, J.; Wang, Z. Microscopic Picture of Constraint Release Effects in Entangled Star Polymer Melts. *Macromolecules* **2016**, 49, 5677-5691.

[12] Park, S. J.; Shanbhag, S.; Larson, R. G. A Hierarchical Algorithm for Predicting the Linear Viscoelastic Properties of Polymer Melts with Long-Chain Branching. *Rheol. Acta* **2005**, 44, 319–330.

[13] Larson, R. G. Combinatorial Rheology of Branched Polymer Melts. *Macromolecules* **2001**, 34, 4556–4571.

[14] Milner, S. T.; McLeish, T. C. B. Parameter-Free Theory for Stress Relaxation in Star Polymer Melts. *Macromolecules* **1997**, 30, 2159–2166.

[15] Read, D.J.; Jagannathan, K.; Sukumaran, S.K.; Auhl, D. A Full-Chain Constitutive Model for Bidisperse Blends of Linear Polymers. *J. Rheol.* **2012**, 56, 823-873.

[16] Pilyugina, E.; Andreev, M.; and Schieber, J.D. Dielectric Relaxation as an Independent Examination of Relaxation Mechanisms in Entangled Polymers Using the Discrete Slip-Link Model. *Macromolecules* **2012**, 45 (14), 5728-5743.

[17] Andreev, M. and Schieber, J.D. Accessible and Quantitative entangled Polymer Rheology Predictions, Suitable for Complex Flow Calculations. *Macromolecules* **2015**, 48(5), 1606-1613.

[18] Andreev, M.; Feng, H.; and Schieber, J.D. Universality and Speedup in Equilibrium and Nonlinear Rheology Predictions of the Fixed Slip-Link Model. *J. Rheol.* **2014**, 58, 723.